

Intensity Duration Frequency Curves and Trends for the City of Seattle

Technical Memorandum

December 29 2017

Seattle Public Utilities CSO Reduction Program



Intensity Duration Frequency Curves and Trends for the City of Seattle

Technical Memorandum

December 29, 2017

Prepared for: James Rufo-Hill
Seattle Public Utilities

Prepared by: John Rath, Sujoy Roy, and Jon Butcher
Tetra Tech Inc.
1420 Fifth Avenue, Suite 600, Seattle, WA 98101
and 3746 Mount Diablo Boulevard, Suite 300,
Lafayette, CA 94549

CONTENTS

Acknowledgements	1
Executive Summary	3
Introduction	5
Background	5
Data Used for Analysis	7
Methods	8
L-Moments Approach	8
Bayesian Approach	8
Results	9
IDF Values Using L-Moments Approach	9
Comparison of L-Moments and Bayesian Approaches for Stationary Models	9
Time Trends in Extreme Values	10
Parameters of Bayesian Regression Models	10
Discussion	10
Summary	11
References	13
Tables	Tables-1
Figures	Figures-1

ACKNOWLEDGEMENTS

This work was funded by Seattle Public Utilities (SPU) through a contract with Tetra Tech in support of the combined sewer overflow (CSO) reduction program; James Rufo-Hill served as the Project Manager. Quality controlled precipitation data used for this analysis were developed by SPU for seventeen rain gauges throughout the City of Seattle. Rizwan Hamid of Aqualyze, Inc. provided a processed data set of these values from 1977-2016; 2017 data were supplied directly by SPU. Additional regional precipitation data from National Weather Service stations were compiled, quality controlled, and provided to us by Philip Pasteris of CH2M Hill.

EXECUTIVE SUMMARY

The City of Seattle is served by a combined sewer system that handles both stormwater runoff and wastewater. Large rain events can exceed the capacity of this sewer system and cause combined sewer overflows (CSOs). These sewage discharges to the receiving waters of Puget Sound can be a source of pollutants, and are limited by the City's discharge permit. The City has in place an extensive program to manage these overflows, termed the *Plan to Protect Seattle's Waterways*. As part of this larger plan and to aid the design and upgrade of new stormwater infrastructure to control CSOs, the City needs a characterization of extreme precipitation events occurring in the watersheds of the storm sewer network. This is usually performed by the development of intensity-duration-frequency (IDF) curves, which characterize the magnitude of rainfall corresponding to different averaging periods (typically ranging from minutes to hours), with a given return period (typically ranging from a year to 1,000 years). Thus, extreme precipitation at a location is represented, not by a single value, but a matrix of values corresponding to the averaging duration and the return period. This document provides an update of the IDF curves for the City given the most complete precipitation record available.

Seattle Public Utilities (SPU) collects precipitation data at seventeen stations which were used for this analysis. Quality controlled data from these stations, composited to a 5 minute interval, were available for 1977-2017. In addition, supporting analyses were performed using data from a set of regional stations operated by the National Weather Service.

An initial evaluation of annual extremes was used to make a determination on excluding individual storms because of their non-representative character, by comparing across stations in the same year, and considering the largest storms in each year. However, the data on annual maxima did not suggest unusual behavior in individual data points, and all storms are used in the analysis presented here.

The 5-minute precipitation data, integrated to various other intervals, were used to develop the IDF curves by fitting the data to a standard probability distribution that is commonly used for developing IDF curves in the United States, the generalized extreme value (GEV) distribution. The parameter fit to this probability distribution was accomplished using two approaches, the L-moments method, which has been used in all prior work for SPU, and a Bayesian estimation method, that also allowed for the evaluation of time and other variables in the parameters of the GEV distribution. IDF curves were prepared for the entire region served by SPU (i.e., considering data from all 17 rain gauges), and for individual rain gauges. Values for individual stations may be used in future station-specific hydrologic modeling.

IDF curves were developed using the L-moments approach on a regional basis and on a station-specific basis. These values (referred to as the "stationary" values in the presentation of the results) can be used as is. Table ES-1 presents the updated regional IDF values calculated in this work, using the previously applied L-moments method. The point estimates of the L-moments approach agree well with those of a stationary Bayesian multilevel model. However, the Bayesian approach also provided information on the trends in the rainfall extremes over the period of record.

The trend evaluation of GEV distribution parameters—after accounting for the variation of the oceanic phenomenon known as the Pacific Decadal Oscillation, known to affect precipitation in the Pacific Northwest—showed statistically significant positive trends in various metrics of extreme precipitation. For example, given the matrix of 8X8, or 64 values that represent IDF curves for the SPU region, 55 (or 86%) indicate an increase for the median estimate. For comparison, these trends were also calculated for NWS stations, many of which contain data over longer time periods. The trends at these stations are more variable, but in general, a statistically significant positive trend is apparent at the majority (but not all) of stations with long data records, some extending over a century.

These trends in the SPU station extremes, based on the large volume of underlying data, provide strong quantitative support for anticipated changes in precipitation extremes over future decades in the SPU region. The general concept of increasing precipitation extremes is indicated through global climate model analysis, but the changes computed here are based on observed, local data, and provide credible support for consideration of such trends in future planning for infrastructure design by SPU. The rates of change can be used as calculated in this work, by extrapolation into the future, or, as a bookend for increases computed through the results of downscaled global climate model results.

Table ES-1. IDF values using data for 17 stations from the SPU network, and computed using the L-moments approach.

Duration	Intensity (inches per hour)							
	2-yr	5-yr	10-yr	25-yr	50-yr	100-yr	500-yr	1000-yr
5.0 minutes	1.3400	1.7900	2.1100	2.5400	2.8800	3.2300	4.1200	4.5400
15.0 minutes	0.8170	1.0900	1.2800	1.5400	1.7400	1.9600	2.5000	2.7600
30.0 minutes	0.5560	0.7310	0.8590	1.0400	1.1800	1.3400	1.7600	1.9600
1.0 hours	0.3910	0.5000	0.5780	0.6820	0.7650	0.8510	1.0700	1.1700
6.0 hours	0.1680	0.2210	0.2590	0.3100	0.3500	0.3920	0.4970	0.5470
1.0 days	0.0828	0.1120	0.1350	0.1680	0.1960	0.2280	0.3160	0.3620
3.0 days	0.0416	0.0538	0.0621	0.0729	0.0812	0.0897	0.1100	0.1190
7.0 days	0.0261	0.0324	0.0359	0.0395	0.0418	0.0437	0.0473	0.0485

INTRODUCTION

The City of Seattle (City) is served by a combined sewer system that handles both stormwater runoff and wastewater. Large rain events can exceed the capacity of the sewer system and cause combined sewer overflows (CSOs). These sewage discharges to the receiving waters of Puget Sound can be a source of pollutants, and are limited by the City's discharge permit. Specifically, the City's permit allows no more than one CSO event each year. These overflow events occur during periods of very high rainfall, and there is great interest in characterizing the magnitude of extreme precipitation events accurately to effectively design to mitigate CSOs.

Typically, extreme precipitation information is presented in the form of intensity-duration-frequency (IDF) curves that quantify the amount of precipitation over a given averaging duration and return period (or probability). In general the intensity of rainfall, expressed in units of inches per hour, is highest for shorter averaging durations, and also higher for long return periods. Return periods for IDF curves usually range from one year (i.e., the quantity of rainfall that can be expected to be exceeded each year), to 100 to 1,000 years (i.e., the probability of exceedance in any given year being 0.01 or 0.001, respectively). There is greater uncertainty in values associated with higher return period events, because, by definition, there are fewer data points in this part of the distribution. IDF curve values may be used directly to develop design storms that are used to size infrastructure, or may be a component of a hydrologic modeling approach where a natural precipitation time series is modified to represent particular extremes.

The current *Stormwater Manual for the City of Seattle* (2016) contains a set of IDF curves for the City regionally and for individual gauging stations. These IDF curves are based on an analysis performed by MGS Engineering Consultants, Inc. for Seattle Public Utilities in 2013. Durations of 5 minutes, 10 minutes, 15 minutes, 20 minutes, 30 minutes, 45 minutes, 60 minutes, 2 hours, 3 hours, 6 hours, 12 hours, 24 hours, 48 hours, 72 hours, and 7 days were analyzed to develop the IDF curves. The MGS analysis is reported to have used rain gauge data to 2012. A subsequent effort by CH2M Hill using data to 2015 (CH2M Hill, 2016) developed precipitation intensities for the 24-hour duration. Because precipitation may change over time, and because additional data enhance the estimate of the IDF values, there is a need to update the IDF values at a regular frequency. The prior analyses by MGS Engineering Consultants and CH2M Hill both suggest that there has been an increase in extreme events, and thus there is interest in using the most complete and recent record for updating the IDF curves and formally evaluating trends over time.

The present work builds upon and extends prior work performed for SPU. As part of this effort, Tetra Tech obtained quality-controlled 5-minute precipitation data from 17 rain gauges across the City of Seattle beginning in water year 1978 and ending in April 2017 (water years run from October 1 of the preceding year to September 30 of the current year). Precipitation data from National Weather Service gauges for the Puget Sound and surrounding region was obtained from CH2M Hill, with a range of starting and ending dates. The data were used to develop IDF curves for the Seattle metropolitan area, and for individual stations. Tetra Tech further evaluated trends in extreme precipitation over time, after correcting for the effects of the Pacific Decadal Oscillation (PDO), an oceanic index that is correlated with higher rainfall in the Pacific Northwest (Mantua et al., 1997).

This technical memorandum provides an overview of the scientific literature on precipitation extremes, particularly in the context of the Pacific Northwest, an overview of data used for the analysis, and the results of the IDF curve analysis and the estimated trends in precipitation extremes.

BACKGROUND

In general, extreme precipitation is a complex phenomenon and represented both by the averaging duration and the return period, resulting in a matrix of values for a single location. Assuming, for example, that extremes are reported for 8 averaging durations and 8 return periods at a location or region (as done in this work), the extreme precipitation is represented as matrix of 64 values. In the United States, IDF values are typically developed by

fitting observed data to an extreme-value probability distribution called the generalized value distribution (GEV). Parameters for the GEV distribution are fitted through a methodology termed the L-moments approach. The National Oceanic and Atmospheric Administration provides recent IDF values for much of the United States, through a product called Atlas 14 that uses this methodology (NOAA, 2013). Importantly, however, Atlas 14 values have not been developed for the State of Washington.

Although the Atlas 14 IDF estimates, where available, are based on relatively recent data, they do not evaluate trends in extreme precipitation. A significant body of recent literature considers the possibility of there being changes in extremes as a consequence of climate change, both in the recent past in and in future years. When reporting trends, a significant amount of the scientific literature does not consider the full range of extreme metrics, but focuses on a selected few. Considered in this manner, several studies have suggested that precipitation extremes (defined over different averaging durations) have increased over the late 20th and early 21st century. For example, Zhang et al. (2013) estimated that human influence from 1952 to 2005 intensified annual maximum 1-day precipitation in the northern hemisphere by 3.3 percent, corresponding to an average intensification in maximum 1-day precipitation of 5.2 percent per degree increase in observed global mean surface temperature, consistent with the Clausius-Clapeyron relationship (this thermodynamic relationship states that higher temperatures are associated with a higher moisture content in air).

Studies of observational data at selected locations report results that are more mixed. Examining the top 50 extreme precipitation events in two-day precipitation from 60 years of National Climatic Data Center daily precipitation data at six Pacific Northwest coastal stations, Warner et al. (2012) reported that the 1950s, 1980s, and 1990s experienced more extreme events than the 1960s, 1970s, and 2000s, indicative of other drivers in extremes, besides a monotonic trend. Rosenberg et al. (2010) reported an increase in the fitted 1- and 24-hour annual maximum distributions from 1956–1980 to 1981–2005 for the Puget Sound region, although not for other regions studied in the Northwest. Mass et al. (2011) similarly reported an increase in extreme precipitation in Washington, but not in other regions of the Pacific coast, such as Northern California and Central Oregon. An evaluation of 1-day and 5-day precipitation extremes over the Northern Hemisphere with data for 1950–1999 (Min et al., 2011) shows that the Pacific Northwest exhibits increases for both metrics. The 2017 Climate Science Special Report (CSSR) report, published by the U.S. Global Climate Change Program, presents an examination of change in extreme precipitation (Easterling et al., 2017). The CSSR is a technical report that describes the state of science relating to climate change and its physical impacts. Two metrics are presented: the daily maximum precipitation (1948–2015) and the 5-year maximum daily and 2-day precipitation (1901–2016). A summary of daily precipitation change by season, in seven broad regions of the conterminous U.S. indicates a mix of increases and decreases, with the Northwest region showing very small changes in all seasons, and a very small decrease over winter. The 5-day maximum daily and 2-day precipitation shows small increases over the Northwest over the 1901–2016 period; the increases are smaller than computed over the eastern half of the U.S.

Pertinent to these types of regional-scale studies, a review of the CSSR was recently performed by the National Academies of Sciences, Engineering, and Medicine (National Academies, 2017). In the context of extreme precipitation, this review stated:

“Studies of changes in extreme precipitation at individual weather stations find a wide variety of trends (and results can depend profoundly on which metric is selected); spatially aggregating the trends to a relatively large scale does seem to result in a regionally averaged increase in extreme precipitation (e.g., Min et al., 2011; Zhang et al., 2013)... But, the underlying message of the spatial complexity is not well articulated in the draft CSSR, especially when accompanied by language like “Heavy precipitation events across the United States have increased...” The Committee recommends careful consideration of the appropriate level of detail concerning spatial complexity (e.g., plotting station-level or climate-division trends), robustness across metrics (e.g., plotting multiple time series of different metrics), and traceability.”

The review clearly suggests that temporal trends in extremes are more complex when looked at individual locations than across large regions, and all extreme metrics at a given location may not follow the same pattern of monotonic increase. This work supports such a recommendation in considering observed data in a focused region, to perform a robust evaluation of changes in multiple measures of precipitation extremes over time.

DATA USED FOR ANALYSIS

SPU maintains a gauging network of 17 stations across the City of Seattle that was the primary focus of this analysis. The stations are listed in Table 1 and their locations shown on Figure 1 (tables and figures are provided at the end of this technical memorandum). Data were provided to Tetra Tech at 5-minute intervals from water year 1978 (beginning October 1, 1977) to April 2017. The data were subject to quality control by SPU prior to being provided to us. In addition, a set of National Weather Service (NWS) station data (Figure 2) were provided following initial cleaning (performed in a previous task for SPU) by CH2M Hill. The NWS data span a much greater geographic region than the SPU data, and in many instances, a much longer period of record. The daily NWS data were primarily used for supporting the trend evaluation; the IDF curve update focused on the SPU data.

To verify the overall quality of the SPU and NWS data, especially the extent of gaps in the record and the likelihood of outliers in the extremes, the following steps were performed:

- For the SPU data, prepare time series of the 5 highest precipitation values for each station for each year, aggregated for the following durations: 5 minutes, 15 minutes, 30 minutes, 1 hour, 1 day, and 7 days. The existence of individual values distant from other high values in that year could be indicative of erroneous values, although outliers are expected to some extent in a dataset of sample maxima. These plots are shown in Figures 3 through 19. For certain averaging durations and certain stations, the single highest values appears distinct from the remaining four high values for the year. However, there is no systematic pattern of difference at a specific station, or in a specific year across all averaging durations. This form of data inspection did not support the exclusion of any year or any station from the IDF analysis. In any event, when the focus of the analysis is on a small number of extreme events, great caution must be exercised in excluding individual data points from the analysis.
- A similar evaluation was performed for the NWS data, where the averaging was performed over 1, 3, and 7 days. These plots are shown in Figures 20 through 44. As with the SPU data, there was little in the data to suggest that any of the years or stations should be excluded from the analysis.
- The extent of missing data was evaluated in tabular form for the SPU stations, as shown in Table 2. Following the quality control procedures adopted by SPU, including the possibility that data gaps were filled, there will be minimal gaps in the data over the 1977-2017 period. In comparison, there were extensive gaps in the NWS data at virtually all stations (Table 3). Importantly, however, the data record length at some stations was extensive, spanning more than a century.
- Further examination of the SPU data was performed by examining individual annual maxima values over the past decade to see if there was a recent pattern in the occurrence of extreme high precipitation, such that particular years might be excluded from the IDF calculation. This was done for the 5 minute, 1 hour, and 1 day averaging periods (Tables 4 through 6). Again, as in the time series plots, incidences of high values are randomly distributed across stations and years, and there is no basis for excluding any of these data. An exception is the 1-day average precipitation which appears to be the highest in 2008 across most stations (Table 6). However, the 2008 values are within the range of maxima when looked at over the full record (time series plots), and do not appear unusual.
- The NWS data extremes for 1-day precipitation over the past decade were examined in a similar manner (Table 7) and show a random distribution of high values. These data do not support the exclusion of particular years.

In addition to the precipitation time series, the water year average of the PDO values was used, as shown in Figure 45. The PDO is a climate index based on patterns of variation in sea surface temperatures in the North Pacific (Mantua et al. 1997) and is related to precipitation in the Northwest. PDO conditions can last for decades, and are important to consider in evaluating temporal trends in extremes.

The NWS data were available at most stations at the daily level. Use of daily data can underestimate the 24-hour maximum, where a storm spans a portion of two days. The difference in averaging is referred to as constrained (data accumulated over calendar days) or unconstrained (24-hour value calculated as a rolling total). Using the sub-daily SPU data, a ratio between the unconstrained and constrained values for the region was calculated, as shown on Figure 46. A ratio of 1.13 was applied to the NWS data for analysis of extremes.

METHODS

IDF curves were estimating using two statistical approaches. Both approaches fit the annual maximum precipitation series to the generalized extreme value (GEV) distribution. This distribution was chosen for its flexibility and its widespread use in other analyses, such as NOAA (2013), Cheng and AghaKouchak (2014), and previous analyses of SPU data (CH2M Hill, 2016).

The GEV distribution is specified in terms of three parameters, μ , σ , and ξ (mu, sigma, and xi). They are, respectively, location, scale, and shape parameters of the GEV distribution. For a non-exceedance probability p (associated with the n -year event where $n = 1/(1 - p)$), the corresponding return level is

$$\mu + \frac{\sigma}{\xi} \cdot \left(\left(\log \frac{1}{p} \right)^{-\xi} - 1 \right).$$

Thus, changes in μ lead to an equivalent change in every return level. Changes in σ represent an increase in variability of the underlying distribution and also affect the return levels. The extreme tail behavior of the annual maximum distribution is dominated by ξ appearing as an exponent in the above equation.

L-Moments Approach

The first approach was a regional frequency analysis using L-moments, following Hosking and Wallis (1997) as implemented in the R packages *lmom* and *lmomRFA* (written by Hosking of Hosking and Wallis (1997)). This is a widely used approach that has been used in the NOAA precipitation atlas and previous analyses of SPU data. The approach works by expressing the GEV distribution's parameters in terms of the data sample's L-moments, which are analogous to the standard moments (mean, standard deviation, skewness, etc.) except that they are based on the data's order statistics. This gives them some measure of robustness compared to standard moments. If the data from the sites of interest are found to be consistent with the notion of belonging to a single homogenous region, then this approach assumes a single regional growth curve that describes the relationship between return frequency and precipitation and a site-specific scaling factor known as the "index flood." Uncertainty in the estimates is simulated from repeated samples of a synthetic dataset with L-moment statistics similar to those of the observed data.

Bayesian Approach

The second approach used Bayesian multilevel regression models with posterior inference carried out using the Stan modeling language via the *rstan* package. Bayesian inference has some similarities to maximum likelihood approaches, but it takes a slightly different perspective of considering unknown parameters to be random variables and using the rules of conditional probability to calculate the probability distribution of the unknown parameters, conditional on the data and any prior knowledge about the parameters. One of the main advantages of a likelihood-based model is the ability to incorporate regression information (for example time trend or

dependence on large-scale climatic indices) directly into the model. Further advantages of the Bayesian paradigm include automatically incorporating parameter uncertainty in the model and natural estimation of models with hierarchical/multilevel structure. In this analysis, that structure is the regionalization of GEV and regression parameters: the site-specific unknowns are drawn from a simultaneously estimated regional model. In order to compare results with the L-moments approach, Tetra Tech fit a stationary Bayesian multilevel that includes the regional structure but not regression on time or climatic covariates.

The regression model involves a linear regression of two of the GEV parameters on time and PDO. Each site j has its own regression with each regression parameter $(\mu_0, a, b, \sigma_0, c, d)$ following a regional distribution to account for expected similarities in parameters between sites in a homogenous region:

$$\begin{aligned}\mu_j(t) &= \mu_{0,j} + a_j \cdot t + b_j \cdot \text{PDO}(t) \\ \sigma_j(t) &= \sigma_{0,j} + c_j \cdot t + d_j \cdot \text{PDO}(t).\end{aligned}$$

Compared to μ and σ , the shape parameter ξ generally requires a lot of data to produce accurate estimates and therefore is not used as a regression outcome here.

The NWS data represent a much larger and more heterogeneous geographic area. Together with the large gaps in this dataset, this would make a hierarchical model more challenging to establish. For this reason, and because the NWS trends are meant to serve as context for the SPU results, trends were estimated on the NWS data using maximum likelihood estimation of a non-hierarchical version of the model above.

RESULTS

IDF Values Using L-Moments Approach

Results of the IDF analysis for the SPU stations on a regional basis, expressed as a precipitation rate in inches per hour, are shown in Table 8 and Figure 47. As is typical with IDF curves, intensities are highest at shorter averaging durations. An IDF analysis using the NWS data is shown in Figure 48 and Table 9. At shorter return periods, or higher probabilities, the results from the NWS and SPU data are similar, but there is a divergence at return periods greater than 25 years.

The IDF values can also be reported at a station level, as shown in Figures 49 and 50, with intervals from 5 minutes to 1 hour, and from 6 hours to 7 days. Station-specific IDF values may be needed when a decision related to precipitation extremes needs to be made in specific geographic region, such as a modeling or design-related decision at a specific location.

Comparison of L-Moments and Bayesian Approaches for Stationary Models

Before examining the results of the trend analysis, the similarity of estimates between the L-moments and Bayesian approaches were verified. Figure 51 shows a comparison of the regional IDF values between the L-moments approach and the stationary version (i.e., not including PDO or time trend) of the Bayesian multilevel model. The point estimates are quite similar. The uncertainty in the estimates differs for several of the averaging durations at the longer periods, but this is likely attributed to differences in the regionalization scheme and uncertainty estimation between the models. In particular, the L-moments approach uses one ξ parameter for every site whereas the Bayesian method has the sites having separate ξ parameters that are related by a common regional distribution. One point of caution is what the very large uncertainty bounds can imply about the IDF curve; for example, the lower bound of the 7-day panel for the L-moments model in Figure 51 has a ξ sufficiently negative that the 50-year and 1,000-year events are approximately of the same magnitude. Figure 52 shows a similar figure for the individual sites' IDF relationships.

Time Trends in Extreme Values

Time trends are reported for different averaging periods based on the GEV model incorporating the variability of time and PDO (Figures 53 through 60). There is a positive slope with time for averaging durations and return frequencies. The range of the trend estimate (10th and 90th percent interval) increases for the longer return frequencies.

A comparison of the stationary model IDF estimates (using the L-moments approach above) with the trend model is shown in Figures 61 through 68. For most return periods, and over different averaging durations, the trend model supports a slightly higher intensity of rainfall than the stationary model. For a more nuanced comparison, the difference between the trend model and the stationary model is shown in Table 10, for the median, 25th and 75th percentile value of rainfall intensity. Table 11 presents the same information as a percentage change between the trend and stationary models. Over most of the range (55 of 64 values at the median level), the difference is positive, meaning the rainfall intensity is higher with the trend model. Importantly though, this is not true of all values, and, there is a difference in the range depending on the type of event being considered.

Parameters of Bayesian Regression Models

For many durations, the data are consistent with dependence on time and/or PDO because there is significant posterior probability mass for the linear regression parameters being non-zero. Said another way, there are cases in which the location parameter (μ , μ) and/or the scale parameter (σ , σ) have significant non-zero regression coefficients (Figures 69 through 76).

As discussed in the methods section, changes to μ and σ to first order (although the mean of the distribution also depends on σ) represent changes in average and variability of the distribution of the annual maximum series.

The shorter duration events (up to 1 hour) tend to have positive trends with PDO in both the location and the scale parameters. There is also more modest evidence of time trend in the location and scale parameters (Figures 69 through 72). The longer duration events tend to have negative relationships between PDO and the scale parameter. They tend to have positive trend in the location parameter (Figures 73 through 76).

DISCUSSION

The following are key discussion points based on the results of the analysis:

- The SPU 17-station quality-controlled data appear robust for the IDF analysis, with minimal need for additional data cleaning. There was no statistical basis for excluding any years or any stations from the overall analysis. The NWS data provided a useful complement to the SPU data, and were helpful in better evaluating the trends over time, because of their longer record.
- IDF curves were developed using the L-moments approach on a regional basis and on a station-specific basis. These values (referred to as the “stationary” values in the presentation of the results) can be used as is. The point estimates of the L-moments approach agree well with those of a stationary Bayesian multilevel model; the two approaches differ somewhat in their characterization of parameter uncertainty.
- The trend model results provide important additional insight into the changes in extremes over time, and should be considered directly or by extrapolating to a future period, assuming the trends continue as estimated to date. Extrapolated trends from these observed data records may be compared to estimates derived from climate models as part of future analysis being performed for SPU.
- Consistency in trend estimates in the NWS dataset between the period in which SPU data was observed and the period of complete record builds confidence that trend estimates are not strongly dependent on the timing of the SPU data.

- When the stationary IDF values were computed with the NWS data, the rainfall intensity values were comparable at shorter return periods, although there was a divergence at longer return periods. In these cases, the SPU-computed intensity was higher and may be considered more conservative.
- Precipitation trends at the SPU stations appear to be broadly consistent with location-specific studies based on observed data in the literature. In particular, the trend results seem generally consistent with other studies that found increases in extreme precipitation in Washington. The trend-based approach to the IDF analysis provides an alternative approach to consider extremes over a long-term horizon for CSO planning and design, in addition to obtaining estimates from downscaled global climate models.
- Differences in behavior of the return levels with respect to the covariates among different durations could be explained by differences in storm mechanisms driving those events. The differences in the estimates for the shape parameter between short- and long-duration events is further potential evidence of this.
- Another possible explanation is that building up longer duration events from 5-minute data could underestimate those events if they consist of smaller intensity rainfall spread over a longer duration. If there is collocated data collected using measurement techniques designed for longer durations, it would be possible to examine this hypothesis.
- The trend analysis of NWS data with the maximum likelihood model showed a more mixed collection of increasing and decreasing trends (Figures 77 to 80). In particular, increasing trends in precipitation were observed less consistently than for the SPU data. For example, 7 of 25 stations considered showed decreases in precipitation over the 1977-present time frame, the remained showed increases over this time. Several of the stations showed different signs of trend (positive and negative) for the full record versus the post-1977 record. These stations provide support to the idea that precipitation extremes may have increased, although it is clear that it is not a uniform phenomenon, over stations that represent a substantially larger degree of geographic and topographical variation than the SPU stations.
- For the vast majority of NWS stations with long, relatively complete records, the differences between trend estimates during the period of SPU data and during the entire record were minimal. One notable exception is the Sedro Woolley site for 1-day durations.

SUMMARY

This document provides an update of IDF curves for the City of Seattle given the most complete and up-to-date precipitation record available, using four decades of data from seventeen stations. Supporting analysis were performed using data from a set of regional stations operated by the National Weather Service; these data spanned a greater spatial and temporal extent than the SPU data.

An initial evaluation of annual extremes was used to make a determination on excluding individual storms because of their non-representative character. However, the data on annual maxima did not suggest unusual behavior in the data, and no data were excluded from the quality controlled data sets we worked with. All storms, including several large storms over the last 15 years, are used in the analysis presented here.

The 5-minute precipitation data, integrated to various other intervals, were used to develop the IDF curves by fitting the data to a standard probability distribution that is commonly used for developing IDF curves in the United States, the generalized extreme value (GEV) distribution. The parameter fit to this probability distribution was accomplished using two approaches, the L-moments method, which has been used in all prior work for SPU, and a Bayesian estimation method, that also allowed for the evaluation of time and other variables in the parameters of the GEV distribution. IDF curves were prepared for the entire region served by SPU (i.e., considering data from all 17 rain gauges), and for individual rain gauges.

IDF curves were developed using the L-moments approach on a regional basis and on a station-specific basis. These values can be used as is. The point estimates of the L-moments approach agree well with those of a stationary Bayesian multilevel model. However, the Bayesian approach also provided information on the trends in the rainfall extremes over the period of record.

The trend evaluation of GEV distribution parameters—after accounting for the variation of the oceanic phenomenon known as the Pacific Decadal Oscillation, known to affect precipitation in the Pacific Northwest—showed statistically significant positive trends in various metrics of extreme precipitation for the SPU stations. For example, given the matrix of 8X8, or 64 values that represent IDF curves for the SPU region, 55 (or 86%) indicate a statistically significant increase for the median estimate. For comparison, these trends were also calculated for NWS stations, many of which contain data over longer time periods. In general, a statistically significant positive trend is apparent at the majority (but not all) of stations with long data records, some extending over a century. The trends in the NWS stations are supportive of the findings for the SPU stations, but less clear because of the much larger geographic range and topographic variation in these stations.

The trends in the SPU station extremes, based on the large volume of underlying data, provide strong quantitative support for anticipated changes in precipitation extremes over future decades in the SPU region. The general concept of increasing precipitation extremes is indicated through global climate model analysis, but the changes computed here are based on observed, local data, and provide credible support for consideration of such trends in future planning for infrastructure design by SPU. The rates of change can be used as calculated in this work, by extrapolation into the future, or, as a bookend for increases computed through the results of downscaled global climate model results.

REFERENCES

- CH2M (2016) Seattle Public Utilities Combined Sewer Overflow Reduction Program: Precipitation Intensity, Duration, and Frequency Update, Draft Report.
- Cheng, L., and AghaKouchak, A. (2014). Nonstationary precipitation intensity-duration-frequency curves for infrastructure design in a changing climate. *Scientific reports*, 4.
- City of Seattle (2016) City Of Seattle Stormwater Manual, Appendix F Hydrologic Analysis and Design
- Easterling, D.R., K.E. Kunkel, J.R. Arnold, T. Knutson, A.N. LeGrande, L.R. Leung, R.S. Vose, D.E. Waliser, and M.F. Wehner, 2017: Precipitation change in the United States. In: Climate Science Special Report: Fourth National Climate Assessment, Volume I [Wuebbles, D.J., D.W. Fahey, K.A. Hibbard, D.J. Dokken, B.C. Stewart, and T.K. Maycock (eds.)]. U.S. Global Change Research Program, Washington, DC, USA, pp. 207-230, doi: 10.7930/J0H993CC.
- Hosking, J. R. M., and Wallis, J. R. (1997). *Regional frequency analysis: an approach based on L-moments*. Cambridge University Press.
- Mantua, N. J., S. R. Hare, Y. Zhang, J. M. Wallace, and R. C. Francis. 1997. A Pacific decadal climate oscillation with impacts on salmon. *Bulletin of the American Meteorological Society* 78:1069–1079.
- Mass, C., Skalenakis, A. and Warner, M., 2011. Extreme precipitation over the west coast of North America: Is there a trend? *Journal of Hydrometeorology*, 12(2), pp.310-318.
- Min, S.-K., X. Zhang, F. W. Zwiers, and G. C. Hegerl. 2011. Human contribution to more-intense precipitation extremes. *Nature* 470(7334):378-381. DOI: 10.1038/nature09763.
- National Oceanographic and Atmospheric Administration (NOAA) (2013). *Precipitation-Frequency Atlas of the United States*.
- Rosenberg, E.A., Keys, P.W., Booth, D.B., Hartley, D., Burkey, J., Steinemann, A.C. and Lettenmaier, D.P., 2010. Precipitation extremes and the impacts of climate change on stormwater infrastructure in Washington State. *Climatic Change*, 102(1), pp.319-349.
- The National Academies of Sciences, Engineering, and Medicine (National Academies). 2017. Review of the Draft Climate Science Special Report. Washington, DC: The National Academies Press. doi: <https://doi.org/10.17226/24712>.
- Warner, M.D., Mass, C.F. and Salathé Jr, E.P., 2012. Wintertime extreme precipitation events along the Pacific Northwest coast: Climatology and synoptic evolution. *Monthly Weather Review*, 140(7), pp.2021-2043.
- Zhang, X., H. Wan, F. W. Zwiers, G. C. Hegerl, and S.-K. Min. 2013. Attributing intensification of precipitation extremes to human influence. *Geophysical Research Letters* 40(19):5252-5257. DOI: 10.1002/grl.51010.

TABLES

Table 1. SPU Stations Used in Analysis

Station ID	Alternate ID in 2015 Stormwater Manual Table F.2	Station Name
RG01	45-S001	Haller Lake Shop
RG02	45-S002	Magnusson Park
RG03	45-S003	UW Hydraulics Lab
RG04	45-S004	Maple Leaf Reservoir
RG05	45-S005	Fauntleroy Ferry Dock
RG07	45-S007	Whitman Middle School
RG08	45-S008	Ballard Locks
RG09	45-S009	Woodland Park Zoo
RG10_30	45-S010 and RG-30	Rainier Ave Elementary (1978-2008); SPL Rainier Beach Branch (2009-2017)
RG11	45-S011	Metro-KC Denny Regulating
RG12	45-S012	Catherine Blaine Jr Elem School
RG14	45-S014	Lafayette Elementary School
RG15	45-S015	Puget Sound Clean Air Monitoring Station
RG16	45-S016	Metro-KC E Marginal Way
RG17	45-S017	West Seattle Reservoir Treatment Shop
RG18	45-S018	Aki Kurose Middle School
RG20_25	45-S020 and RG25	TT Minor Elementary (1978-2010); Garfield Community Center (2010-2017)

Table 2. Completeness Statistics for SPU Data

Site	Start	End	N Missing	N Total ^a	Percent Missing
RG01	1976-09-01 00:05:00	2017-04-30 23:55:00	0	4,277,375	0%
RG02	1976-09-01 00:05:00	2017-04-30 23:55:00	4	4,277,375	9.4e-05%
RG03	1976-09-01 00:05:00	2017-04-30 23:55:00	6	4,277,375	0.00014%
RG04	1976-09-01 00:05:00	2017-04-30 23:55:00	1	4,277,375	2.3e-05%
RG05	1976-09-01 00:05:00	2017-04-30 23:55:00	5	4,277,375	0.00012%
RG07	1976-09-01 00:05:00	2017-04-30 23:55:00	3	4,277,375	7e-05%
RG08	1976-09-01 00:05:00	2017-04-30 23:55:00	4	4,277,375	9.4e-05%
RG09	1976-09-01 00:05:00	2017-04-30 23:55:00	5	4,277,375	0.00012%
RG10 30	1976-09-01 00:05:00	2017-04-30 23:55:00	6	4,277,375	0.00014%
RG11	1976-09-01 00:05:00	2017-04-30 23:55:00	6	4,277,375	0.00014%
RG12	1976-09-01 00:05:00	2017-04-30 23:55:00	5	4,277,375	0.00012%
RG14	1976-09-01 00:05:00	2017-04-30 23:55:00	4	4,277,375	9.4e-05%
RG15	1976-09-01 00:05:00	2017-04-30 23:55:00	2	4,277,375	4.7e-05%
RG16	1976-09-01 00:05:00	2017-04-30 23:55:00	6	4,277,375	0.00014%
RG17	1976-09-01 00:05:00	2017-04-30 23:55:00	8	4,277,375	0.00019%
RG18	1976-09-01 00:05:00	2017-04-30 23:55:00	5	4,277,375	0.00012%
RG20 25	1976-09-01 00:05:00	2017-04-30 23:55:00	6	4,277,375	0.00014%

a. Total number of values is based on number of 5-minute periods possible between start and end of observed data at each station. Missing values are primarily associated with original dataset ending slightly before October 1, 2016.

Table 3. Completeness Statistics for NWS Data

Site	Start	End	N Missing	N Total ^a	Percent Missing
Anacortes-Daily	1892-09-01	2015-11-30	2,841	45,015	6.3%
Arlington-Daily	1922-12-01	2015-12-27	4,137	33,995	12%
Bellingham 3 SSW-Daily	1985-08-01	2015-12-27	36	11,106	0.32%
Bellingham Intl. AP-Daily	1949-01-01	2015-12-29	866	24,469	3.5%
Blaine-Daily	1893-10-01	2015-12-28	5,415	44,648	12%
Bremerton-Daily	1899-05-01	2015-12-30	3,344	42,612	7.8%
Buckley 1NE-Daily	1913-01-01	2012-04-15	863	36,265	2.4%
Centralia 1W-Daily	1950-10-03	2000-12-13	14,284	18,335	78%
Centralia-Daily	1893-01-01	2015-12-27	4,810	44,920	11%
Chimacum 4S-Daily	1926-10-01	2015-11-30	300	32,568	0.92%
Coupeville 1S-Daily	1895-11-01	2015-11-30	5,059	43,859	12%
Everett-Daily	1894-09-01	2015-12-30	8,055	44,315	18%
Kent-Daily	1912-04-01	2015-12-29	3,816	37,893	10%
Landsburg	1903-04-01	2015-12-24	2,317	41,176	5.6%
Longview	1925-07-01	2015-11-30	638	33,025	1.9%
Mc Millin Resv.	1941-03-01	2015-12-30	512	27,333	1.9%
Monroe-Daily	1929-02-01	2015-12-28	1,464	31,742	4.6%
Mt. Vernon-Daily	1956-01-01	2005-01-31	372	17,929	2.1%
Olympia AP	1948-01-01	2015-12-29	3	24,835	0.012%
SEA Sand Pnt WSFO	1986-10-01	2015-12-30	529	10,683	5%
SEA-TAC-Daily	1945-01-01	2015-12-29	3	25,930	0.012%
Seattle Boeing Fld	1948-01-02	2016-01-17	12,131	24,853	49%
Sedro Woolley-Daily	1896-08-01	2015-11-30	1,904	43,585	4.4%
Snoqualmie Falls	1898-10-01	2015-12-28	1,498	42,822	3.5%
Tacoma #1-Daily	1982-03-01	2015-12-29	352	12,357	2.8%
Tacoma Narrows AP-Daily	1999-01-09	2015-12-29	32	6,199	0.52%

a. Total number of values is based on number of 1-day periods possible between start and end of observed data at each station.

Table 4. Recent Annual Maxima for SPU 5-Minute Data

Site	Maximum Recorded 5-Minute Rainfall Depth (inches)										
	2007	2008	2009	2010	2011	2012	2013	2014	2015	2016	2017
RG01	0.09	0.08	0.1	0.11	0.09	0.1	0.17	0.14	0.1	0.13	0.1
RG02	0.12	0.12	0.13	0.09	0.1	0.14	0.12	0.31	0.17	0.08	0.1
RG03	0.15	0.09	0.11	0.14	0.12	0.11	0.17	0.11	0.27	0.12	0.11
RG04	0.12	0.07	0.07	0.16	0.11	0.1	0.14	0.18	0.13	0.12	0.12
RG05	0.14	0.12	0.09	0.18	0.1	0.12	0.13	0.1	0.21	0.12	0.18
RG07	0.12	0.16	0.07	0.2	0.14	0.14	0.14	0.14	0.14	0.12	0.16
RG08	0.12	0.13	0.12	0.11	0.16	0.09	0.25	0.09	0.16	0.12	0.07
RG09	0.12	0.07	0.1	0.09	0.13	0.08	0.21	0.11	0.16	0.1	0.07
RG10 30	0.19	0.1	0.16	0.11	0.11	0.11	0.2	0.12	0.14	0.08	0.1
RG11	0.14	0.08	0.09	0.09	0.11	0.11	0.14	0.3	0.2	0.11	0.13
RG12	0.14	0.11	0.18	0.14	0.11	0.21	0.25	0.12	0.21	0.11	0.1
RG14	0.12	0.1	0.12	0.12	0.09	0.12	0.09	0.13	0.13	0.23	0.09
RG15	0.12	0.08	0.09	0.11	0.09	0.08	0.11	0.1	0.15	0.08	0.1
RG16	0.19	0.1	0.09	0.11	0.09	0.12	0.21	0.12	0.06	0.08	0.11
RG17	0.14	0.12	0.12	0.08	0.12	0.17	0.25	0.09	0.06	0.08	0.13
RG18	0.1	0.1	0.12	0.09	0.1	0.14	0.29	0.13	0.14	0.08	0.11
RG20 25	0.21	0.09	0.14	0.11	0.16	0.15	0.12	0.15	0.14	0.15	0.13

Darker-colored cells indicate greater rainfall depth.

Table 5. Recent Annual Maxima for SPU 1-Hour Data

Site	Maximum Recorded 1-Hour Rainfall Depth (inches)										
	2007	2008	2009	2010	2011	2012	2013	2014	2015	2016	2017
RG01	0.34	0.49	0.42	0.54	0.35	0.31	0.59	0.34	0.5	0.6	0.38
RG02	0.39	0.41	0.55	0.46	0.34	0.34	0.62	0.62	0.44	0.34	0.33
RG03	0.64	0.41	0.65	0.38	0.31	0.31	0.61	0.36	1.18	0.36	0.31
RG04	0.39	0.46	0.35	0.39	0.33	0.34	0.48	0.38	0.49	0.45	0.34
RG05	0.66	0.53	0.44	0.37	0.32	0.26	0.46	0.37	0.9	0.39	0.3
RG07	0.33	0.46	0.46	0.44	0.39	0.67	0.6	0.33	0.66	0.51	0.55
RG08	0.48	0.42	0.39	0.5	0.39	0.28	0.56	0.32	0.72	0.49	0.3
RG09	0.31	0.46	0.45	0.39	0.37	0.37	0.52	0.36	0.72	0.45	0.33
RG10 30	0.53	0.53	0.51	0.58	0.36	0.37	0.44	0.54	0.44	0.41	0.39
RG11	0.49	0.44	0.44	0.37	0.4	0.29	0.54	0.73	0.69	0.32	0.47
RG12	0.34	0.45	0.39	0.42	0.46	0.56	0.56	0.39	0.65	0.47	0.36
RG14	0.54	0.47	0.39	0.79	0.42	0.3	0.48	0.48	0.42	0.38	0.35
RG15	0.54	0.45	0.4	0.48	0.34	0.25	0.53	0.37	0.58	0.28	0.31
RG16	0.61	0.47	0.43	0.58	0.4	0.31	0.43	0.33	0.43	0.41	0.39
RG17	0.66	0.47	0.54	0.51	0.31	1.01	0.43	0.34	0.43	0.37	0.38
RG18	0.47	0.53	0.46	0.43	0.46	0.43	0.41	0.35	0.44	0.39	0.38
RG20 25	0.92	0.51	0.4	0.43	0.31	0.33	0.57	0.61	0.49	0.5	0.53

Darker-colored cells indicate greater rainfall depth.

Table 6. Recent Annual Maxima for SPU 1-Day Data

Site	Maximum Recorded 1-Day Rainfall Depth (inches)										
	2007	2008	2009	2010	2011	2012	2013	2014	2015	2016	2017
RG01	1.51	5.17	1.55	1.85	3.15	2.39	3.18	1.55	2.32	2.3	2.44
RG02	1.68	4.84	1.37	1.6	3.17	1.95	2.51	1.75	2.14	1.75	2.42
RG03	1.81	4.84	1.49	1.53	3.44	2.14	2.79	1.61	2.4	1.87	2.31
RG04	1.68	5.18	1.37	1.84	3.33	2.42	2.56	1.49	2.06	1.97	2.31
RG05	2.05	4.8	2.17	1.47	3.26	2.16	2.93	1.57	2.55	1.83	2.48
RG07	1.45	5.01	1.64	1.73	3.4	2.49	3.18	1.59	2.68	2.41	2.48
RG08	1.74	4.7	1.58	1.64	3.5	2.05	2.94	1.54	2.24	2.18	2.25
RG09	1.6	5.18	1.62	1.88	3.89	2.42	2.94	1.77	2.41	2.24	2.43
RG10 30	3.44	4.18	2.01	1.79	3.85	2.24	2.67	1.72	2.3	1.91	2.33
RG11	1.8	4.91	1.7	1.48	3.43	1.88	2.68	1.71	2.57	2	2.39
RG12	1.66	5.61	1.84	1.66	3.57	2.26	2.92	1.78	2.56	2.3	2.49
RG14	1.64	5.28	2.09	1.53	4.01	2.41	3.11	1.77	2.84	2.07	2.54
RG15	1.64	4.79	1.75	1.6	3.53	2.13	2.78	1.63	2.64	1.91	2.45
RG16	2.69	5.04	2.08	1.79	3.88	2.21	2.72	1.79	2.37	1.91	2.33
RG17	2.69	5.04	2.22	1.58	3.62	2.29	2.78	1.77	2.37	1.79	2.31
RG18	2.66	4.43	2.01	1.81	3.67	2.29	2.79	1.77	2.47	2	2.33
RG20 25	2.13	4.72	1.78	1.52	3.2	2.01	2.61	1.77	2.81	2.07	2.33

Darker-colored cells indicate greater rainfall depth.

Table 7. Recent Annual Maxima for NWS 1-Day Data (depth, inches)

Site	Maximum Recorded 1-Day Rainfall Depth (inches)									
	2007	2008	2009	2010	2011	2012	2013	2014	2015	
Anacortes-Daily	1.7	1.2	NA	1.7	2	1.1	NA	1	NA	
Arlington-Daily	1.8	1.6	2	2.2	1.7	3.4	1.9	1.4	2.9	
Bellingham 3 SSW-Daily	2.6	1.5	2.2	3.1	2.5	1.7	1.3	1.2	2.9	
Bellingham Intl. AP-Daily	2	1.1	1.7	1.2	1.8	1.2	NA	1.3	1.4	
Blaine-Daily	2.1	2.7	1.6	1.4	2.4	1.8	2.2	4	2.2	
Bremerton-Daily	2.7	8.5	3.6	2.5	6.2	4.7	2.9	2.4	1.9	
Buckley 1NE-Daily	5.8	NA	2.6	1.4	1.8	NA	NA	NA	NA	
Centralia-Daily	3.9	3.2	2.8	2.9	1.9	2.2	2	0.97	1.7	
Chimacum 4S-Daily	1.7	2.3	0.98	1.9	1.6	2.3	1.9	1.5	1.7	
Coupeville 1S-Daily	1.2	0.91	1.4	1.8	1.4	1.1	1.4	0.87	1.2	
Everett-Daily	1.6	2.8	1.4	2	1.4	2.5	1.7	1.4	1.7	
Kent-Daily	3.7	2.5	2.5	1.9	2.5	1.6	NA	NA	NA	
Landsburg	4.5	2.8	3.3	2.2	2.2	2.4	2.2	2.1	1.7	
Longview	4.6	3.2	3.9	1.3	2.8	2.2	NA	NA	1.6	
Mc Millin Resv.	4.1	2.4	2.8	1.6	2.2	1.8	NA	NA	NA	
Monroe-Daily	2.1	4.4	2.7	NA	2.7	2.3	2.3	2.1	1.9	
Mt. Vernon-Daily	NA	NA	NA	NA	NA	NA	NA	NA	NA	
Olympia AP	4.9	3.6	5.4	1.9	2.1	3.1	3.3	2	2.8	

Site	Maximum Recorded 1-Day Rainfall Depth (inches)								
	2007	2008	2009	2010	2011	2012	2013	2014	2015
SEA-TAC-Daily	3.7	4.3	2.6	1.7	2.5	2	2.4	2.1	2.5
SEA Sand Pnt WSFO	2.4	4.7	1.3	1.3	2.5	2.1	2.9	1.6	2.5
Seattle Boeing Fld	2.4	4.5	1.7	1.2	2.5	2.1	2.8	1.6	2.8
Sedro Woolley-Daily	1.5	1.7	2.9	2.9	3.6	3.1	1.8	2.4	3.6
Snoqualmie Falls	2.8	3.6	3.1	NA	NA	NA	NA	2.3	2.3
Tacoma #1-Daily	3	2.8	3.1	1.2	2.2	5.3	2.3	2.9	1.9
Tacoma Narrows AP-Daily	3.8	2.5	3.8	1.7	1.7	2.7	2.5	2.2	1.7

Darker-colored cells indicate greater rainfall depth.

Table 8. Regional L-Moment IDF Values for SPU Data

Duration	Intensity (inches per hour)							
	2-yr	5-yr	10-yr	25-yr	50-yr	100-yr	500-yr	1000-yr
5.0 minutes	1.3400	1.7900	2.1100	2.5400	2.8800	3.2300	4.1200	4.5400
15.0 minutes	0.8170	1.0900	1.2800	1.5400	1.7400	1.9600	2.5000	2.7600
30.0 minutes	0.5560	0.7310	0.8590	1.0400	1.1800	1.3400	1.7600	1.9600
1.0 hours	0.3910	0.5000	0.5780	0.6820	0.7650	0.8510	1.0700	1.1700
6.0 hours	0.1680	0.2210	0.2590	0.3100	0.3500	0.3920	0.4970	0.5470
1.0 days	0.0828	0.1120	0.1350	0.1680	0.1960	0.2280	0.3160	0.3620
3.0 days	0.0416	0.0538	0.0621	0.0729	0.0812	0.0897	0.1100	0.1190
7.0 days	0.0261	0.0324	0.0359	0.0395	0.0418	0.0437	0.0473	0.0485

Source: Hosking and Wallis, 1997

Table 9. Regional L-Moment IDF Values for NWS Data

Duration	Intensity (inches per hour)							
	2-yr	5-yr	10-yr	25-yr	50-yr	100-yr	500-yr	1000-yr
1.0 days	0.0833	0.1080	0.126	0.1500	0.1680	0.1880	0.2380	0.2610
3.0 days	0.0457	0.0584	0.067	0.0782	0.0867	0.0953	0.1160	0.1250
7.0 days	0.0287	0.0361	0.041	0.0470	0.0514	0.0557	0.0656	0.0697

Note: Heterogeneity test indicates a subset of stations may be more appropriate for NWS data.

Table 10. Stationary and Trend Intensity Return Levels Using Posterior 25th, 50th, and 75th Percentiles

Duration	Frequency	25 th Percentile		Median		75 th Percentile	
		Stationary	Trend	Stationary	Trend	Stationary	Trend
5.0 minutes	2-yr	1.3300	1.3300	1.3400	1.3500	1.3600	1.3800
	5-yr	1.7800	1.7900	1.8000	1.8200	1.8200	1.8700
	10-yr	2.0900	2.1100	2.1100	2.1600	2.1500	2.2100
	25-yr	2.4900	2.5200	2.5400	2.6000	2.5900	2.6800
	50-yr	2.8000	2.8500	2.8700	2.9400	2.9300	3.0500
	100-yr	3.1100	3.1700	3.2000	3.3000	3.3000	3.4400
	500-yr	3.8700	3.9800	4.0400	4.1900	4.2200	4.4200
	1000-yr	4.2100	4.3400	4.4200	4.6000	4.6600	4.9000
15.0 minutes	2-yr	0.8130	0.8240	0.8220	0.8380	0.8310	0.8530
	5-yr	1.0800	1.1100	1.0900	1.1300	1.1000	1.1500
	10-yr	1.2700	1.3000	1.2800	1.3300	1.3000	1.3600
	25-yr	1.5100	1.5500	1.5300	1.5900	1.5600	1.6400
	50-yr	1.6900	1.7400	1.7300	1.8000	1.7700	1.8600
	100-yr	1.8800	1.9400	1.9300	2.0100	1.9900	2.0900
	500-yr	2.3400	2.4100	2.4400	2.5300	2.5600	2.6700
	1000-yr	2.5400	2.6200	2.6800	2.7700	2.8200	2.9500
30.0 minutes	2-yr	0.5490	0.5660	0.5550	0.5760	0.5610	0.5850
	5-yr	0.7220	0.7420	0.7310	0.7570	0.7400	0.7700
	10-yr	0.8470	0.8700	0.8610	0.8890	0.8750	0.9110
	25-yr	1.0200	1.0400	1.0400	1.0700	1.0700	1.1100
	50-yr	1.1600	1.1900	1.1900	1.2300	1.2300	1.2700
	100-yr	1.3000	1.3400	1.3500	1.3900	1.4000	1.4500
	500-yr	1.6800	1.7200	1.7700	1.8300	1.8800	1.9400
	1000-yr	1.8700	1.9100	1.9800	2.0400	2.1200	2.1900
1.0 hours	2-yr	0.3870	0.3920	0.3910	0.3980	0.3940	0.4040
	5-yr	0.4950	0.5020	0.5000	0.5100	0.5050	0.5180
	10-yr	0.5720	0.5790	0.5790	0.5900	0.5870	0.6010
	25-yr	0.6740	0.6830	0.6870	0.6990	0.6990	0.7170
	50-yr	0.7550	0.7660	0.7730	0.7870	0.7900	0.8110
	100-yr	0.8380	0.8500	0.8640	0.8800	0.8890	0.9120
	500-yr	1.0500	1.0600	1.1000	1.1200	1.1500	1.1800
	1000-yr	1.1500	1.1600	1.2100	1.2300	1.2700	1.3100
6.0 hours	2-yr	0.1670	0.1750	0.1690	0.1770	0.1710	0.1800
	5-yr	0.2190	0.2260	0.2220	0.2300	0.2240	0.2330
	10-yr	0.2550	0.2610	0.2590	0.2660	0.2630	0.2710
	25-yr	0.3030	0.3060	0.3090	0.3130	0.3150	0.3220
	50-yr	0.3400	0.3400	0.3490	0.3510	0.3570	0.3610
	100-yr	0.3770	0.3750	0.3900	0.3890	0.4010	0.4020
	500-yr	0.4690	0.4560	0.4910	0.4810	0.5140	0.5040
	1000-yr	0.5100	0.4930	0.5390	0.5220	0.5690	0.5530
1.0 days	2-yr	0.0823	0.0854	0.0830	0.0869	0.0837	0.0883
	5-yr	0.1110	0.1140	0.1130	0.1160	0.1140	0.1180

Duration	Frequency	25 th Percentile		Median		75 th Percentile	
		Stationary	Trend	Stationary	Trend	Stationary	Trend
	10-yr	0.1330	0.1350	0.1350	0.1380	0.1370	0.1410
	25-yr	0.1640	0.1640	0.1680	0.1690	0.1720	0.1750
	50-yr	0.1900	0.1880	0.1960	0.1950	0.2010	0.2030
	100-yr	0.2180	0.2150	0.2270	0.2240	0.2350	0.2340
	500-yr	0.2960	0.2840	0.3120	0.3000	0.3310	0.3220
	1000-yr	0.3340	0.3190	0.3570	0.3400	0.3830	0.3680
3.0 days	2-yr	0.0412	0.0434	0.0416	0.0440	0.0419	0.0447
	5-yr	0.0534	0.0556	0.0539	0.0564	0.0544	0.0573
	10-yr	0.0614	0.0633	0.0622	0.0645	0.0629	0.0657
	25-yr	0.0715	0.0727	0.0727	0.0746	0.0739	0.0764
	50-yr	0.0790	0.0795	0.0806	0.0820	0.0823	0.0842
	100-yr	0.0865	0.0860	0.0885	0.0892	0.0909	0.0920
	500-yr	0.1030	0.1010	0.1070	0.1050	0.1110	0.1100
7.0 days	1000-yr	0.1110	0.1070	0.1150	0.1120	0.1210	0.1180
	2-yr	0.0254	0.0262	0.0256	0.0266	0.0258	0.0270
	5-yr	0.0318	0.0326	0.0321	0.0330	0.0323	0.0335
	10-yr	0.0354	0.0361	0.0358	0.0366	0.0360	0.0372
	25-yr	0.0393	0.0397	0.0397	0.0405	0.0401	0.0413
	50-yr	0.0418	0.0421	0.0423	0.0430	0.0427	0.0439
	100-yr	0.0439	0.0440	0.0445	0.0451	0.0451	0.0463
	500-yr	0.0478	0.0477	0.0487	0.0493	0.0497	0.0507
1000-yr	0.0491	0.0489	0.0502	0.0507	0.0514	0.0522	

Table 11. Percent Change from Stationary to Trend Model Intensity Return Levels for Posterior 25th, 50th, and 75th Percentiles

Duration	Frequency	25 th Percentile	Median (q50)	75 th Percentile
5.0 minutes	2-yr	0%	0.746%	1.47%
	5-yr	0.562%	1.11%	2.75%
	10-yr	0.957%	2.37%	2.79%
	25-yr	1.2%	2.36%	3.47%
	50-yr	1.79%	2.44%	4.1%
	100-yr	1.93%	3.12%	4.24%
	500-yr	2.84%	3.71%	4.74%
	1000-yr	3.09%	4.07%	5.15%
15.0 minutes	2-yr	1.35%	1.95%	2.65%
	5-yr	2.78%	3.67%	4.55%
	10-yr	2.36%	3.91%	4.62%
	25-yr	2.65%	3.92%	5.13%
	50-yr	2.96%	4.05%	5.08%
	100-yr	3.19%	4.15%	5.03%
	500-yr	2.99%	3.69%	4.3%
	1000-yr	3.15%	3.36%	4.61%
30.0 minutes	2-yr	3.1%	3.78%	4.28%
	5-yr	2.77%	3.56%	4.05%
	10-yr	2.72%	3.25%	4.11%

Duration	Frequency	25 th Percentile	Median (q50)	75 th Percentile
	25-yr	1.96%	2.88%	3.74%
	50-yr	2.59%	3.36%	3.25%
	100-yr	3.08%	2.96%	3.57%
	500-yr	2.38%	3.39%	3.19%
	1000-yr	2.14%	3.03%	3.3%
1.0 hours	2-yr	1.29%	1.79%	2.54%
	5-yr	1.41%	2%	2.57%
	10-yr	1.22%	1.9%	2.39%
	25-yr	1.34%	1.75%	2.58%
	50-yr	1.46%	1.81%	2.66%
	100-yr	1.43%	1.85%	2.59%
	500-yr	0.952%	1.82%	2.61%
	1000-yr	0.87%	1.65%	3.15%
6.0 hours	2-yr	4.79%	4.73%	5.26%
	5-yr	3.2%	3.6%	4.02%
	10-yr	2.35%	2.7%	3.04%
	25-yr	0.99%	1.29%	2.22%
	50-yr	0%	0.573%	1.12%
	100-yr	-0.531%	-0.256%	0.249%
	500-yr	-2.77%	-2.04%	-1.95%
	1000-yr	-3.33%	-3.15%	-2.81%
1.0 days	2-yr	3.77%	4.7%	5.5%
	5-yr	2.7%	2.65%	3.51%
	10-yr	1.5%	2.22%	2.92%
	25-yr	0%	0.595%	1.74%
	50-yr	-1.05%	-0.51%	0.995%
	100-yr	-1.38%	-1.32%	-0.426%
	500-yr	-4.05%	-3.85%	-2.72%
	1000-yr	-4.49%	-4.76%	-3.92%
3.0 days	2-yr	5.34%	5.77%	6.68%
	5-yr	4.12%	4.64%	5.33%
	10-yr	3.09%	3.7%	4.45%
	25-yr	1.68%	2.61%	3.38%
	50-yr	0.633%	1.74%	2.31%
	100-yr	-0.578%	0.791%	1.21%
	500-yr	-1.94%	-1.87%	-0.901%
	1000-yr	-3.6%	-2.61%	-2.48%
7.0 days	2-yr	3.15%	3.91%	4.65%
	5-yr	2.52%	2.8%	3.72%
	10-yr	1.98%	2.23%	3.33%
	25-yr	1.02%	2.02%	2.99%
	50-yr	0.718%	1.65%	2.81%
	100-yr	0.228%	1.35%	2.66%
	500-yr	-0.209%	1.23%	2.01%
	1000-yr	-0.407%	0.996%	1.56%

FIGURES

Source: City of Seattle Stormwater Manual, January 2016

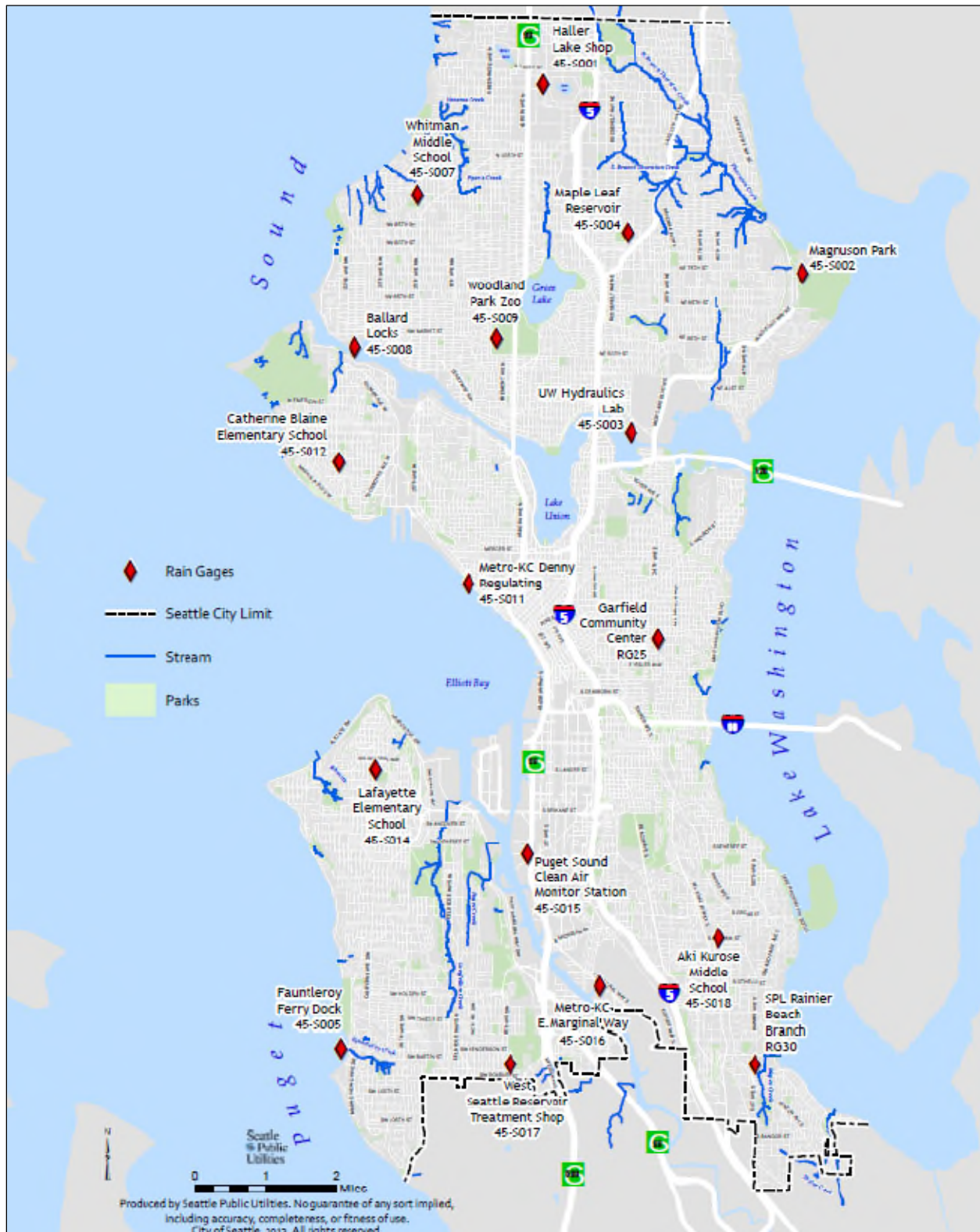


Figure 1. Active Rain Gauges in the SPU Network

Source: CH2M, 2016

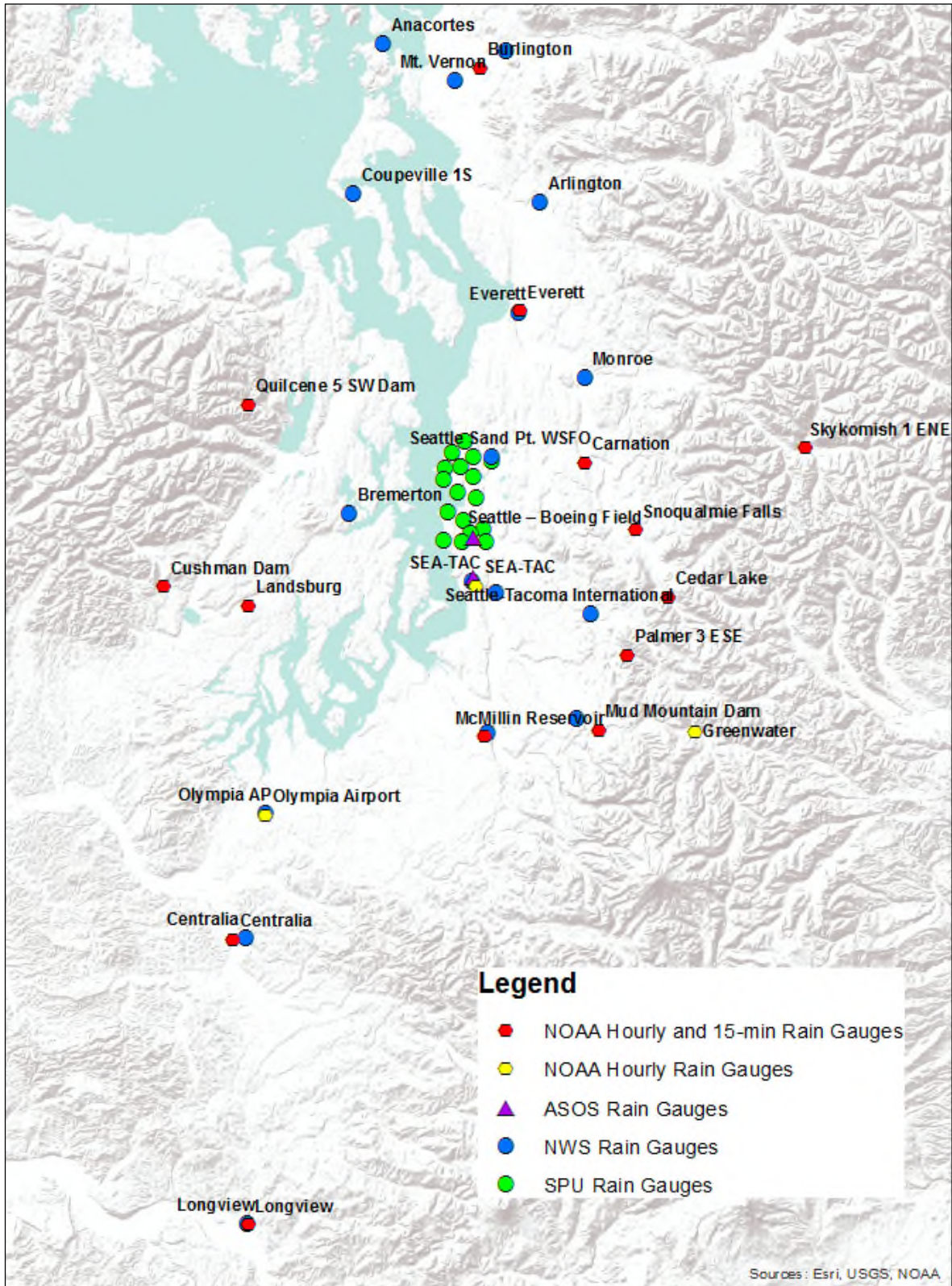
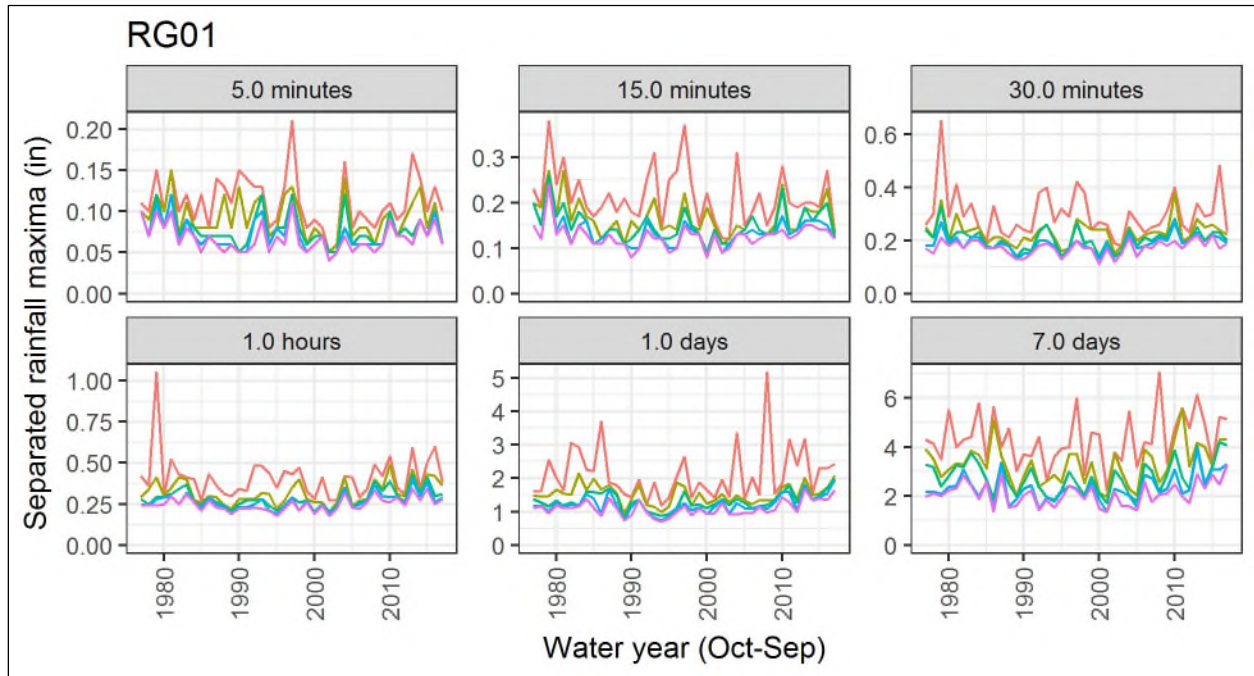
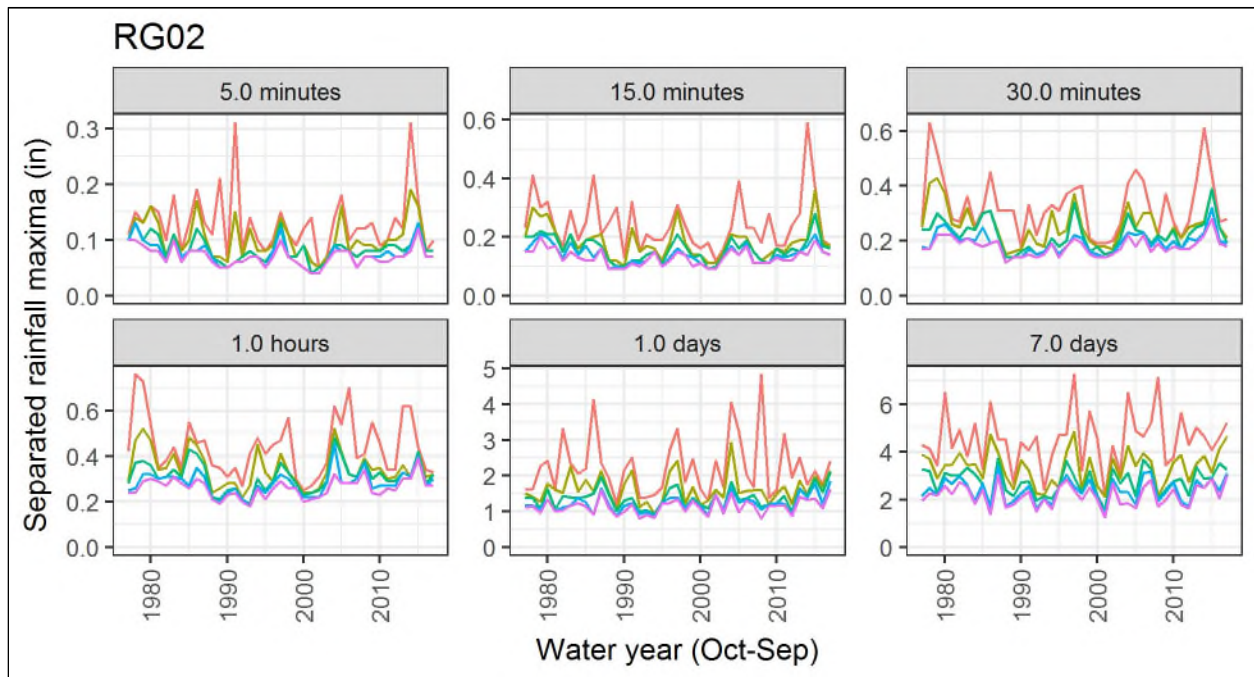


Figure 2. NWS Gauge Locations Reviewed for the Project (SPU gauges shown for comparison)



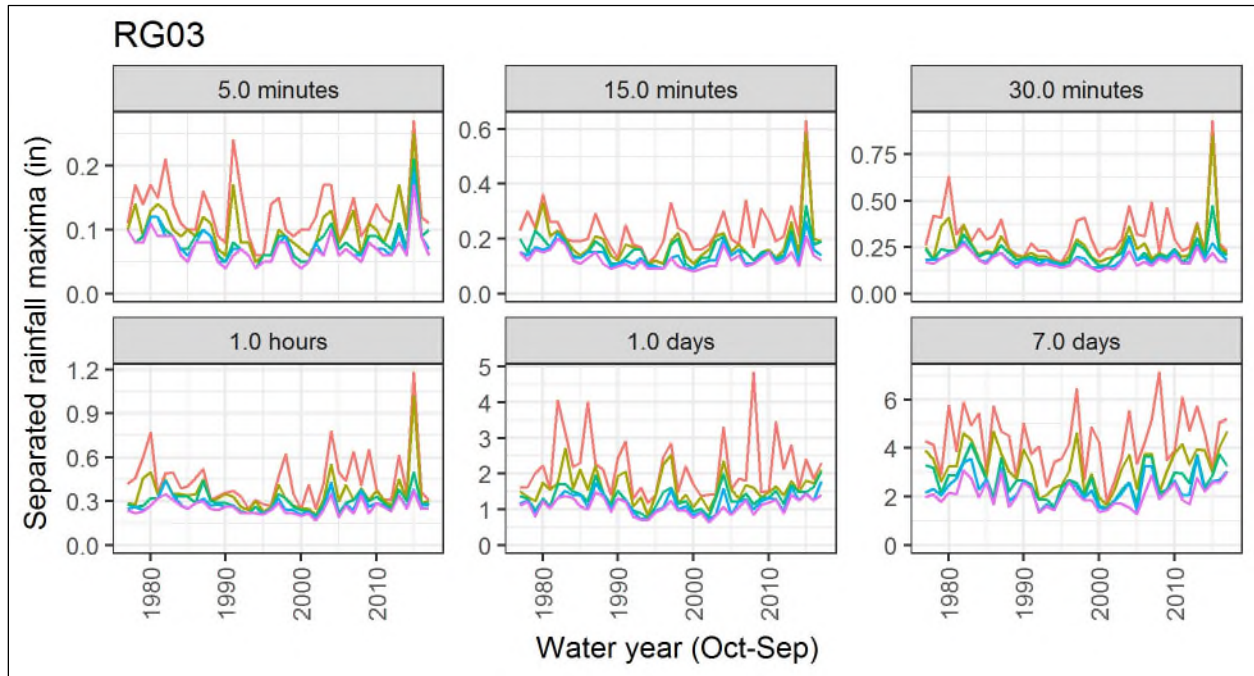
Different colored lines distinguish top 5 values in each water year (separated by at least the length of the relevant duration).

Figure 3. Time Series of Annual Maxima of Rainfall Depth for SPU Site RG01



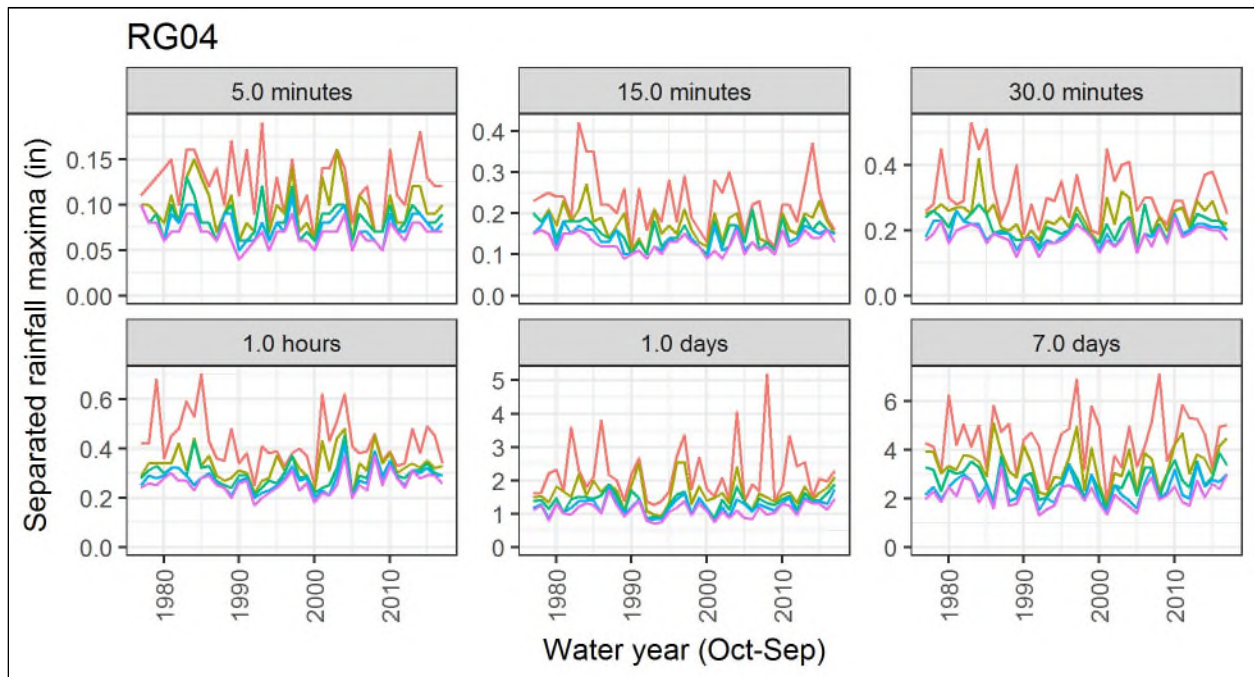
Different colored lines distinguish top 5 values in each water year (separated by at least the length of the relevant duration).

Figure 4. Time Series of Annual Maxima of Rainfall Depth for SPU Site RG02



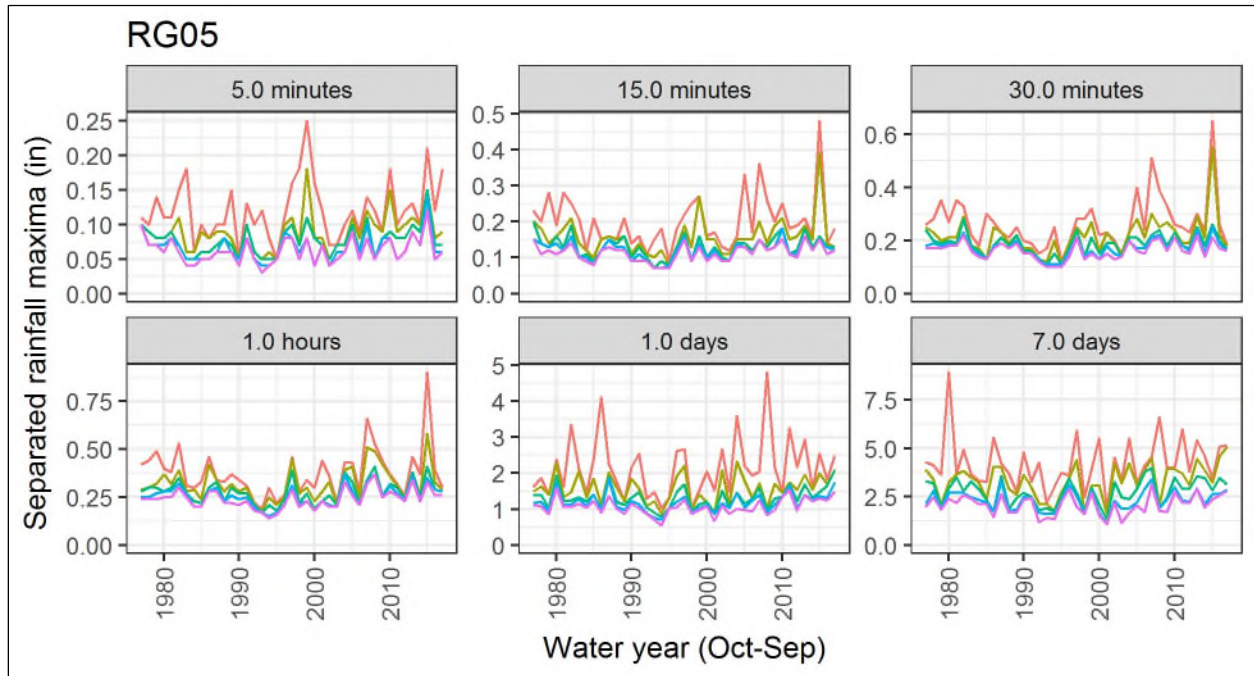
Different colored lines distinguish top 5 values in each water year (separated by at least the length of the relevant duration).

Figure 5. Time Series of Annual Maxima of Rainfall Depth for SPU Site RG03



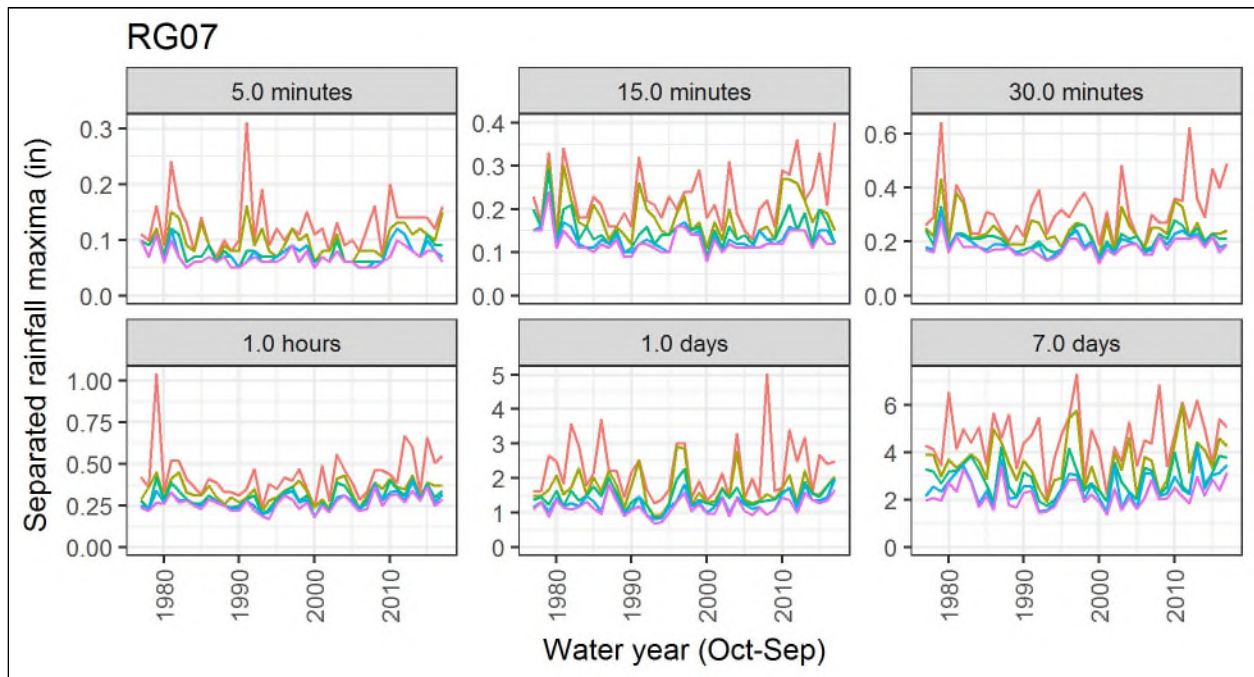
Different colored lines distinguish top 5 values in each water year (separated by at least the length of the relevant duration).

Figure 6. Time Series of Annual Maxima of Rainfall Depth for SPU Site RG04



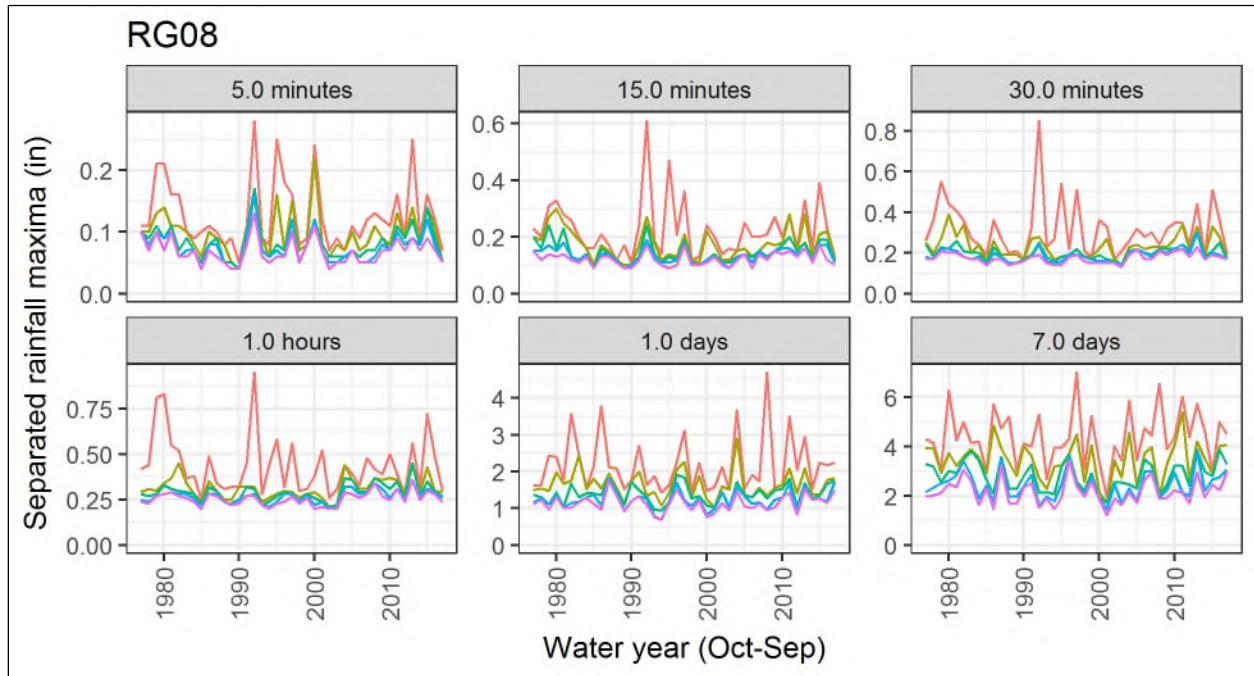
Different colored lines distinguish top 5 values in each water year (separated by at least the length of the relevant duration).

Figure 7. Time Series of Annual Maxima of Rainfall Depth for SPU Site RG05



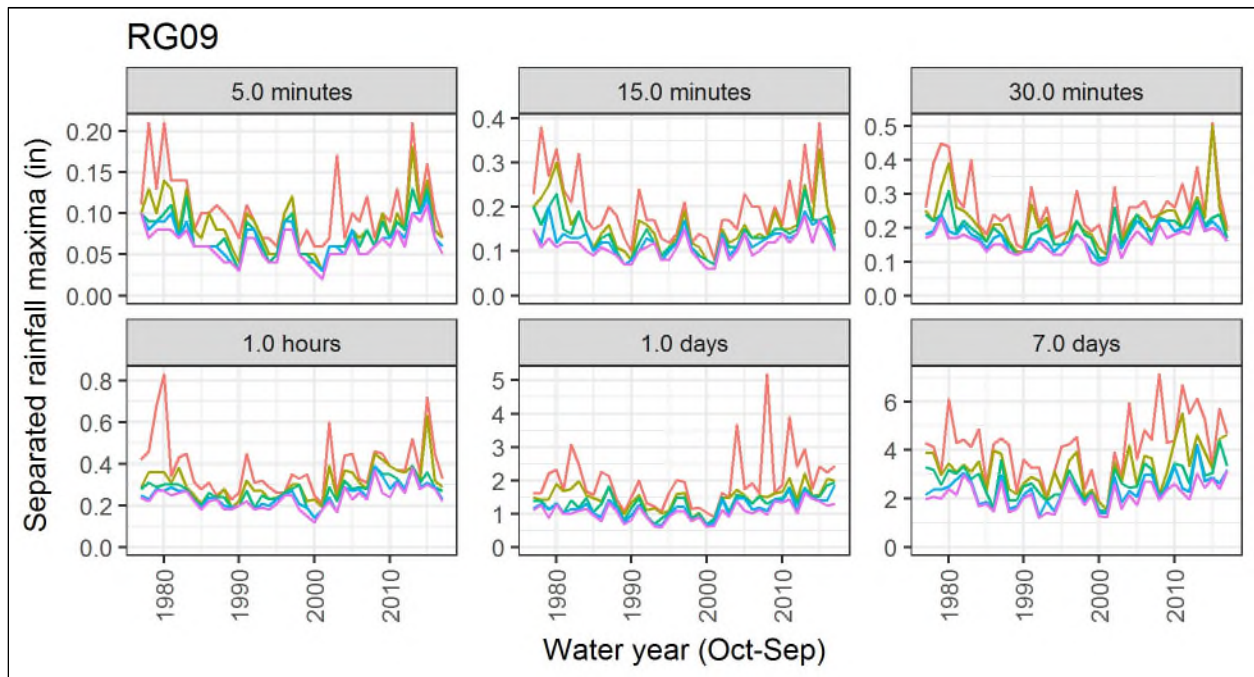
Different colored lines distinguish top 5 values in each water year (separated by at least the length of the relevant duration).

Figure 8. Time Series of Annual Maxima of Rainfall Depth for SPU Site RG07



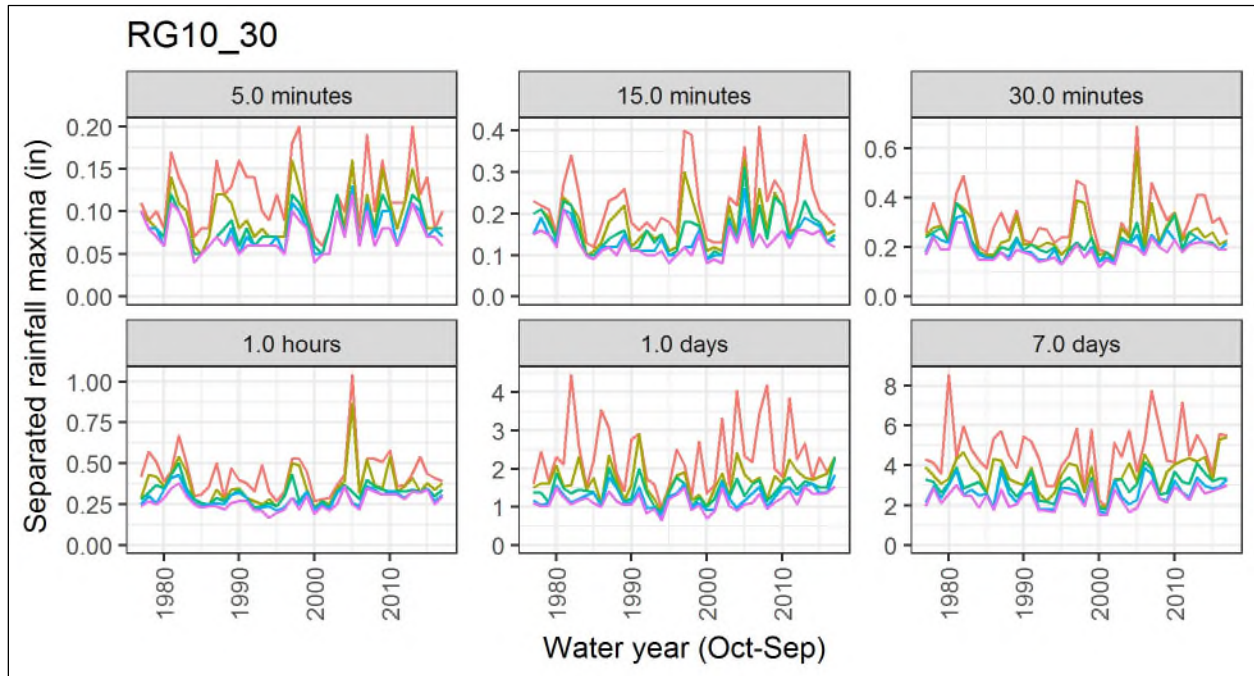
Different colored lines distinguish top 5 values in each water year (separated by at least the length of the relevant duration).

Figure 9. Time Series of Annual Maxima of Rainfall Depth for SPU Site RG08



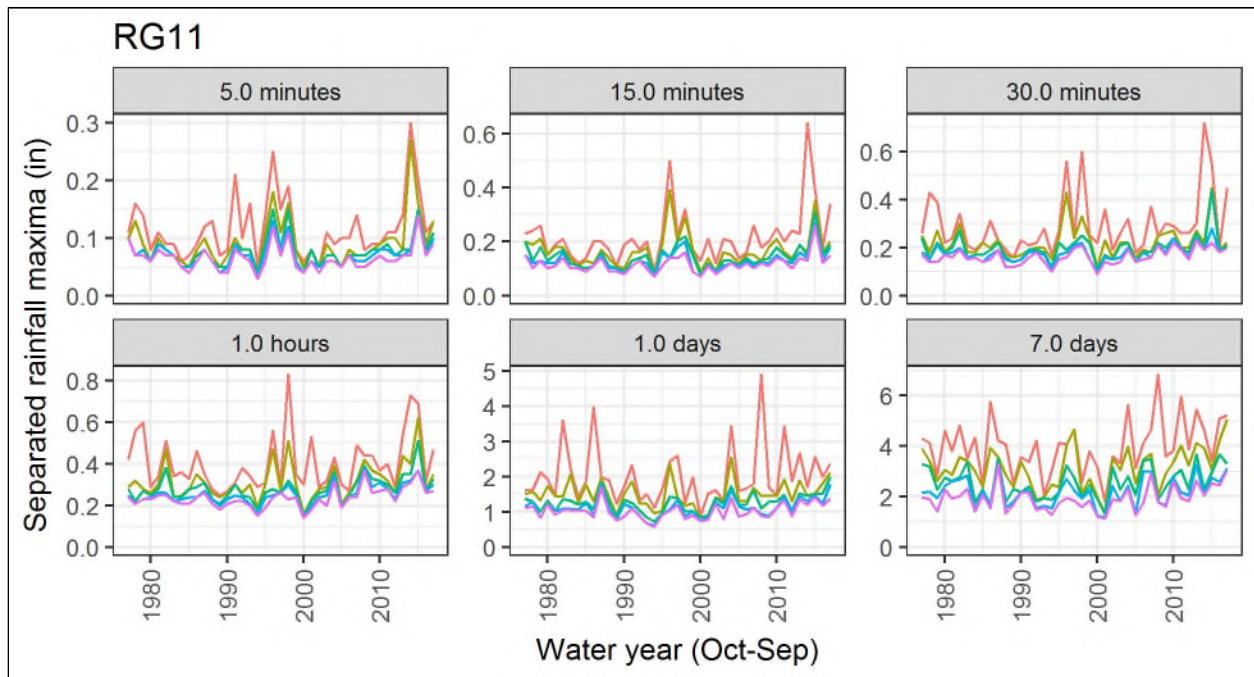
Different colored lines distinguish top 5 values in each water year (separated by at least the length of the relevant duration).

Figure 10. Time Series of Annual Maxima of Rainfall Depth for SPU Site RG09



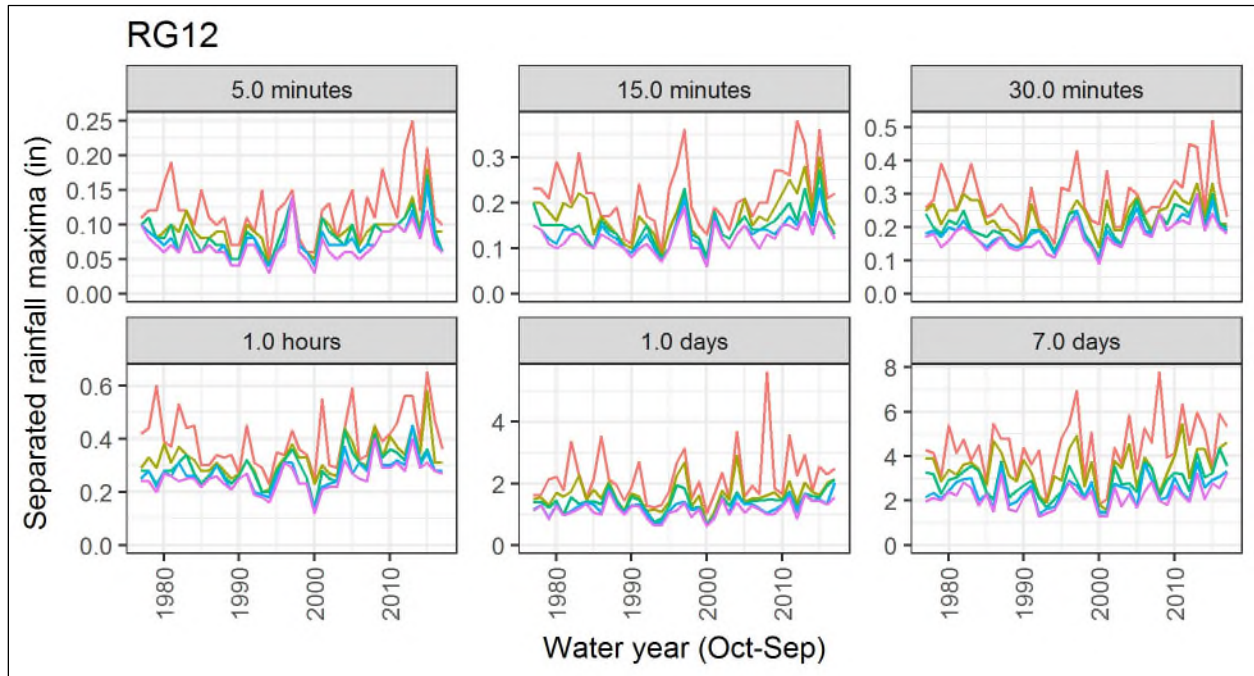
Different colored lines distinguish top 5 values in each water year (separated by at least the length of the relevant duration).

Figure 11. Time Series of Annual Maxima of Rainfall Depth for SPU Site RG10 30



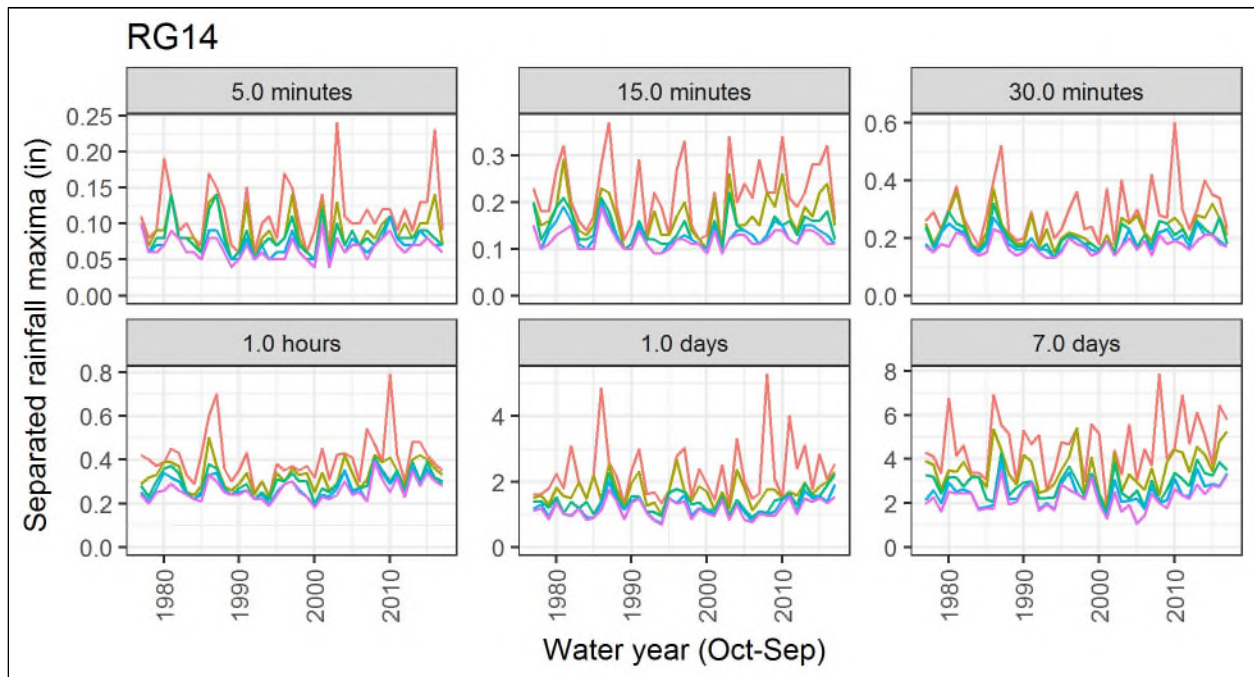
Different colored lines distinguish top 5 values in each water year (separated by at least the length of the relevant duration).

Figure 12. Time Series of Annual Maxima of Rainfall Depth for SPU Site RG11



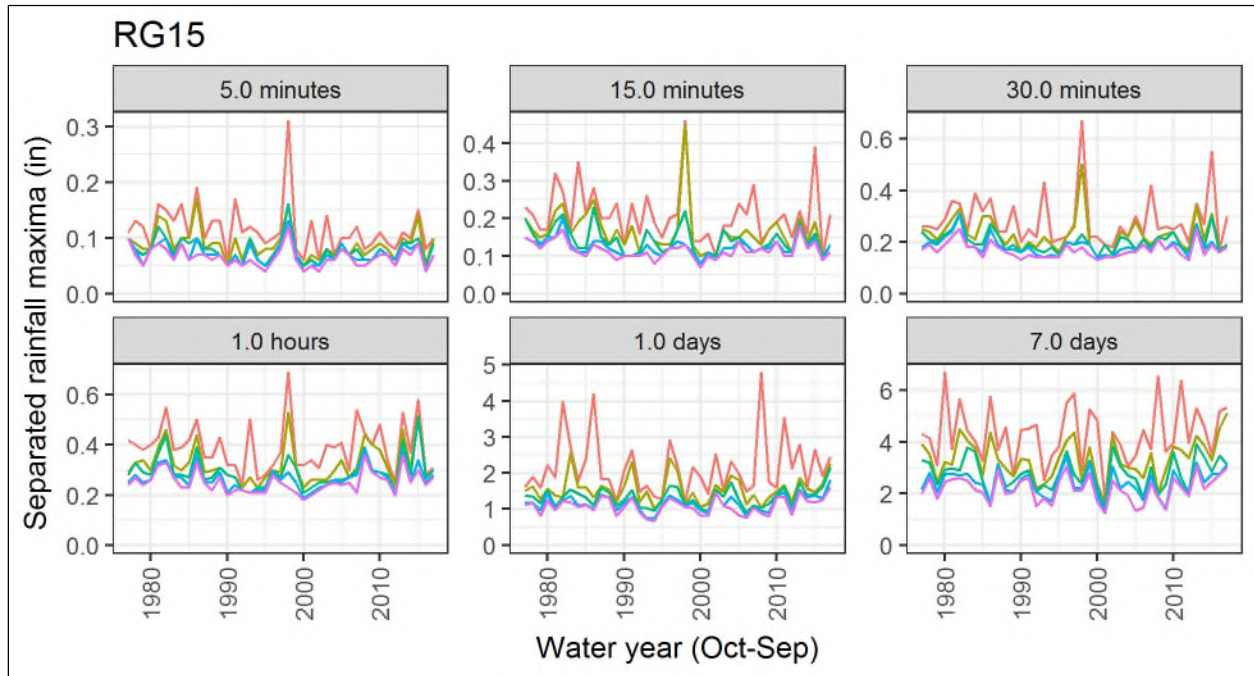
Different colored lines distinguish top 5 values in each water year (separated by at least the length of the relevant duration).

Figure 13. Time Series of Annual Maxima of Rainfall Depth for SPU Site RG12



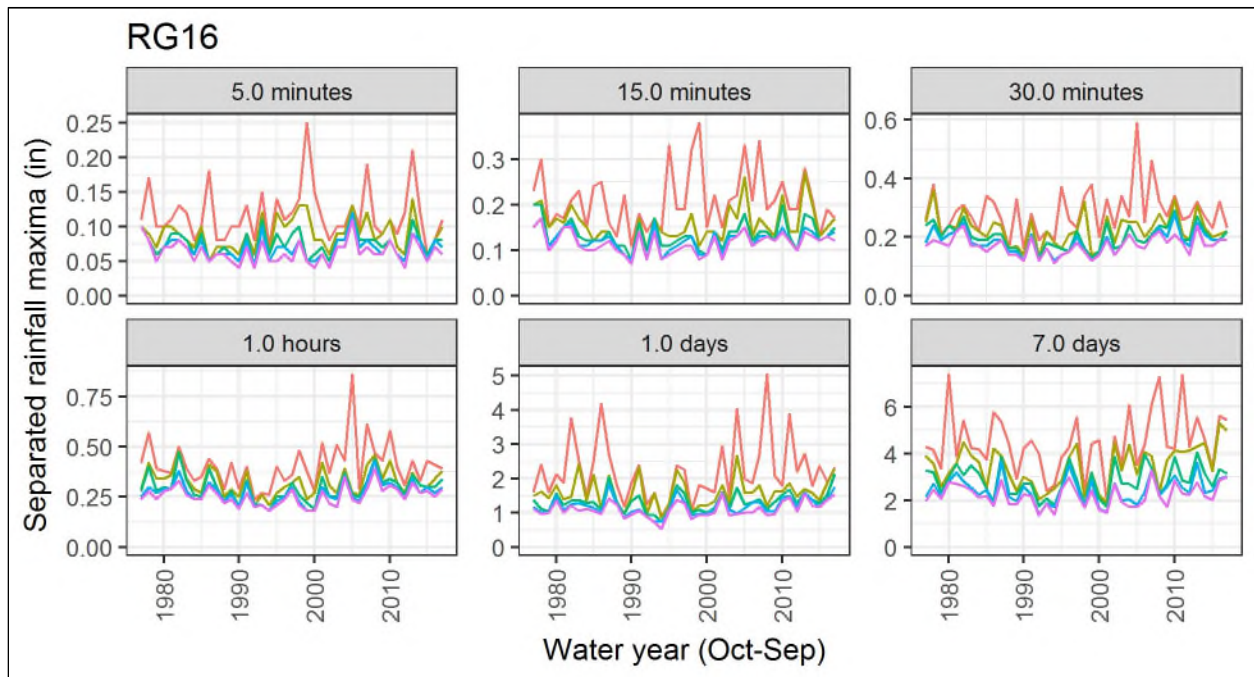
Different colored lines distinguish top 5 values in each water year (separated by at least the length of the relevant duration).

Figure 14. Time Series of Annual Maxima of Rainfall Depth for SPU Site RG14



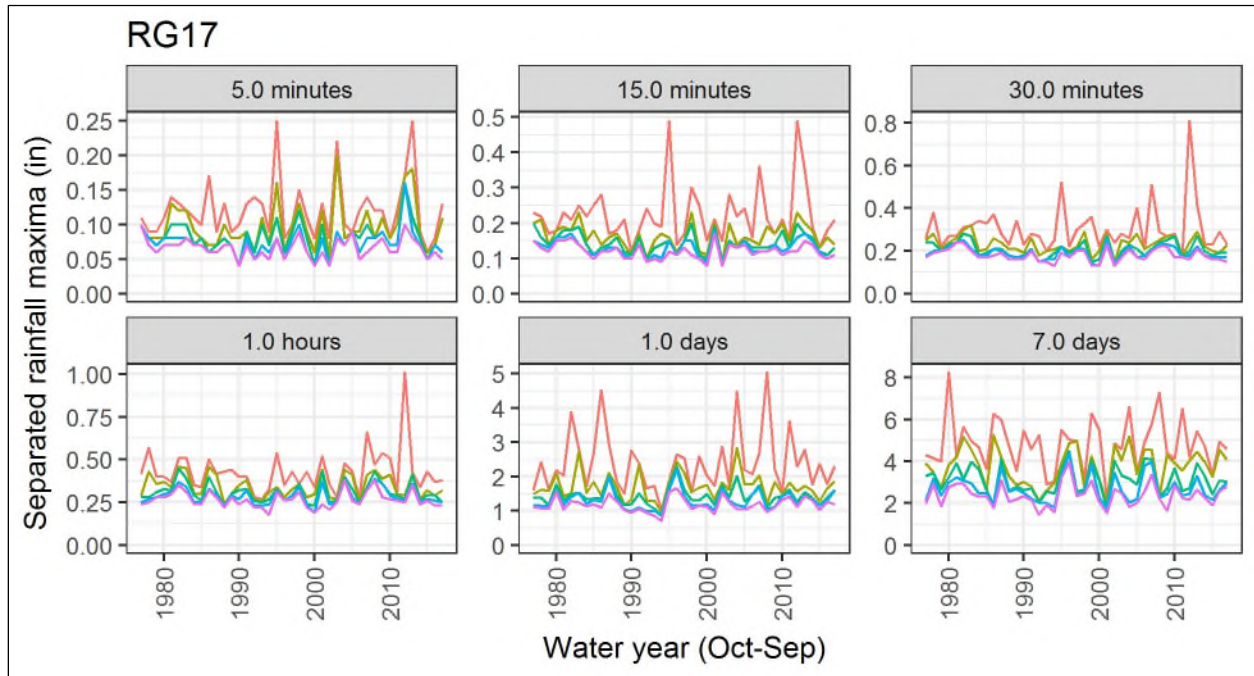
Different colored lines distinguish top 5 values in each water year (separated by at least the length of the relevant duration).

Figure 15. Time Series of Annual Maxima of Rainfall Depth for SPU Site RG15



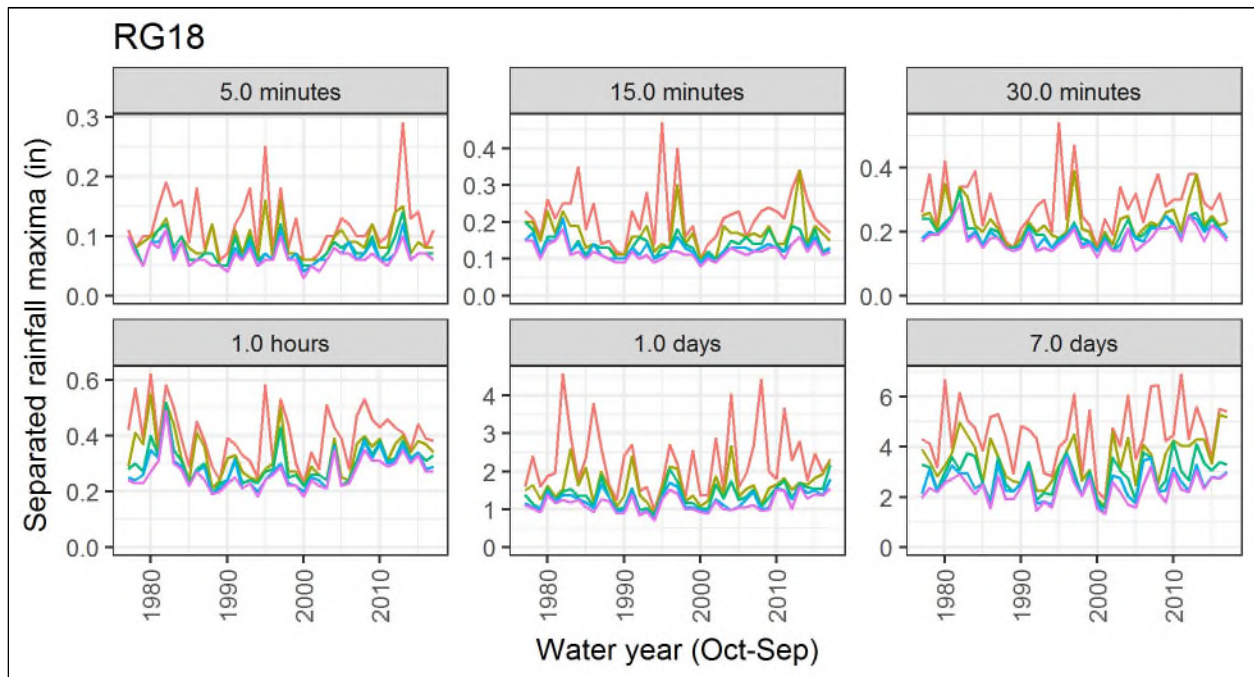
Different colored lines distinguish top 5 values in each water year (separated by at least the length of the relevant duration).

Figure 16. Time Series of Annual Maxima of Rainfall Depth for SPU Site RG16



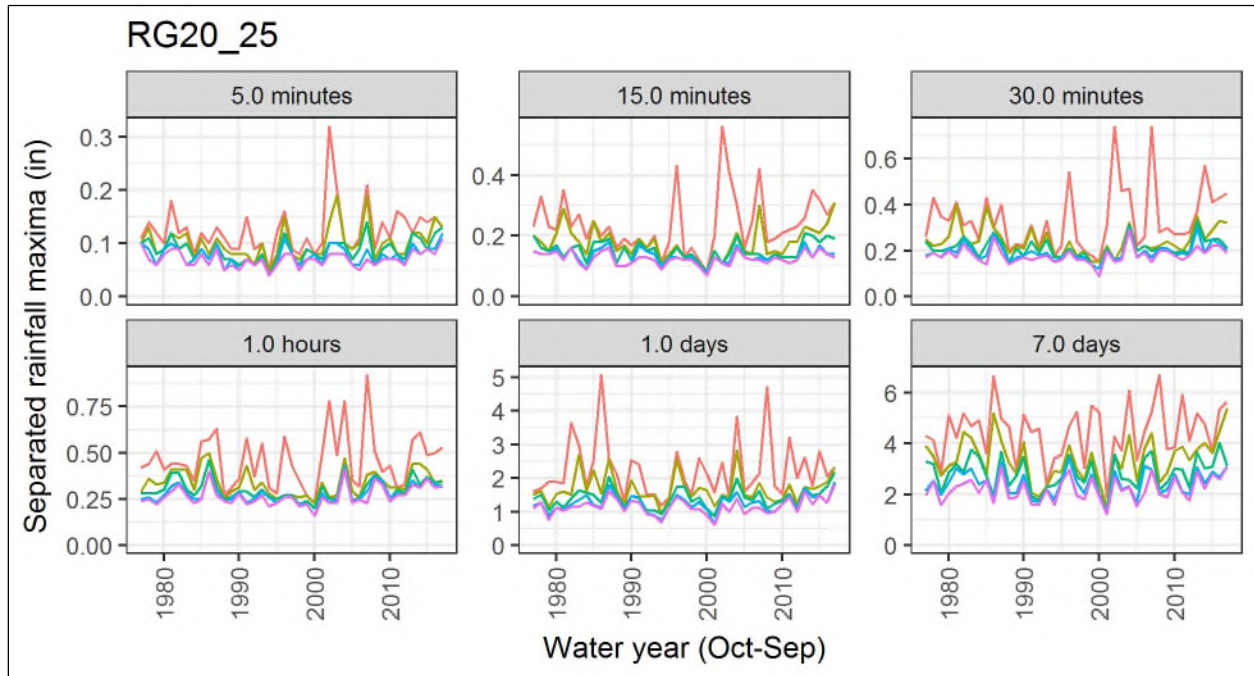
Different colored lines distinguish top 5 values in each water year (separated by at least the length of the relevant duration).

Figure 17. Time Series of Annual Maxima of Rainfall Depth for SPU Site RG17



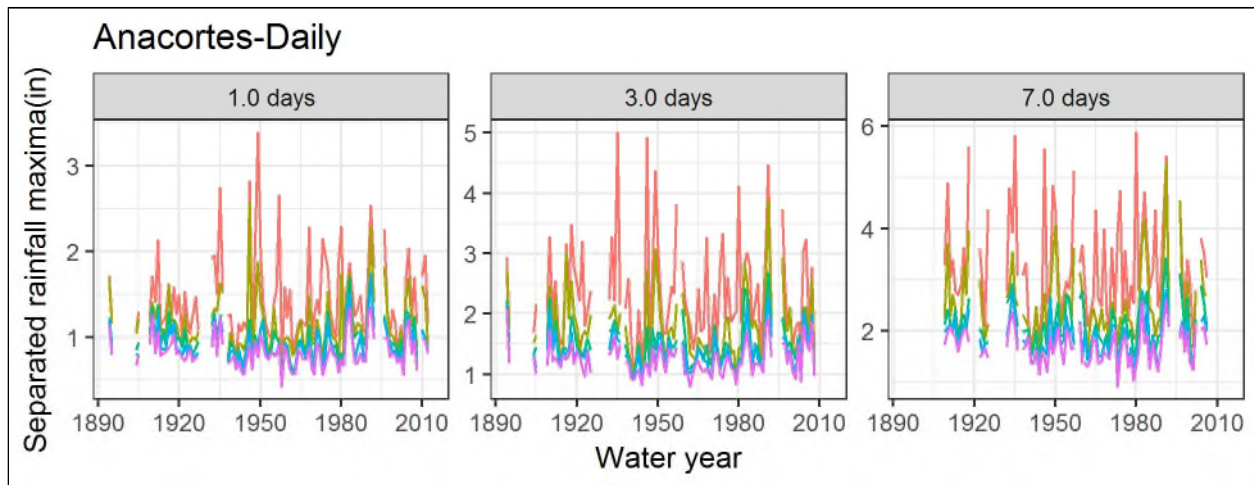
Different colored lines distinguish top 5 values in each water year (separated by at least the length of the relevant duration).

Figure 18. Time Series of Annual Maxima of Rainfall Depth for SPU Site RG18



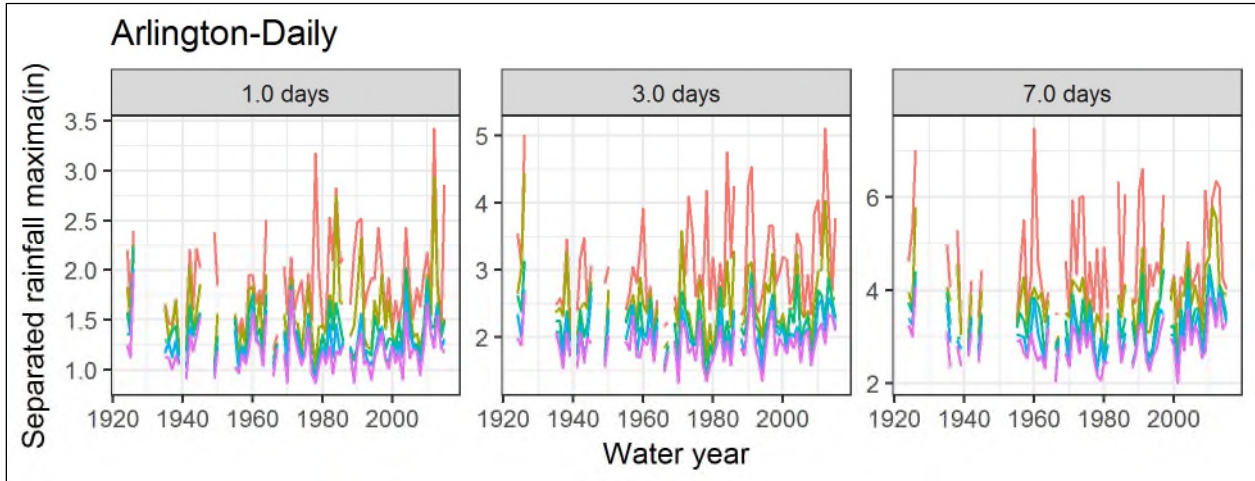
Different colored lines distinguish top 5 values in each water year (separated by at least the length of the relevant duration).

Figure 19. Time Series of Annual Maxima of Rainfall Depth for SPU Site RG20 25



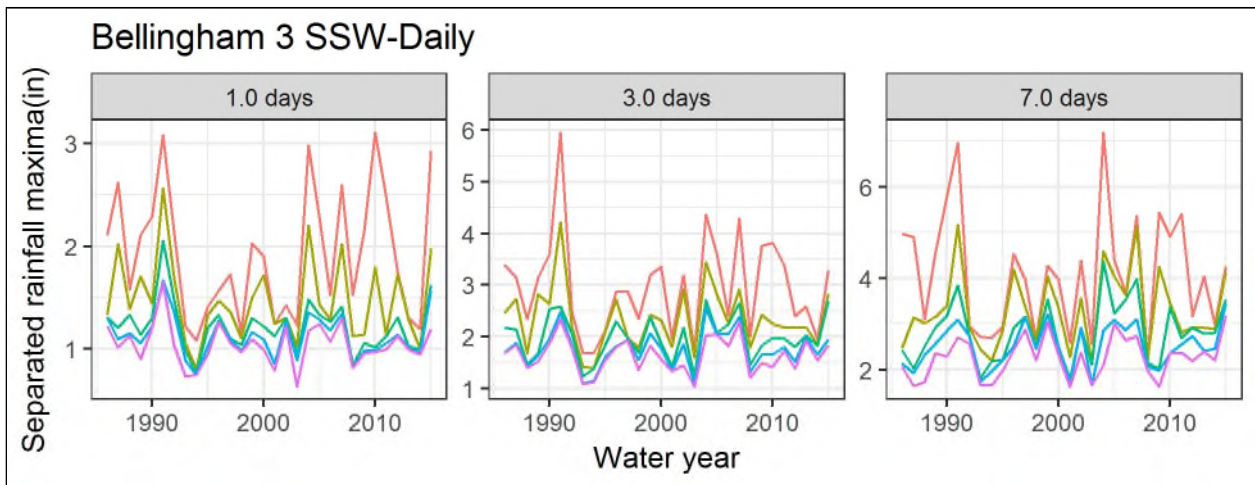
Different colored lines distinguish top 5 values in each water year (separated by at least the length of the relevant duration).

Figure 20. Time Series of Annual Maxima of Rainfall Depth for NWS Site Anacortes-Daily



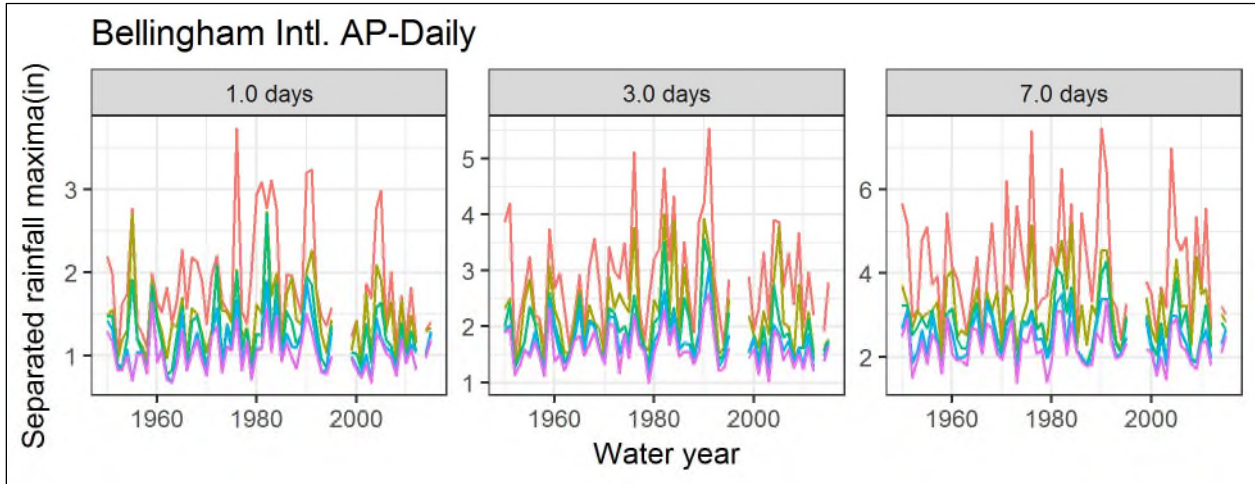
Different colored lines distinguish top 5 values in each water year (separated by at least the length of the relevant duration).

Figure 21. Time Series of Annual Maxima of Rainfall Depth for NWS Site Arlington-Daily



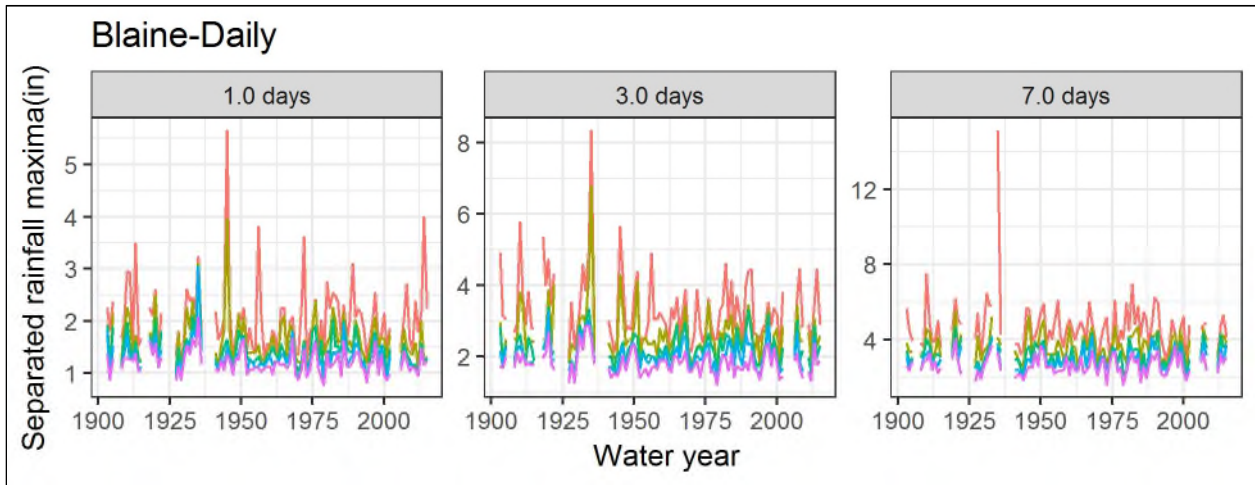
Different colored lines distinguish top 5 values in each water year (separated by at least the length of the relevant duration).

Figure 22. Time Series of Annual Maxima of Rainfall Depth for NWS Site Bellingham 3 SSW-Daily



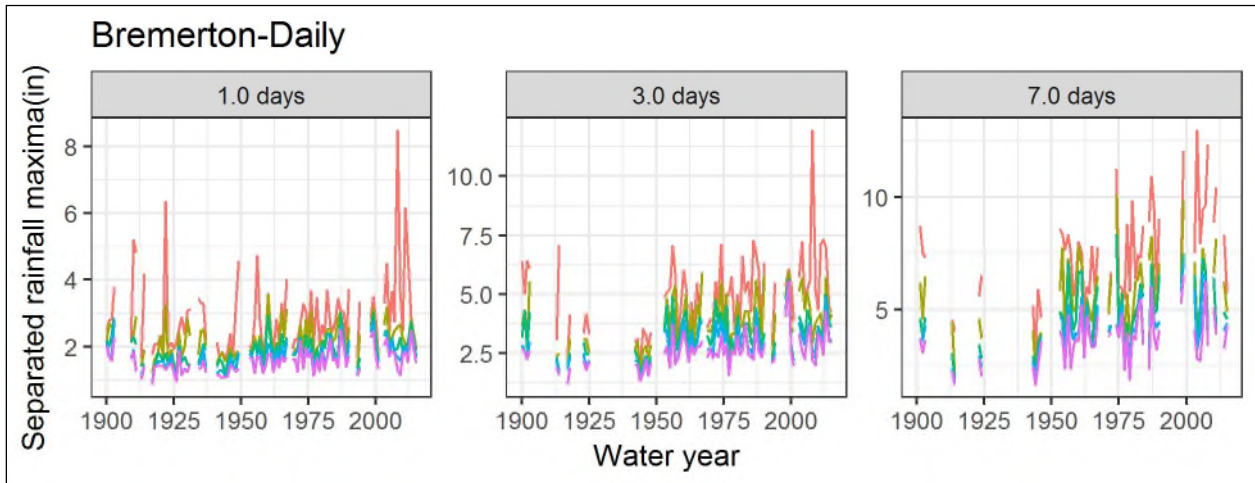
Different colored lines distinguish top 5 values in each water year (separated by at least the length of the relevant duration).

Figure 23. Time Series of Annual Maxima of Rainfall Depth for NWS Site Bellingham Intl. AP-Daily



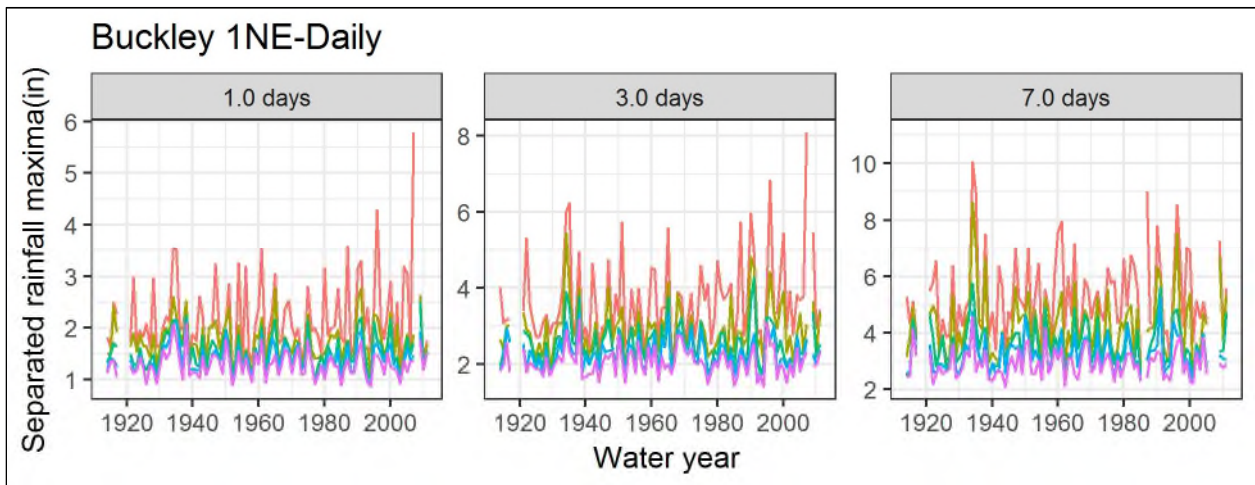
Different colored lines distinguish top 5 values in each water year (separated by at least the length of the relevant duration).

Figure 24. Time Series of Annual Maxima of Rainfall Depth for NWS Site Blaine-Daily



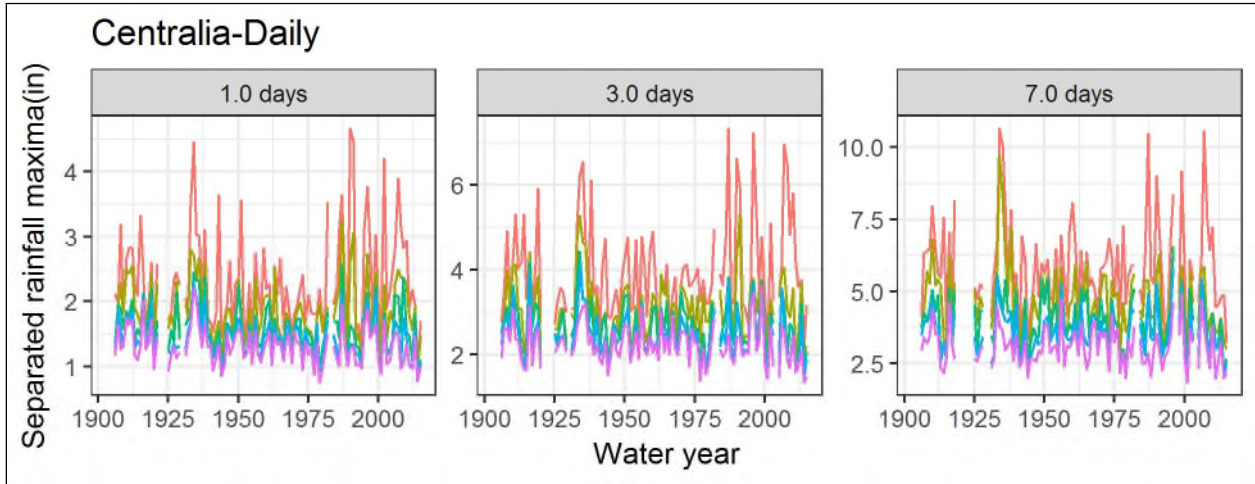
Different colored lines distinguish top 5 values in each water year (separated by at least the length of the relevant duration).

Figure 25. Time Series of Annual Maxima of Rainfall Depth for NWS Site Bremerton-Daily



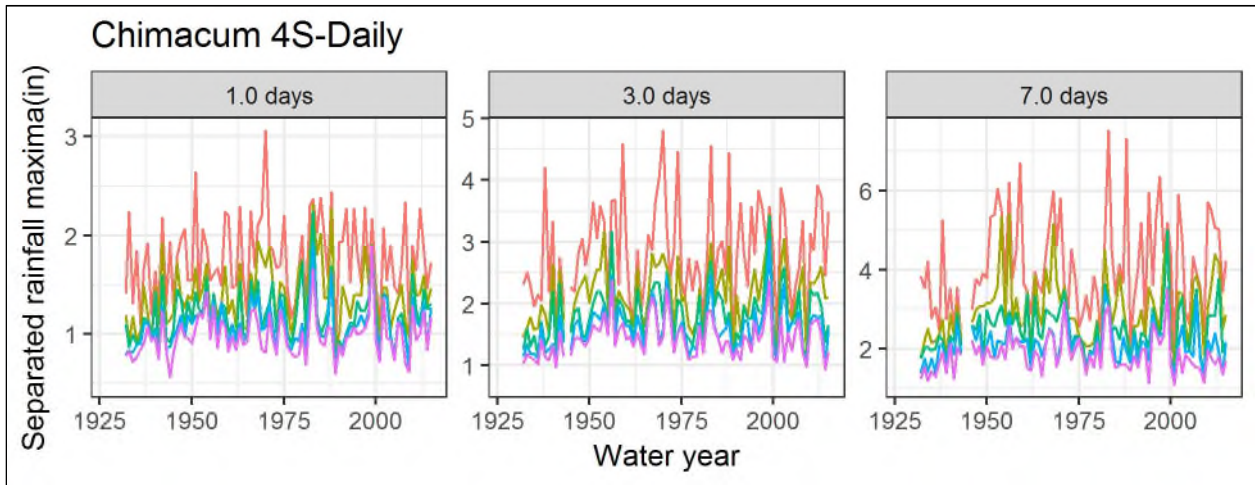
Different colored lines distinguish top 5 values in each water year (separated by at least the length of the relevant duration).

Figure 26. Time Series of Annual Maxima of Rainfall Depth for NWS Site Buckley 1NE-Daily



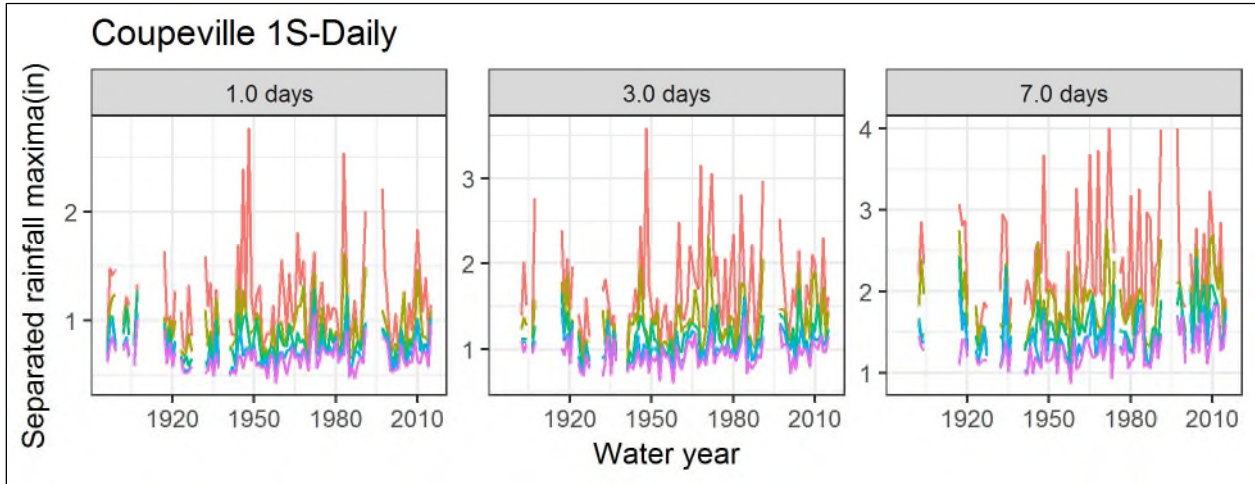
Different colored lines distinguish top 5 values in each water year (separated by at least the length of the relevant duration).

Figure 27. Time Series of Annual Maxima of Rainfall Depth for NWS Site Centralia-Daily



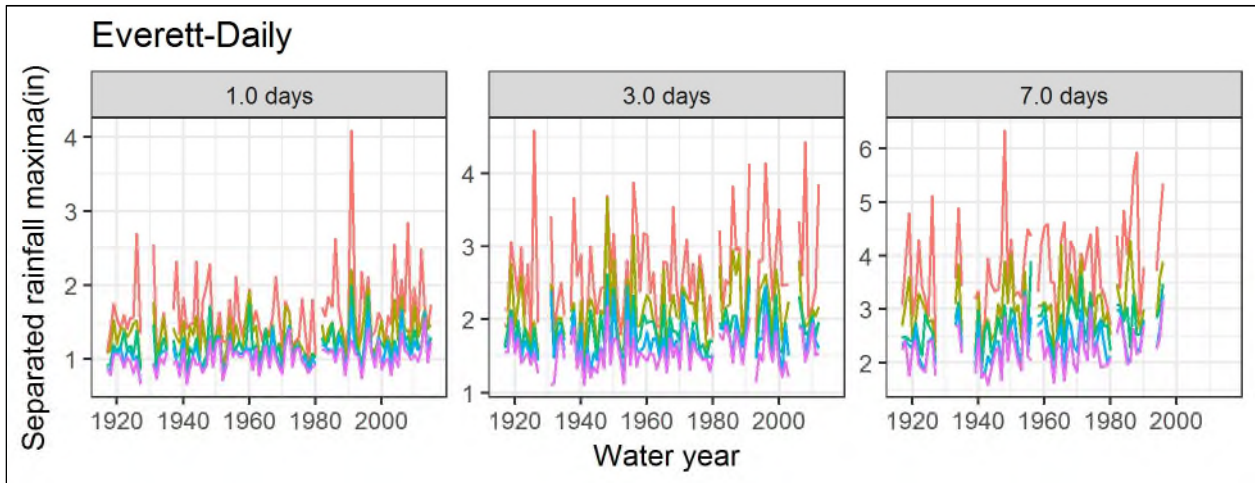
Different colored lines distinguish top 5 values in each water year (separated by at least the length of the relevant duration).

Figure 28. Time Series of Annual Maxima of Rainfall Depth for NWS Site Chimacum 4S-Daily



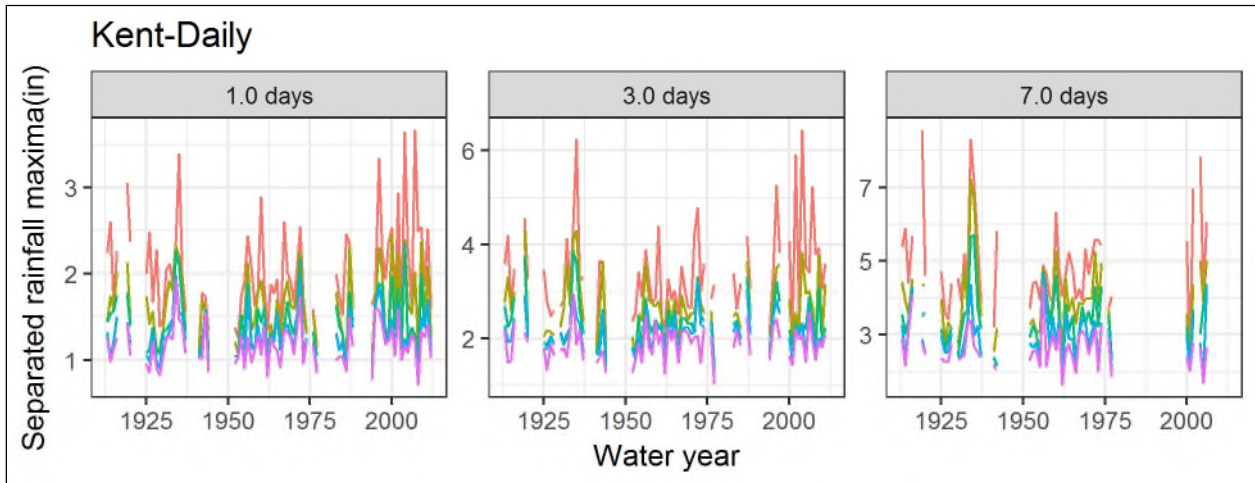
Different colored lines distinguish top 5 values in each water year (separated by at least the length of the relevant duration).

Figure 29. Time Series of Annual Maxima of Rainfall Depth for NWS Site Coupeville 1S-Daily



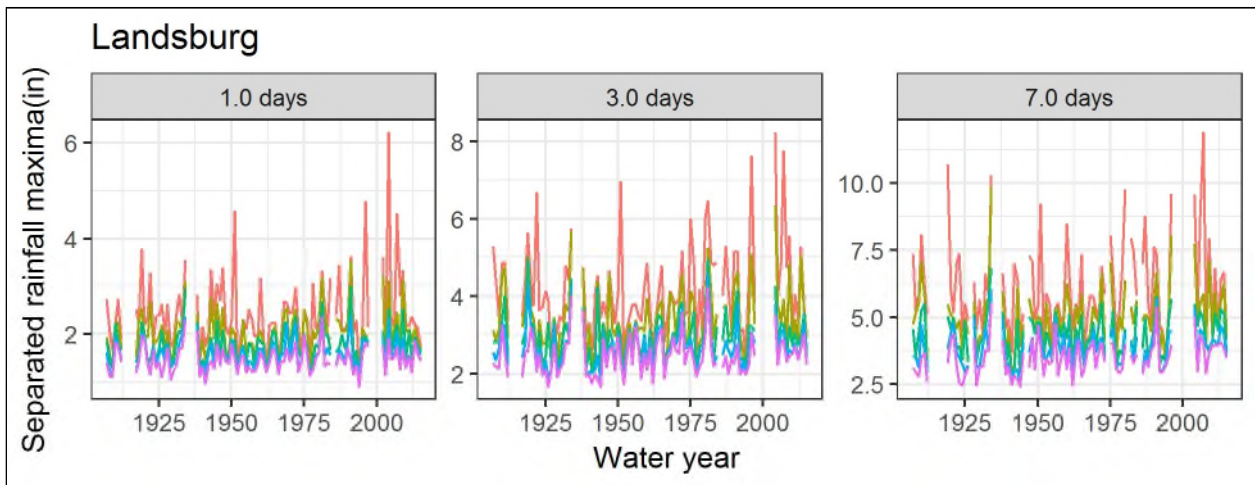
Different colored lines distinguish top 5 values in each water year (separated by at least the length of the relevant duration).

Figure 30. Time Series of Annual Maxima of Rainfall Depth for NWS Site Everett-Daily



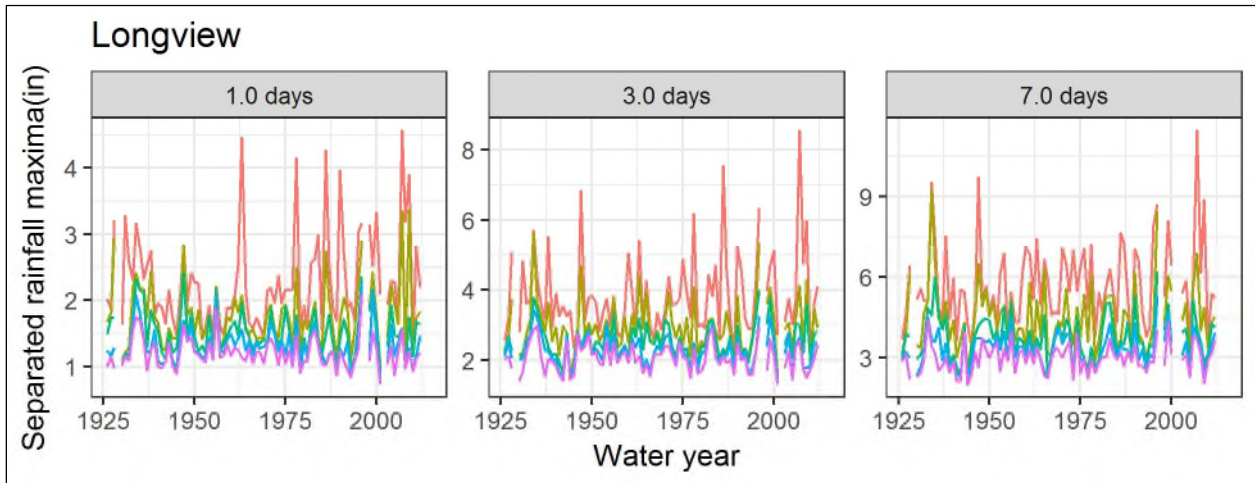
Different colored lines distinguish top 5 values in each water year (separated by at least the length of the relevant duration).

Figure 31. Time Series of Annual Maxima of Rainfall Depth for NWS Site Kent-Daily



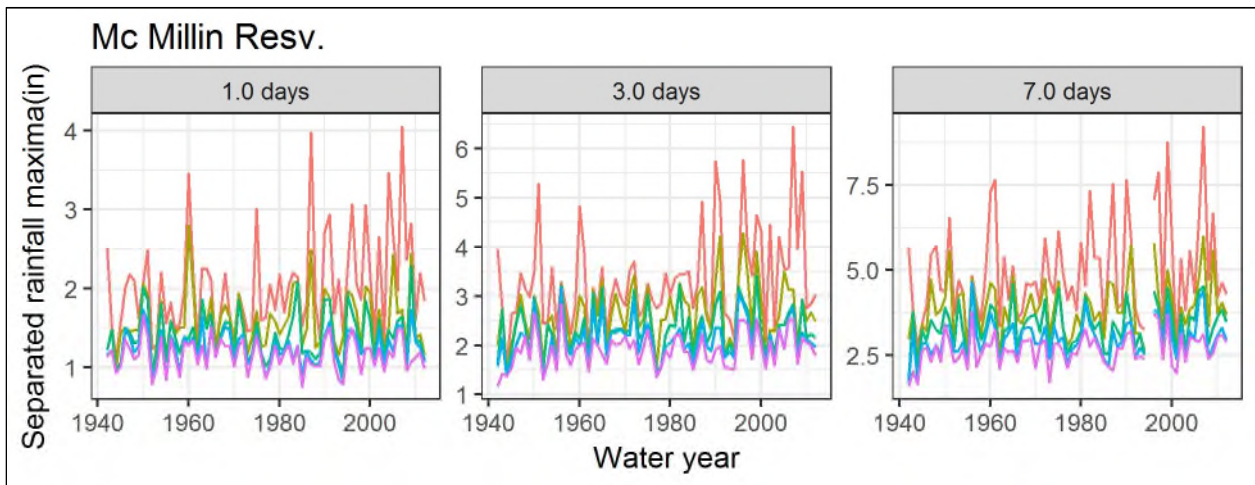
Different colored lines distinguish top 5 values in each water year (separated by at least the length of the relevant duration).

Figure 32. Time Series of Annual Maxima of Rainfall Depth for NWS Site Landsburg



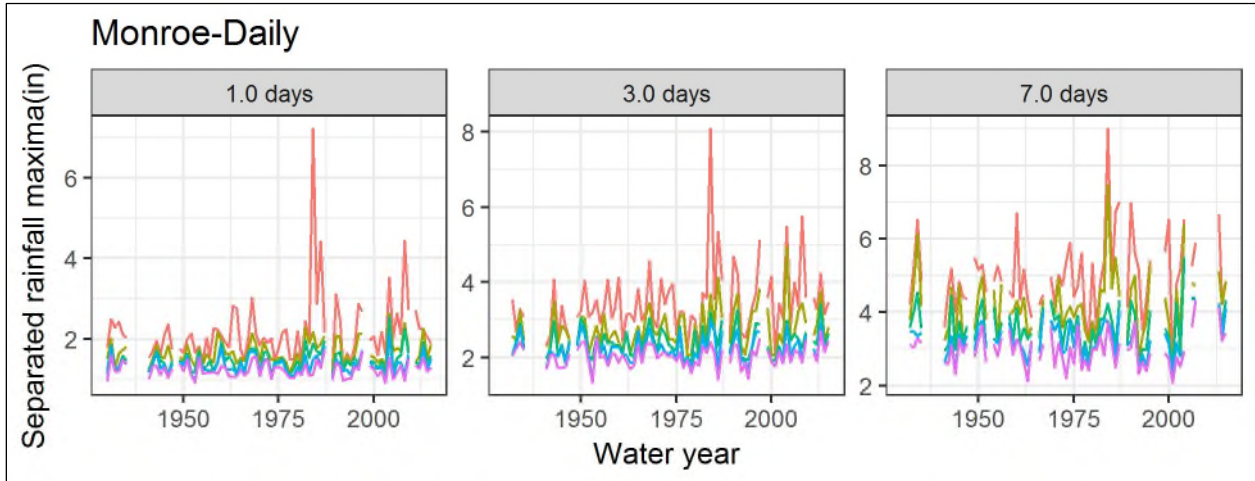
Different colored lines distinguish top 5 values in each water year (separated by at least the length of the relevant duration).

Figure 33. Time Series of Annual Maxima of Rainfall Depth for NWS Site Longview



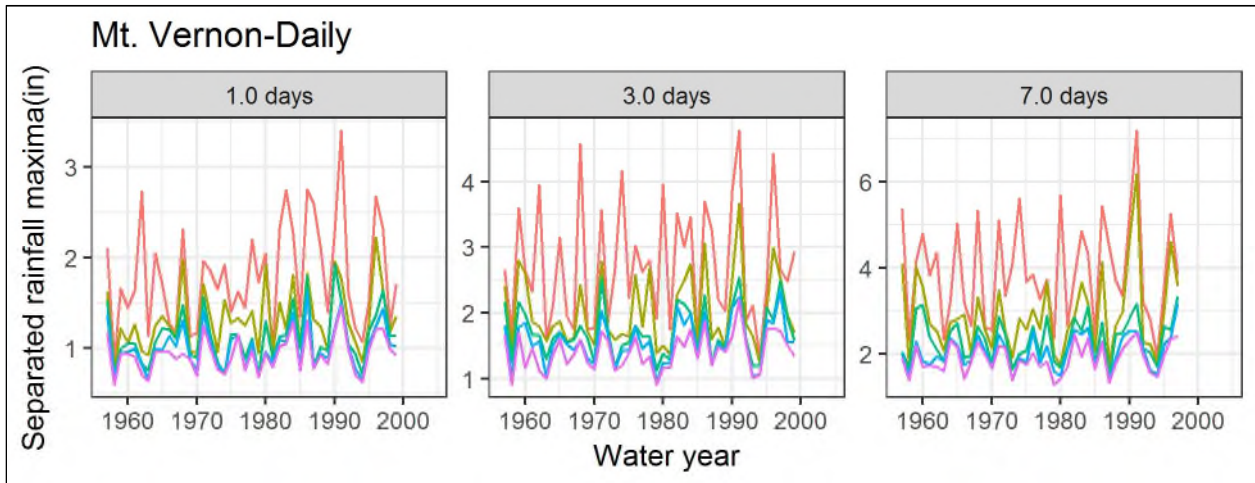
Different colored lines distinguish top 5 values in each water year (separated by at least the length of the relevant duration).

Figure 34. Time Series of Annual Maxima of Rainfall Depth for NWS Site McMillin Resv



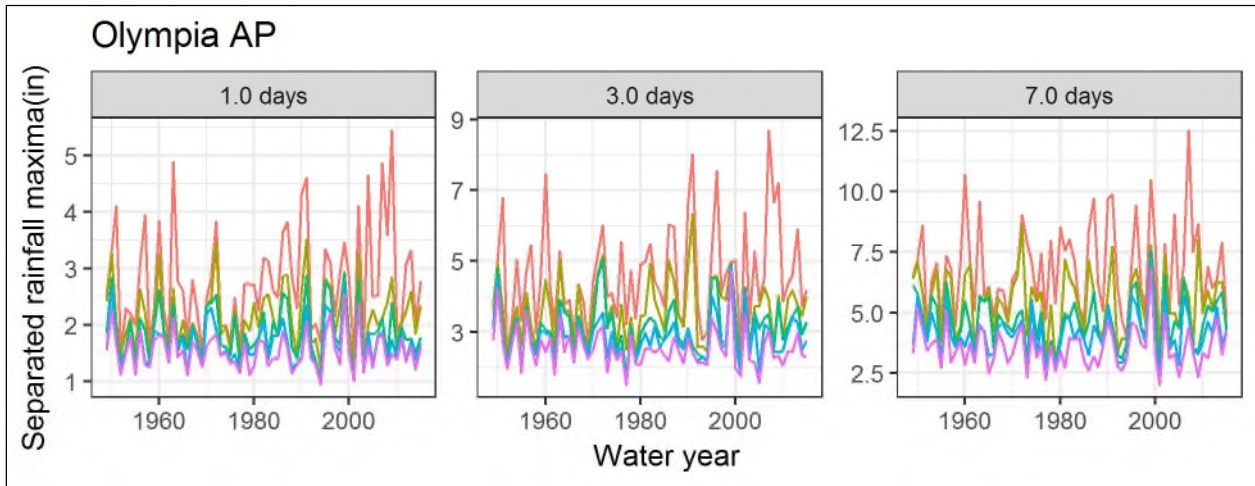
Different colored lines distinguish top 5 values in each water year (separated by at least the length of the relevant duration).

Figure 35. Time Series of Annual Maxima of Rainfall Depth for NWS Site Monroe-Daily



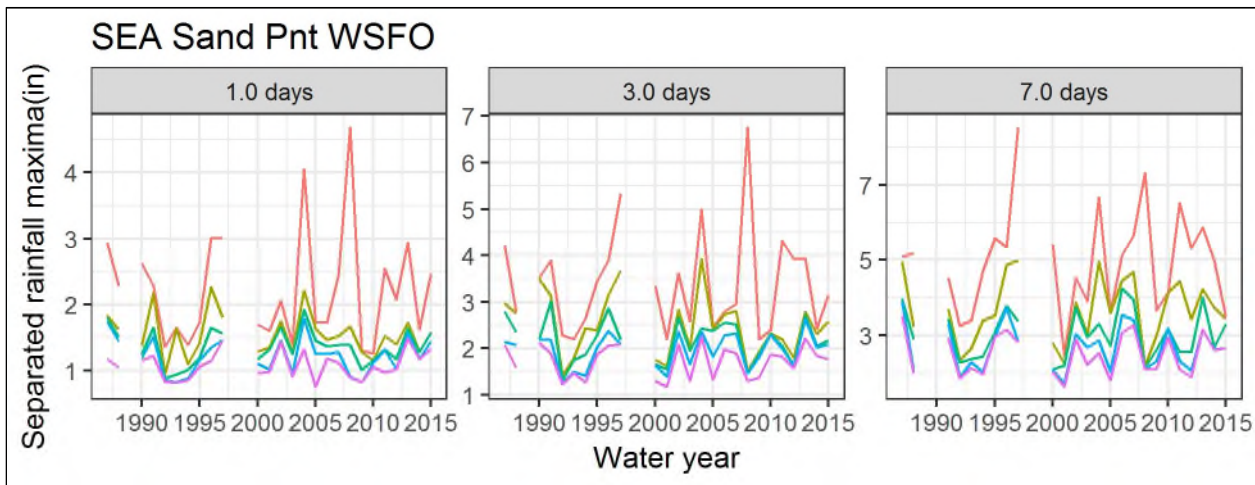
Different colored lines distinguish top 5 values in each water year (separated by at least the length of the relevant duration).

Figure 36. Time Series of Annual Maxima of Rainfall Depth for NWS Site Mt. Vernon-Daily



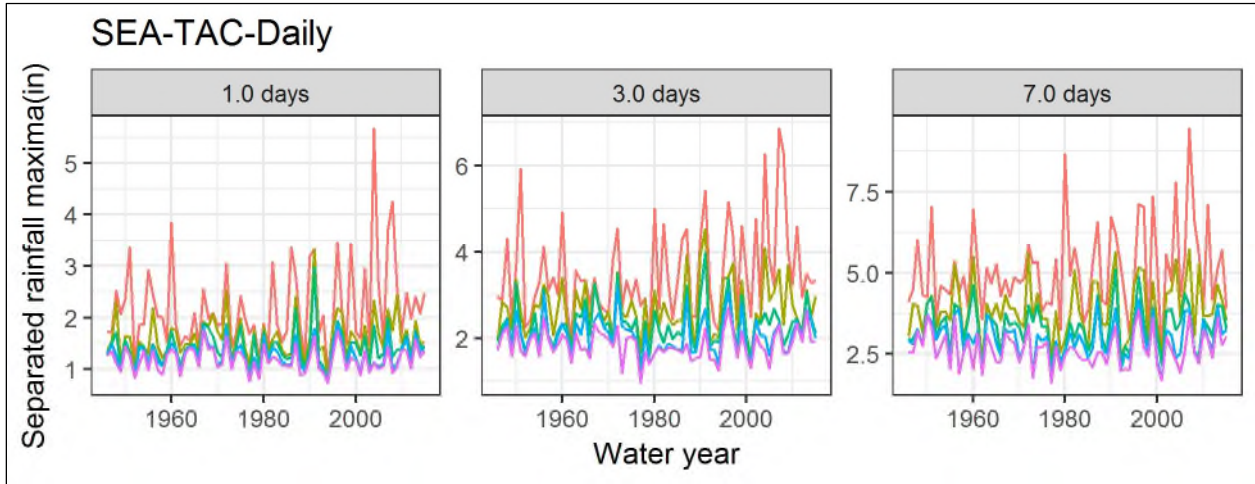
Different colored lines distinguish top 5 values in each water year (separated by at least the length of the relevant duration).

Figure 37. Time Series of Annual Maxima of Rainfall Depth for NWS Site Olympia AP



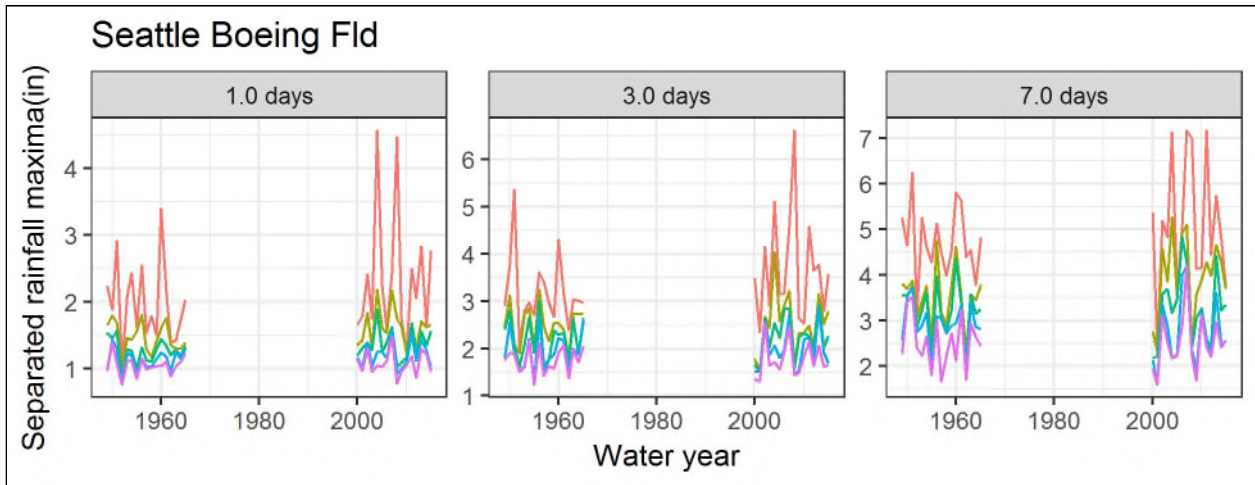
Different colored lines distinguish top 5 values in each water year (separated by at least the length of the relevant duration).

Figure 38. Time Series of Annual Maxima of Rainfall Depth for NWS Site SEA Sand Pnt WSFO



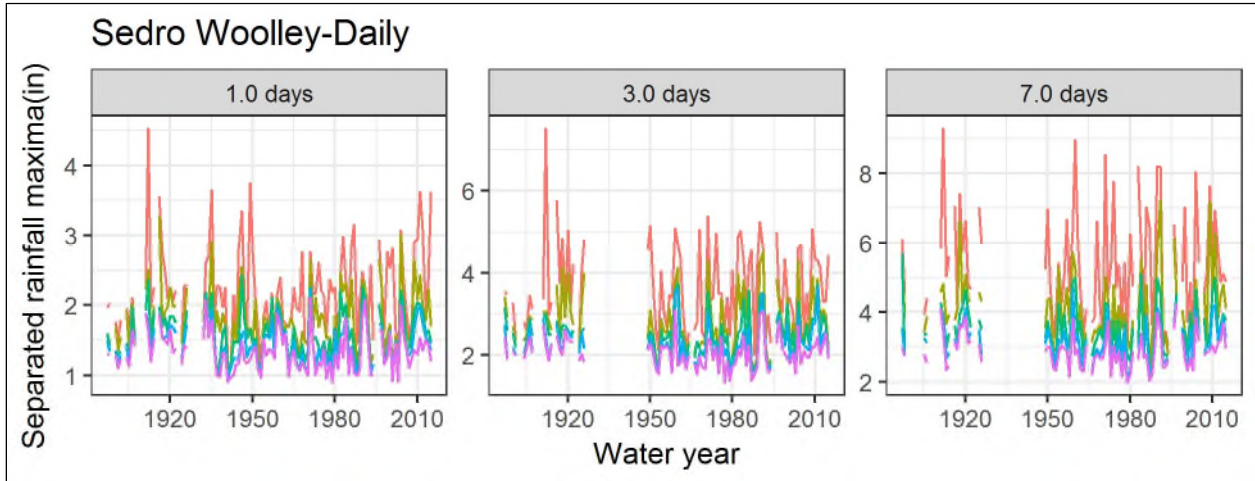
Different colored lines distinguish top 5 values in each water year (separated by at least the length of the relevant duration).

Figure 39. Time Series of Annual Maxima of Rainfall Depth for NWS Site SEA-TAC-Daily



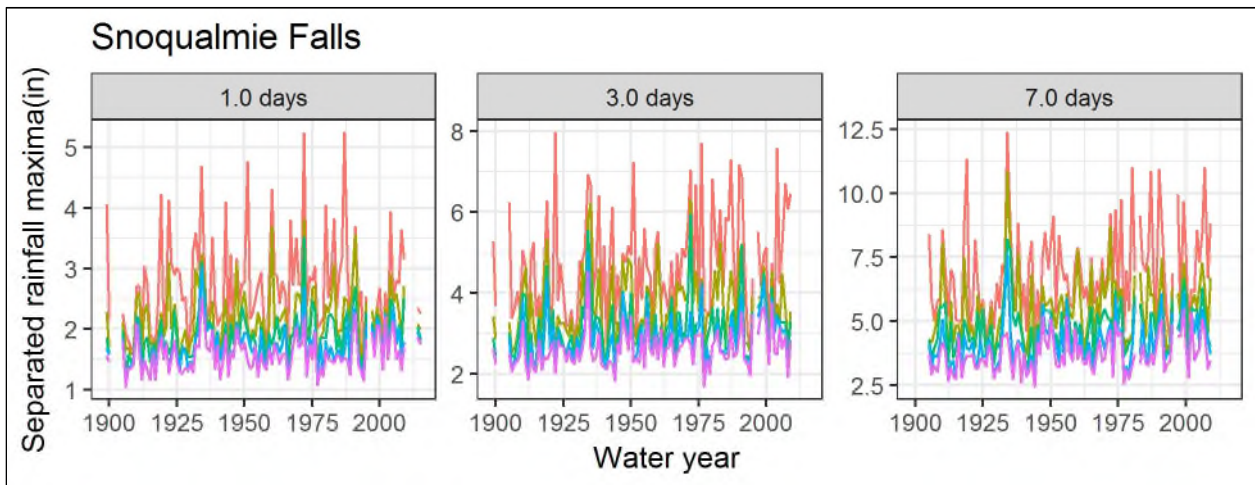
Different colored lines distinguish top 5 values in each water year (separated by at least the length of the relevant duration).

Figure 40. Time Series of Annual Maxima of Rainfall Depth for NWS Site Seattle Boeing Fld



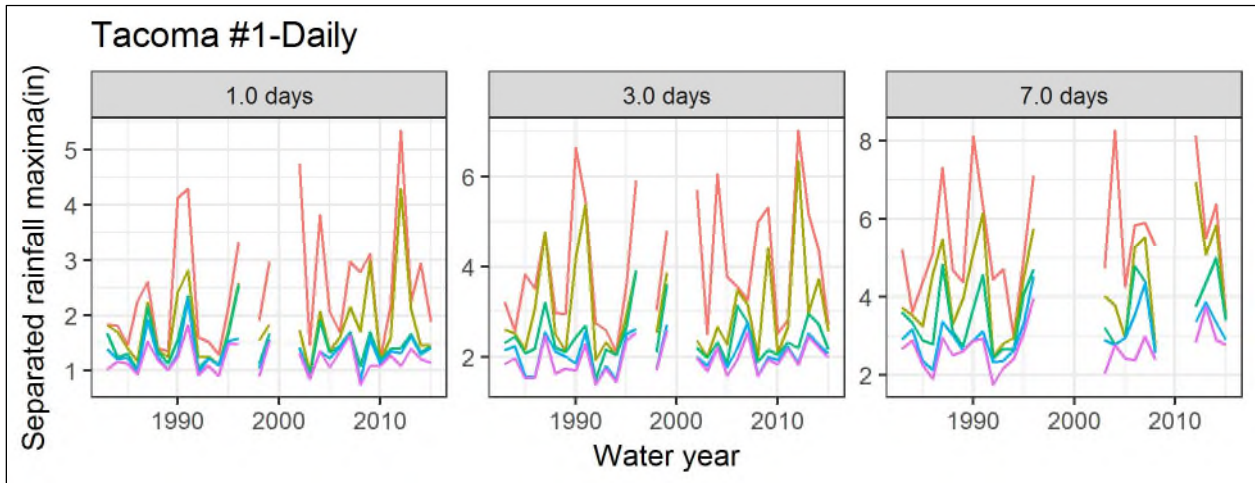
Different colored lines distinguish top 5 values in each water year (separated by at least the length of the relevant duration).

Figure 41. Time Series of Annual Maxima of Rainfall Depth for NWS Site Sedro Woolley-Daily



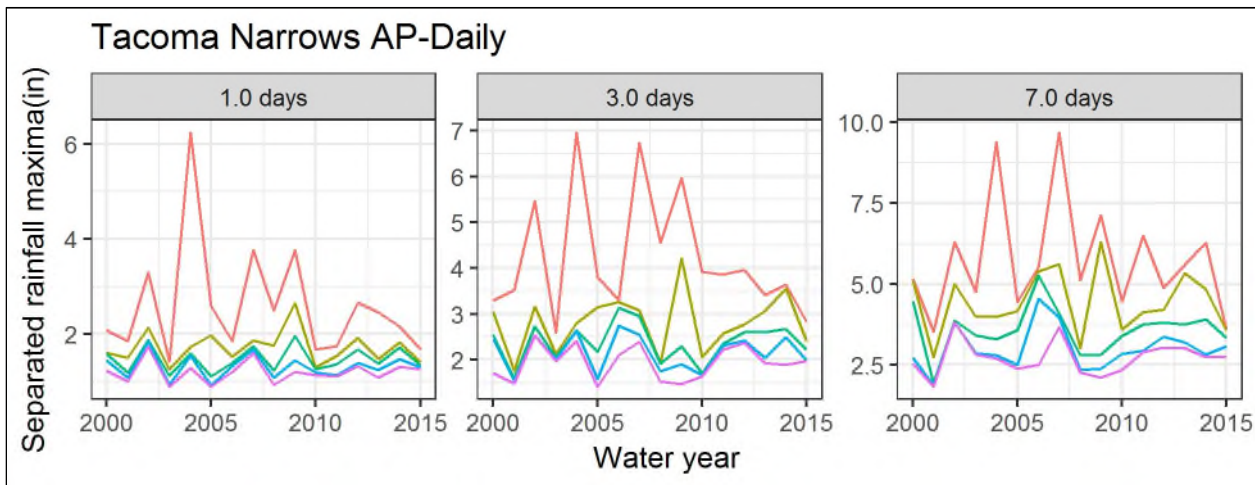
Different colored lines distinguish top 5 values in each water year (separated by at least the length of the relevant duration).

Figure 42. Time Series of Annual Maxima of Rainfall Depth for NWS Site Snoqualmie Falls



Different colored lines distinguish top 5 values in each water year (separated by at least the length of the relevant duration).

Figure 43. Time Series of Annual Maxima of Rainfall Depth for NWS Site Tacoma #1-Daily



Different colored lines distinguish top 5 values in each water year (separated by at least the length of the relevant duration).

Figure 44. Time Series of Annual Maxima of Rainfall Depth for NWS Site Tacoma Narrows AP-Daily

Data obtained from <http://jisao.washington.edu/pdo/PDO.latest.txt>

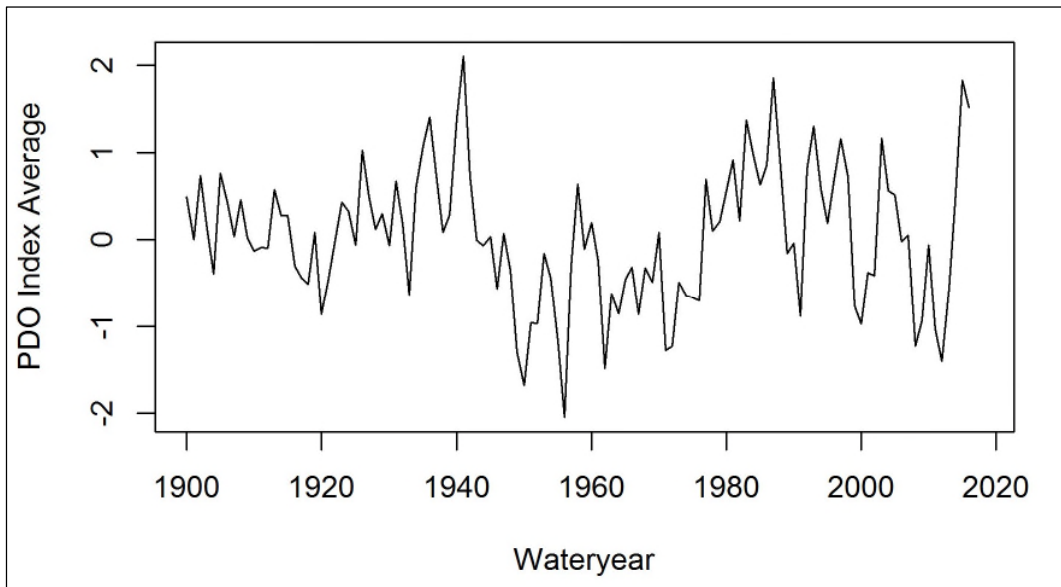
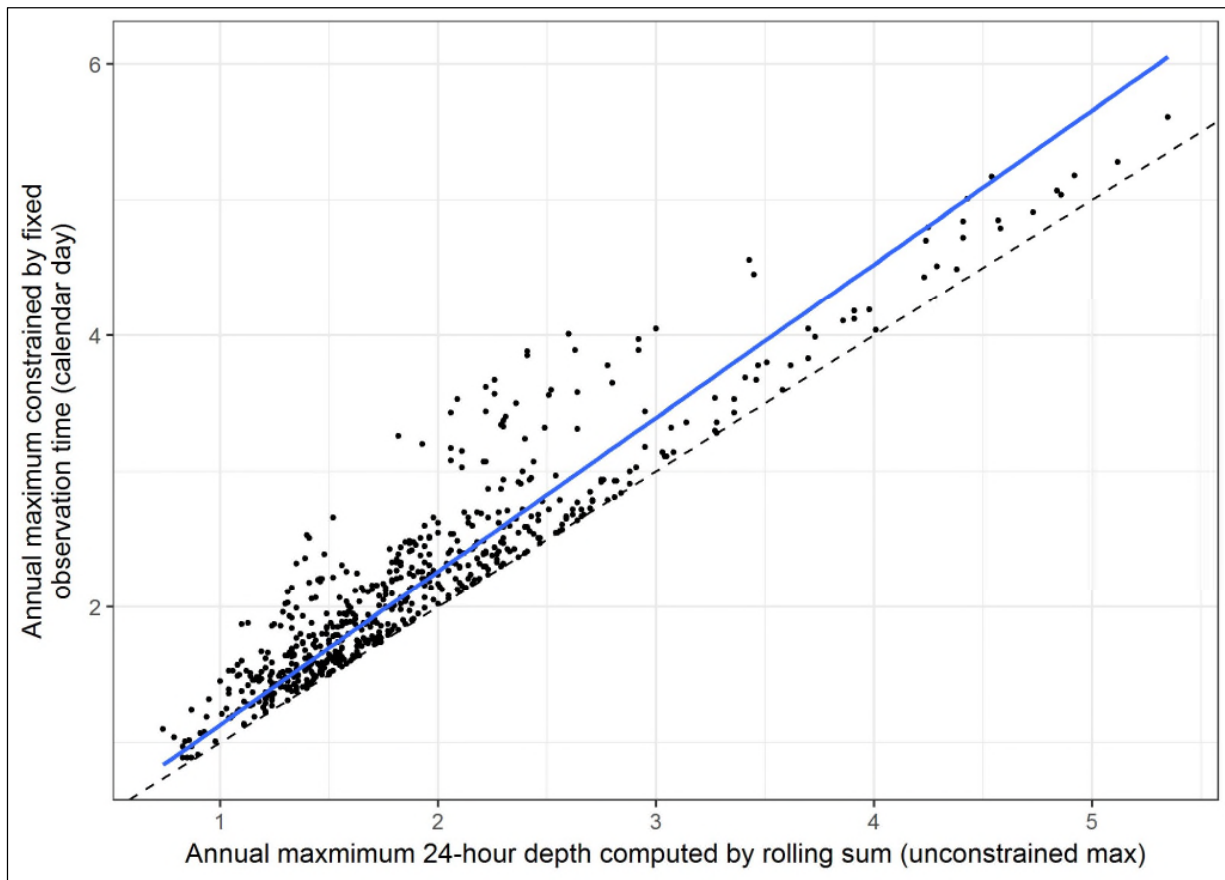


Figure 45. Time Series Plot of Water-Year Average for PDO Monthly Data



Blue line is best-fit. Slope = 1.13; derived from SPU data. This multiplier is applied to NWS data before GEV analysis.

Figure 46. Constrained and Unconstrained 1-Day Precipitation Depths and No-Intercept Best-Fit Line

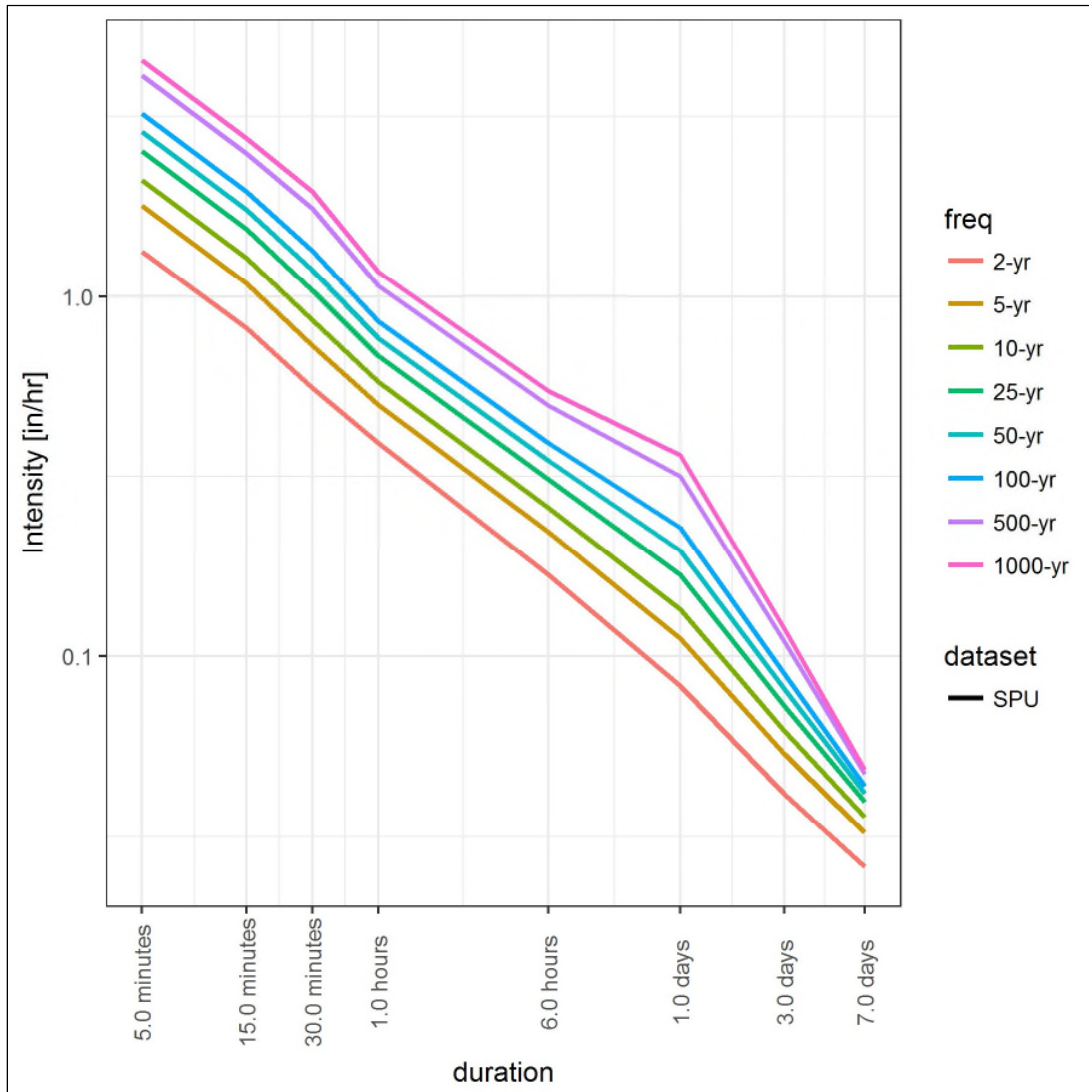
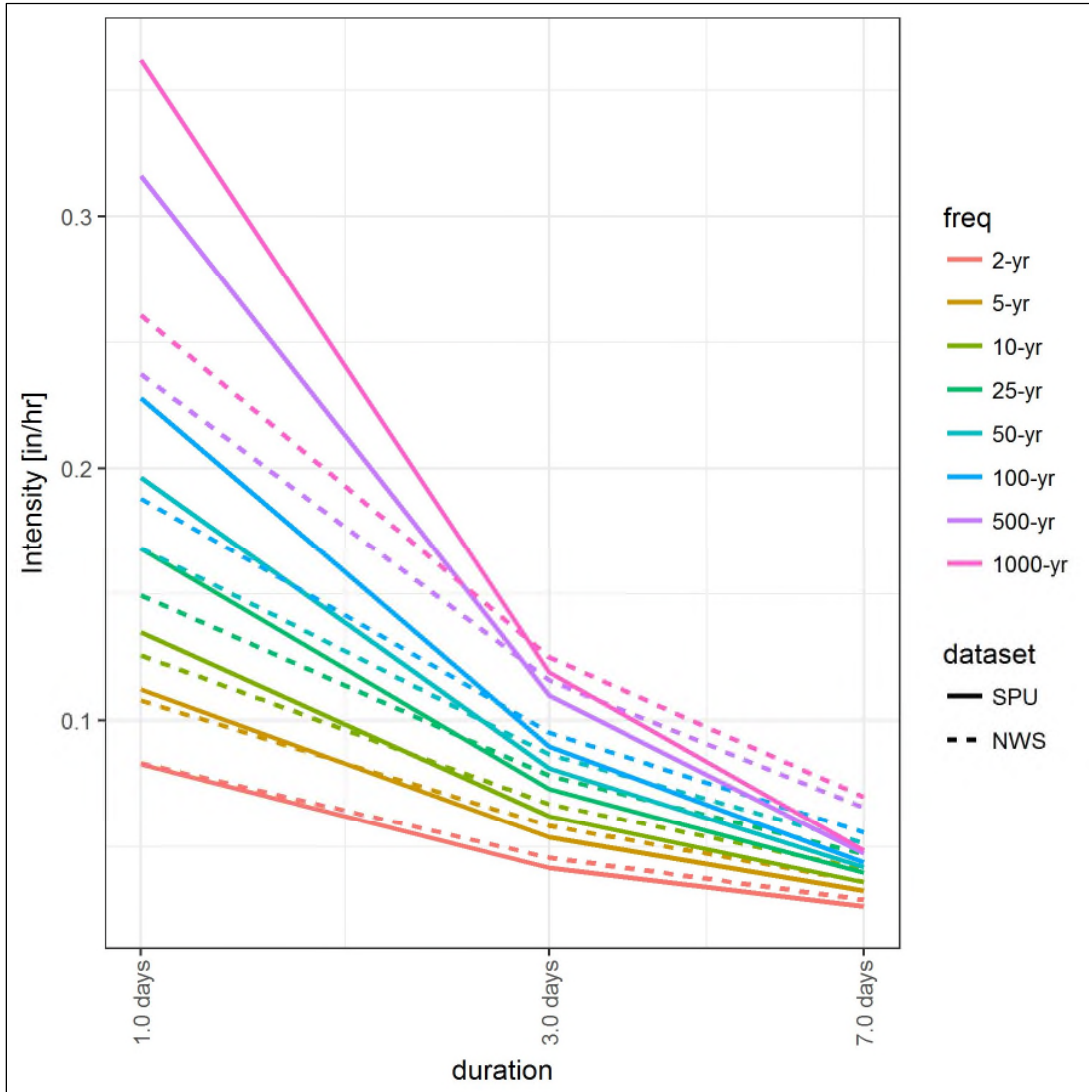


Figure 47. Regional IDF Curves from L-Moment Analysis of SPU Data



Heterogeneity test indicates a subset of stations may be more appropriate for NWS data.

Figure 48. Regional IDF Curves from L-Moment Analysis of SPU and NWS Data

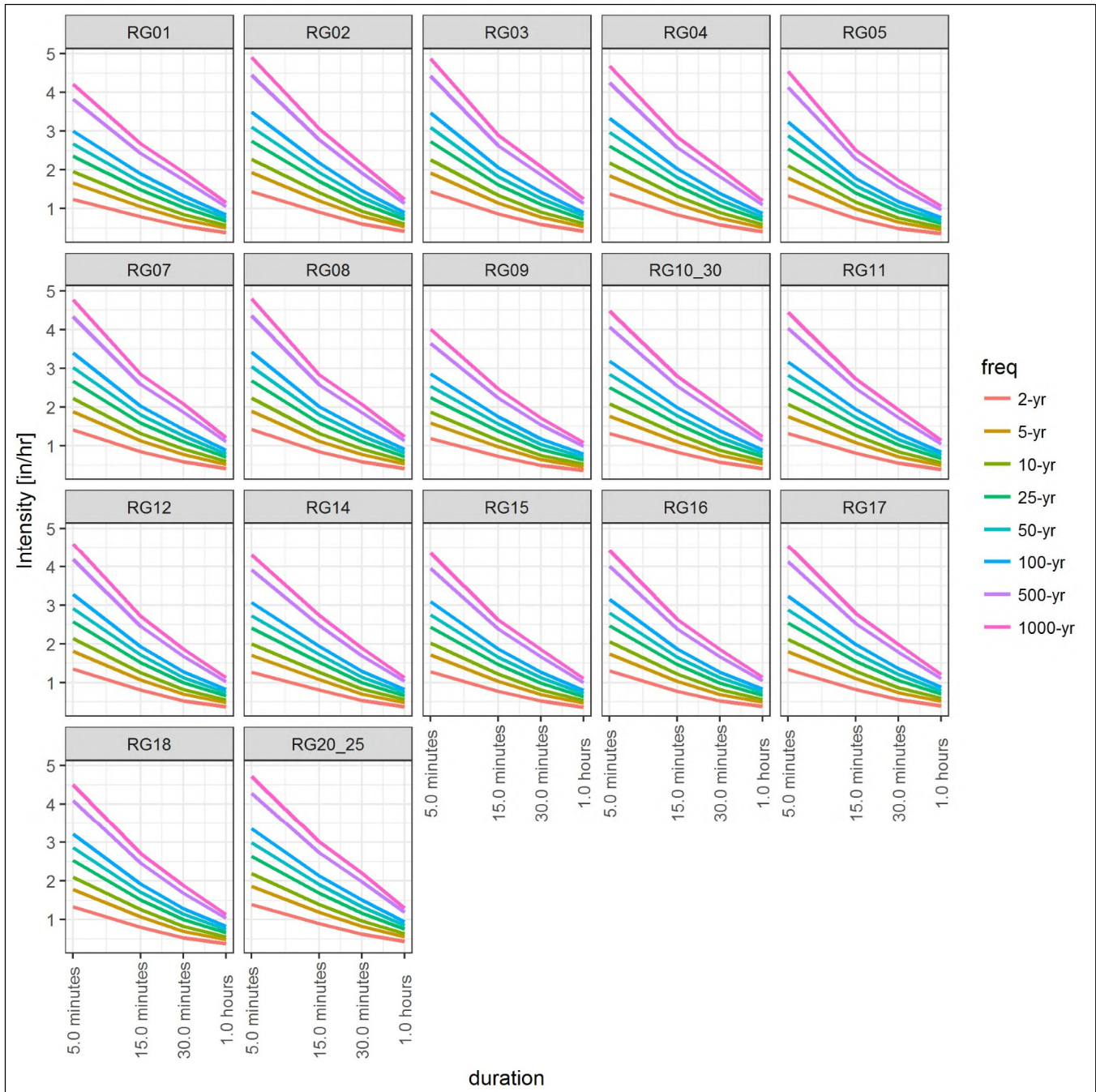


Figure 49. Station-by-Station L-Moment IDF Curves (5 minutes to 1 hour)

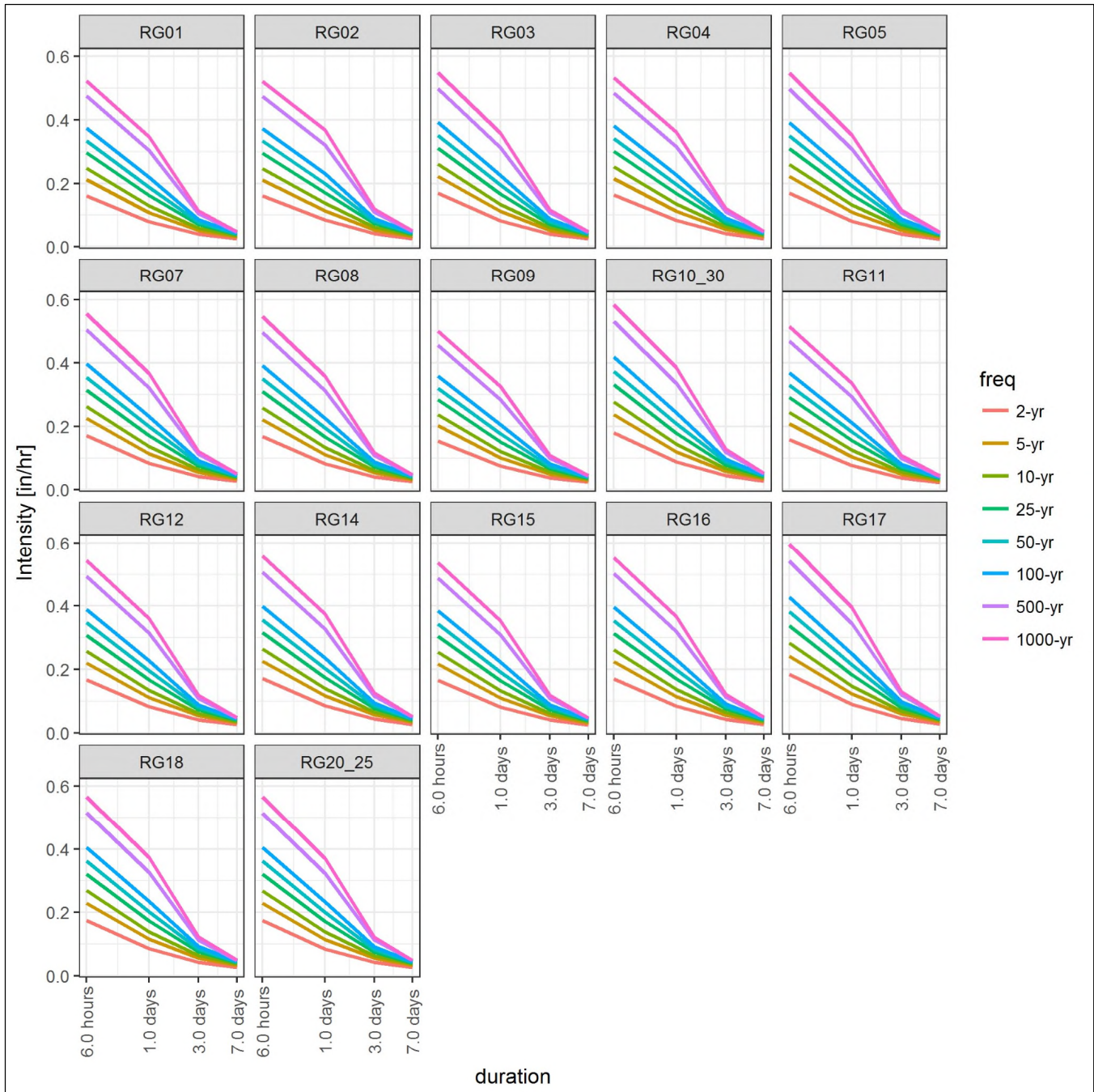


Figure 50. Station-by-Station L-Moment IDF Curves (6 hours to 7 days)

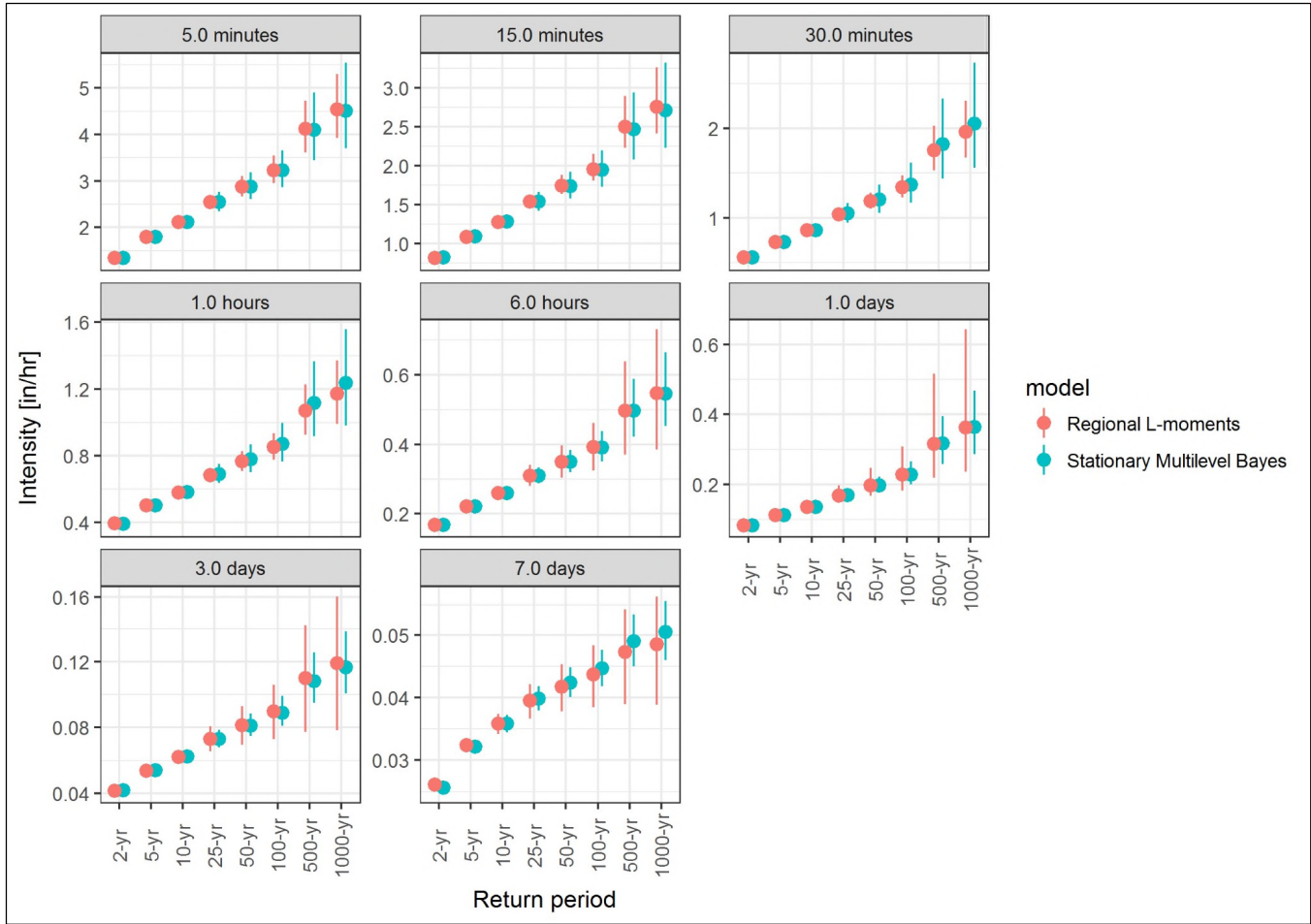


Figure 51. Point Estimates and 5% to 95% Uncertainty Bounds; Regional IDF Curves; L-Moments and Stationary Bayesian Multilevel Models

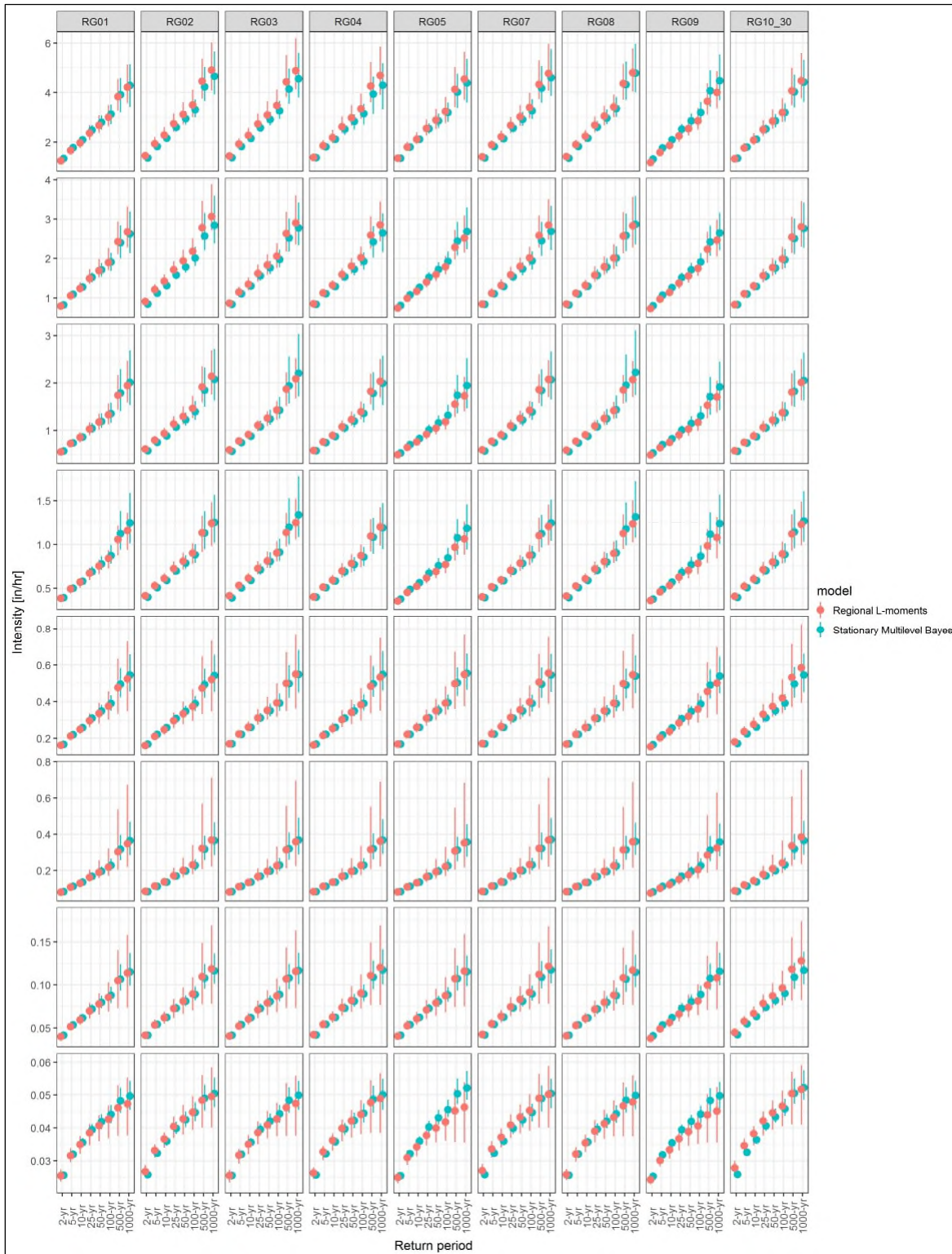


Figure 52a. Point Estimates, 5% to 95% Uncertainty Bounds; Individual Station IDF Curves; L-Moments and Stationary Bayesian Multilevel Models

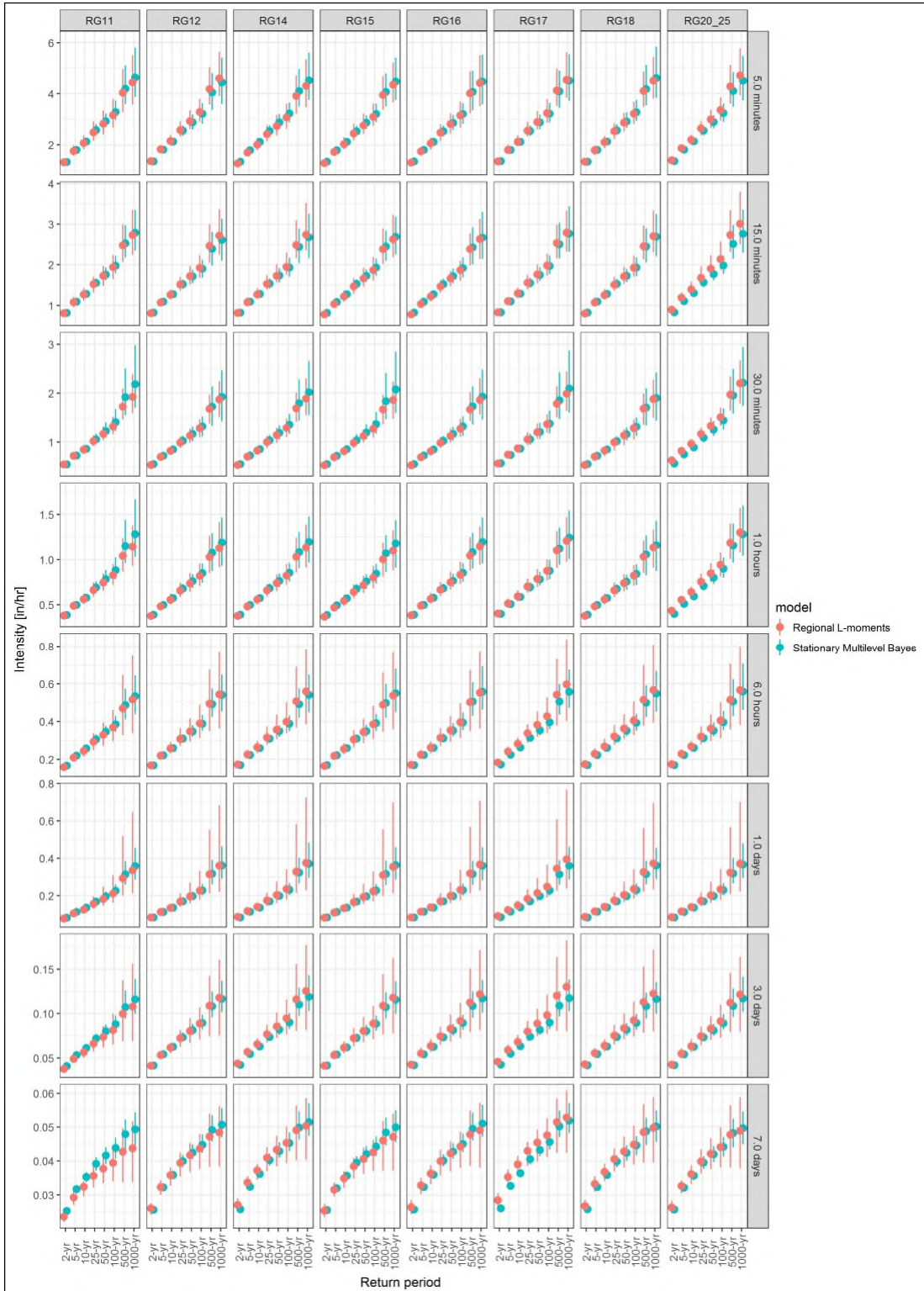
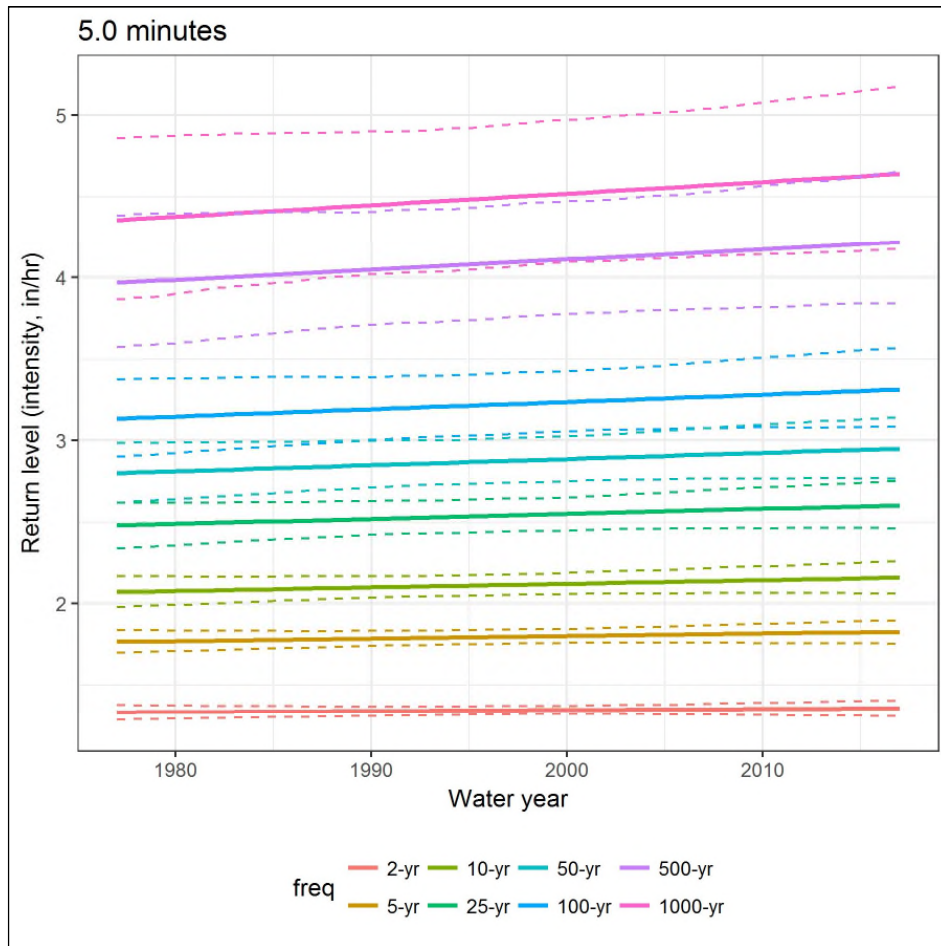
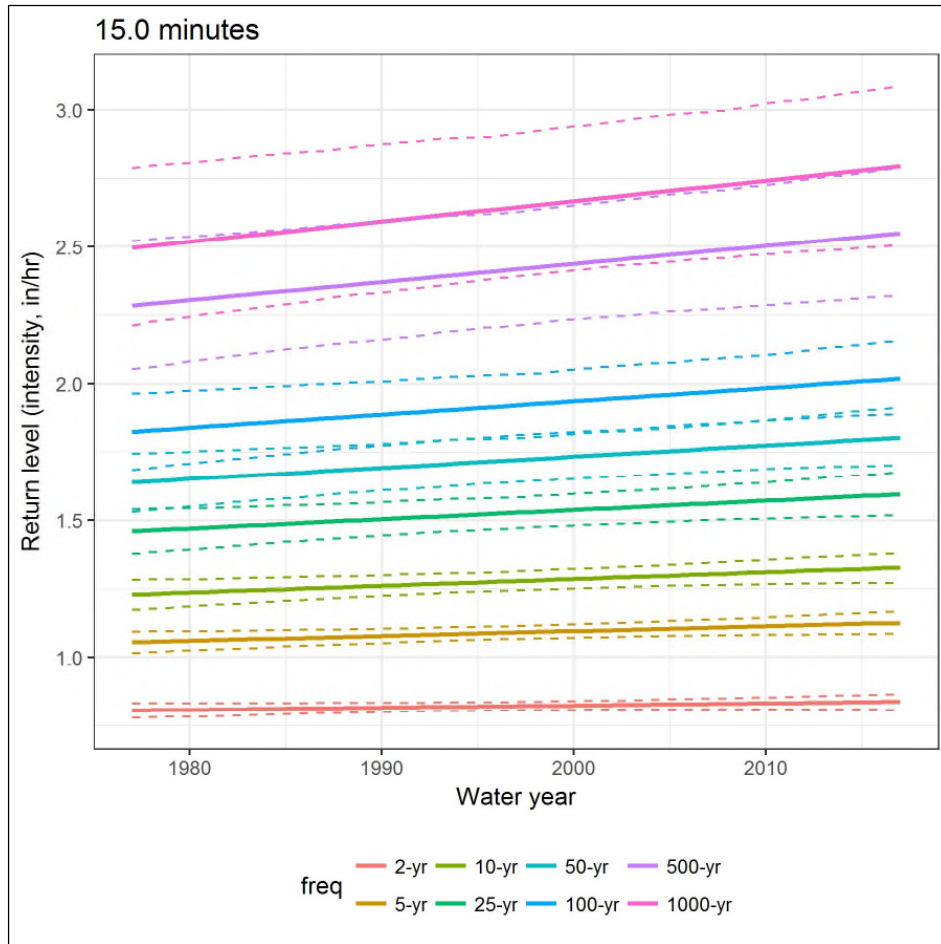


Figure 52b. Point Estimates, 5% to 95% Uncertainty Bounds; Individual Station IDF Curves; L-Moments and Stationary Bayesian Multilevel Models



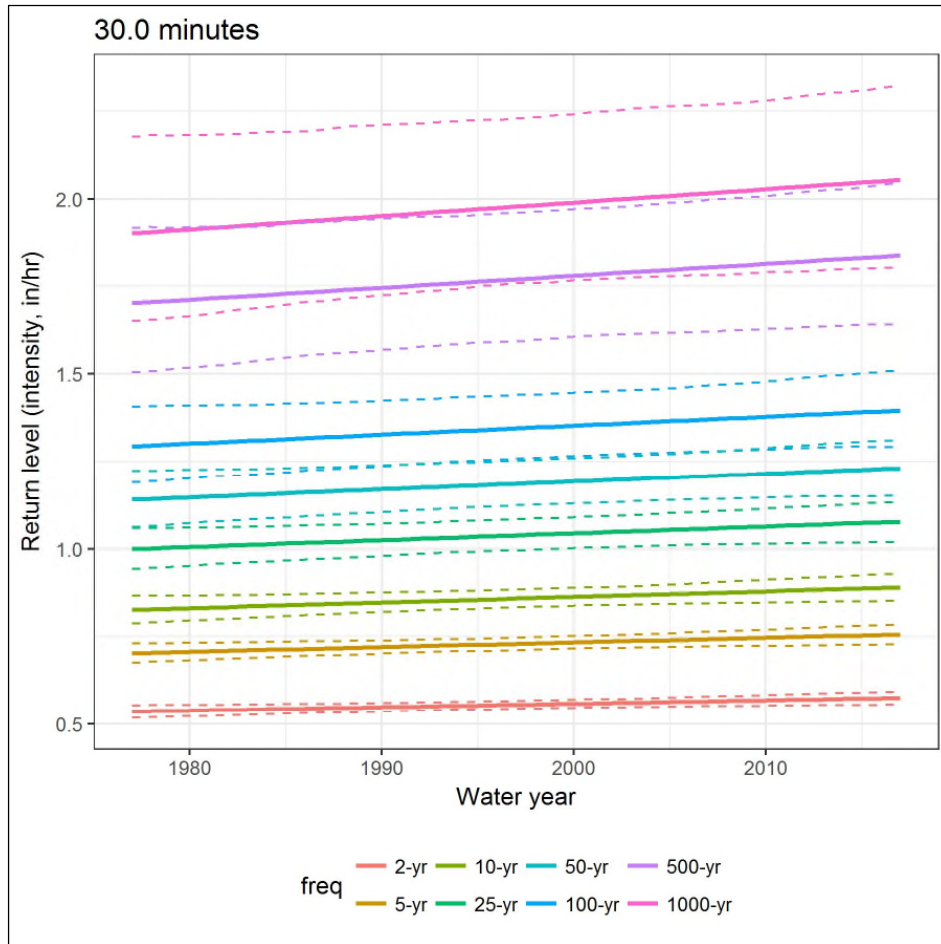
Multilevel GEV model with linear regression for parameters μ and σ using time and PDO as covariates. Solid line is posterior mean for time trend in intensity return level and dashed lines are posterior 10th and 90th percentiles.

Figure 53. Bayesian Time Trend Model for Duration 5.0 Minutes Using SPU Data



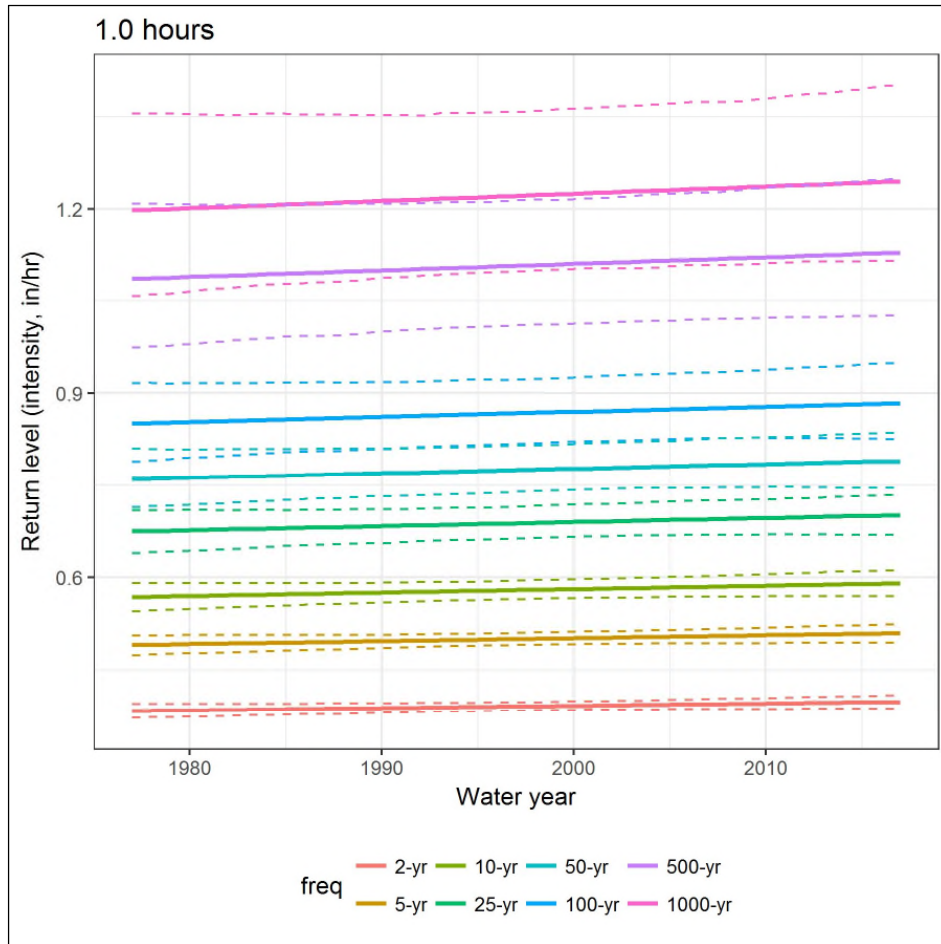
Multilevel GEV model with linear regression for parameters μ and σ using time and PDO as covariates. Solid line is posterior mean for time trend in intensity return level and dashed lines are posterior 10th and 90th percentiles.

Figure 54. Bayesian Time Trend Model for Duration 15.0 Minutes Using SPU Data



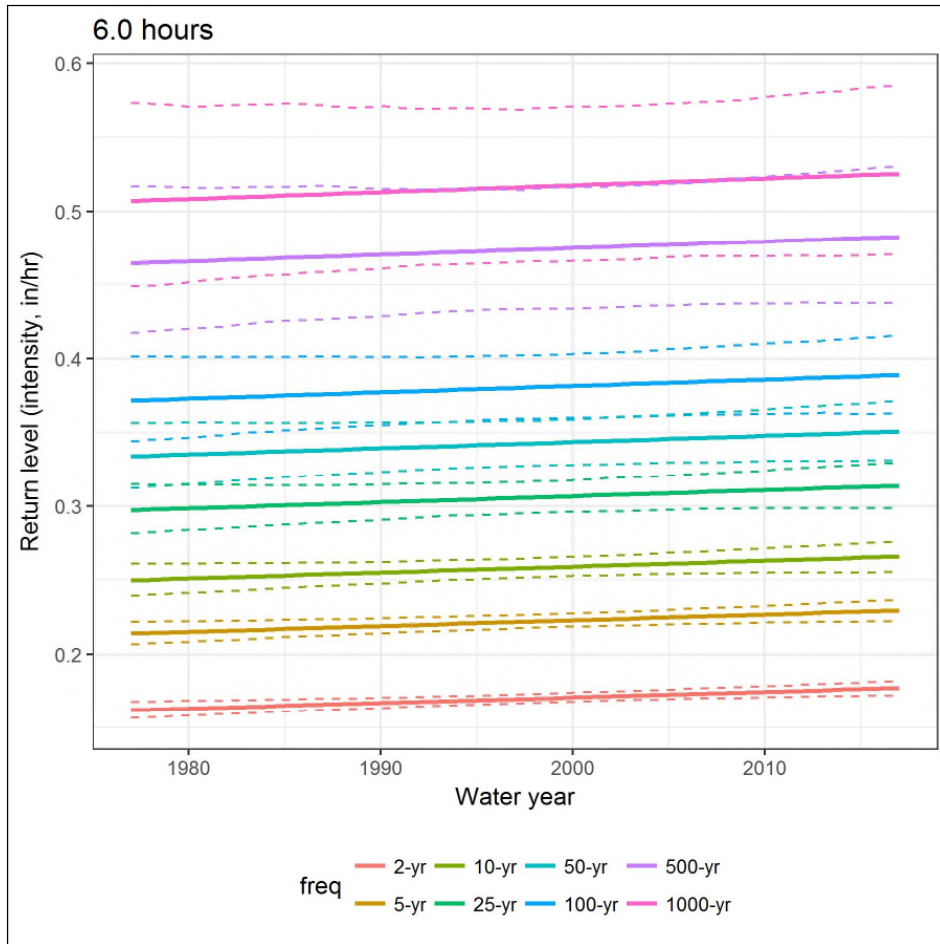
Multilevel GEV model with linear regression for parameters μ and σ using time and PDO as covariates. Solid line is posterior mean for time trend in intensity return level and dashed lines are posterior 10th and 90th percentiles.

Figure 55. Bayesian Time Trend Model for Duration 30.0 Minutes Using SPU Data



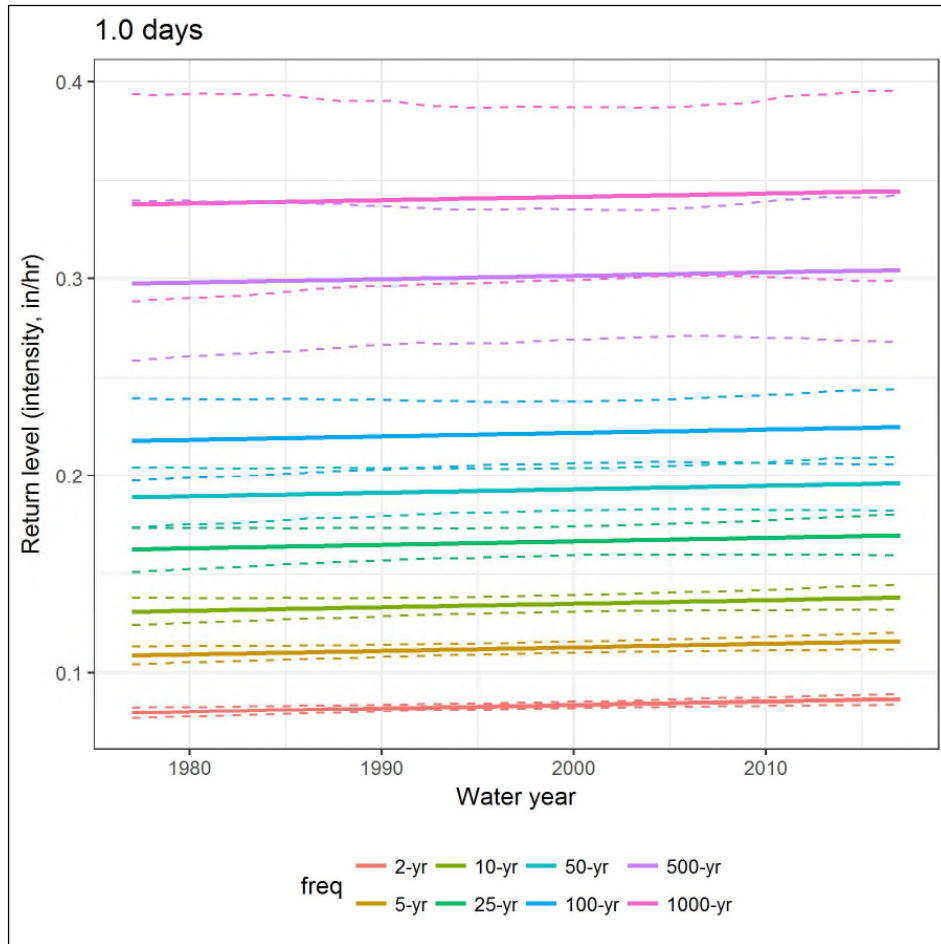
Multilevel GEV model with linear regression for parameters μ and σ using time and PDO as covariates. Solid line is posterior mean for time trend in intensity return level and dashed lines are posterior 10th and 90th percentiles.

Figure 56. Bayesian Time Trend Model for Duration 1.0 Hour Using SPU Data



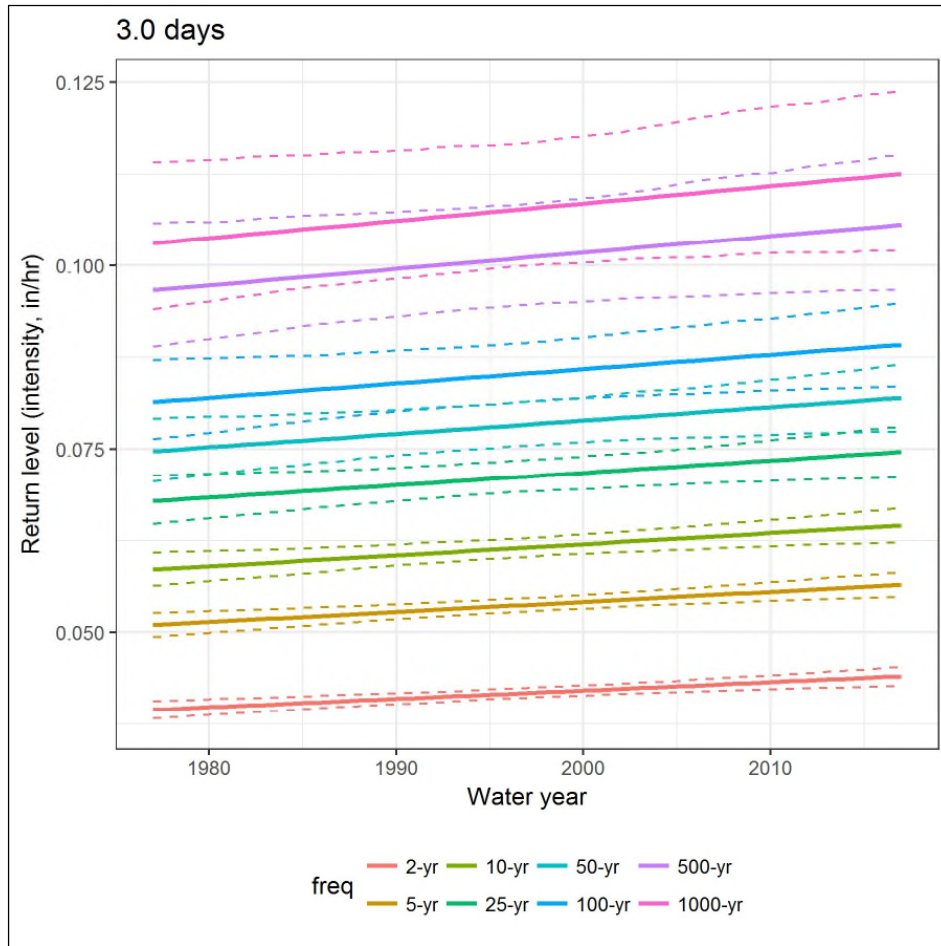
Multilevel GEV model with linear regression for parameters μ and σ using time and PDO as covariates. Solid line is posterior mean for time trend in intensity return level and dashed lines are posterior 10th and 90th percentiles.

Figure 57. Bayesian Time Trend Model for Duration 6.0 Hours Using SPU Data



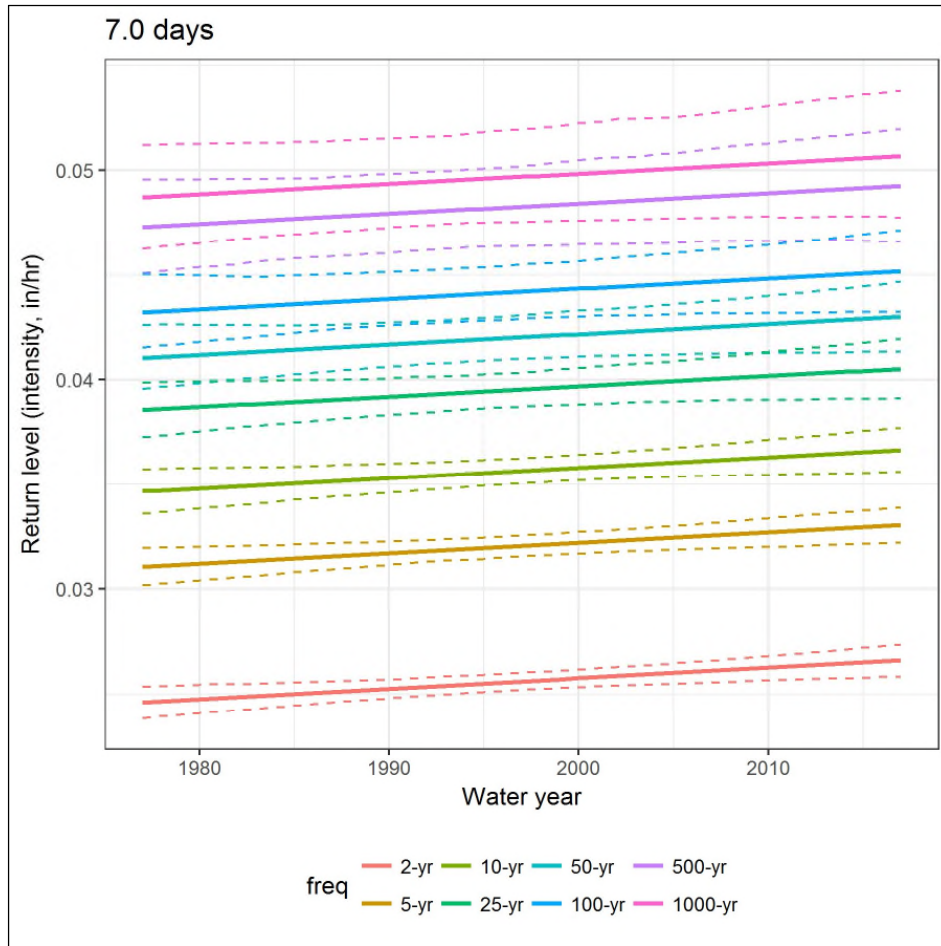
Multilevel GEV model with linear regression for parameters μ and σ using time and PDO as covariates. Solid line is posterior mean for time trend in intensity return level and dashed lines are posterior 10th and 90th percentiles.

Figure 58. Bayesian Time Trend Model for Duration 1.0 Day Using SPU Data



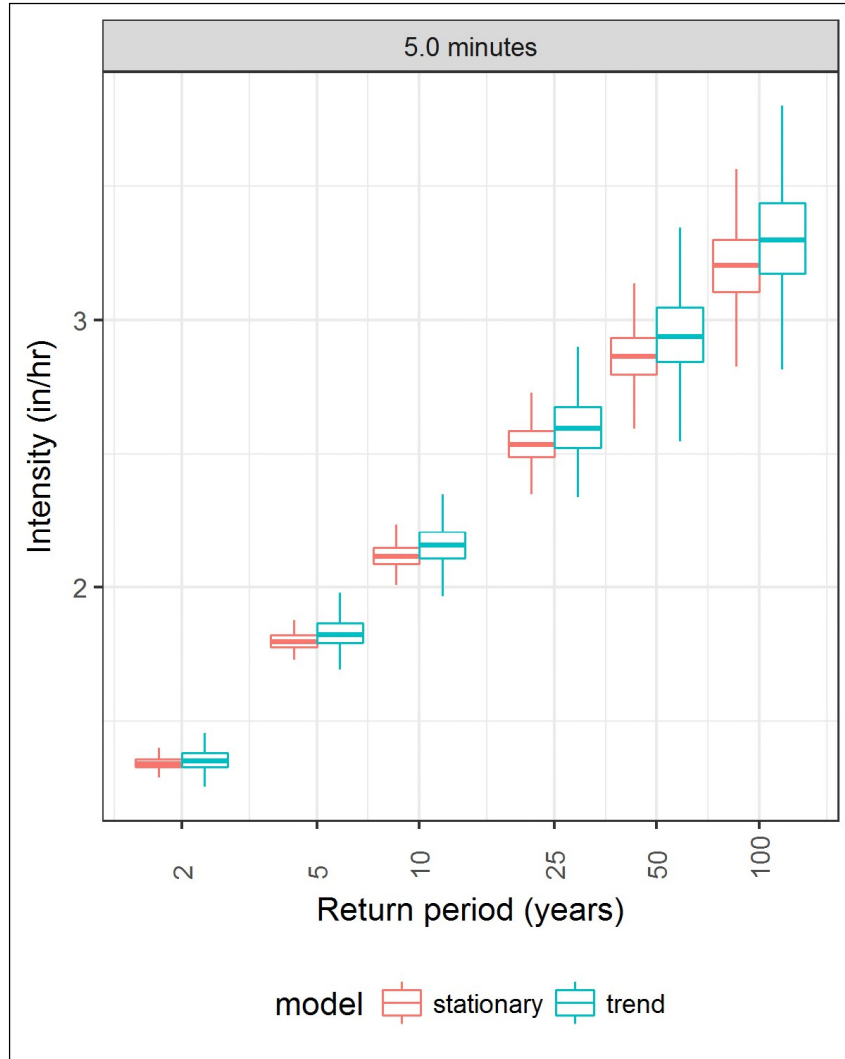
Multilevel GEV model with linear regression for parameters μ and σ using time and PDO as covariates. Solid line is posterior mean for time trend in intensity return level and dashed lines are posterior 10th and 90th percentiles.

Figure 59. Bayesian Time Trend Model for Duration 3.0 Days Using SPU Data



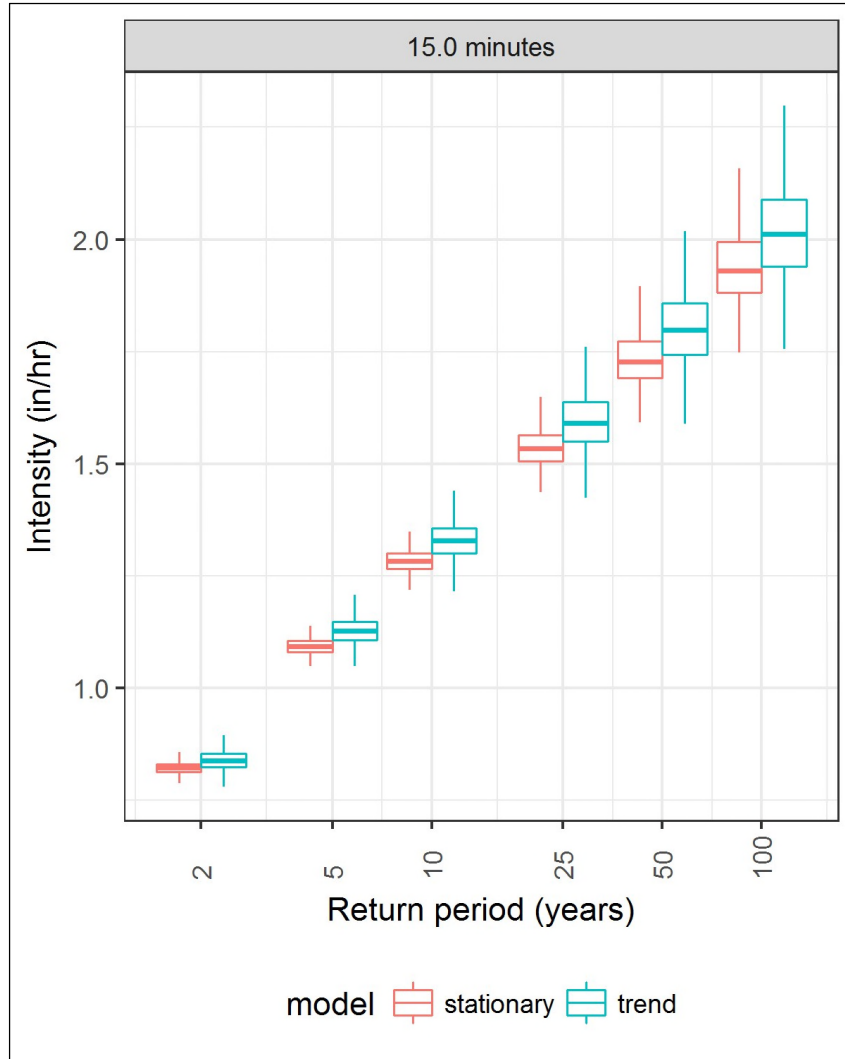
Multilevel GEV model with linear regression for parameters μ and σ using time and PDO as covariates. Solid line is posterior mean for time trend in intensity return level and dashed lines are posterior 10th and 90th percentiles.

Figure 60. Bayesian Time Trend Model for Duration 7.0 Days Using SPU Data



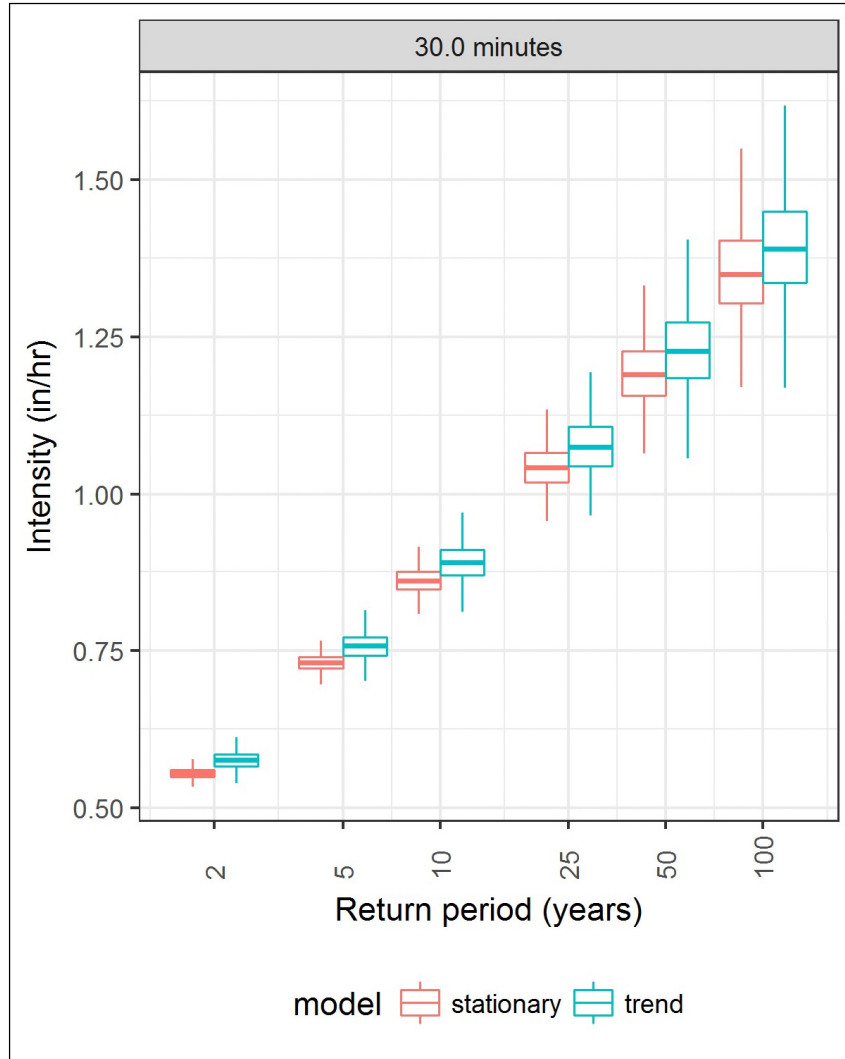
Time and PDO coefficients are fixed to zero.

Figure 61. Comparison of 5-Minute-Duration Intensity Return Levels, Bayesian Time Trend and Stationary



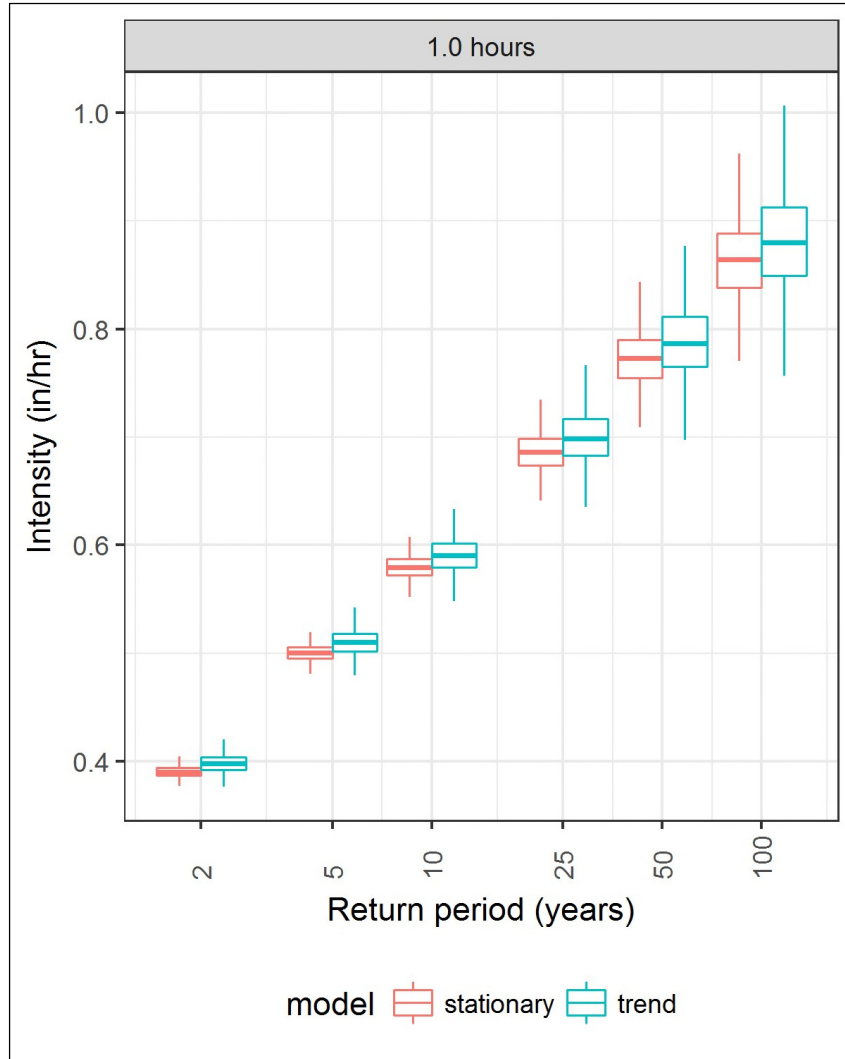
Time and PDO coefficients are fixed to zero.

Figure 62. Comparison of 15-Minute-Duration Intensity Return Levels, Bayesian Time Trend and Stationary



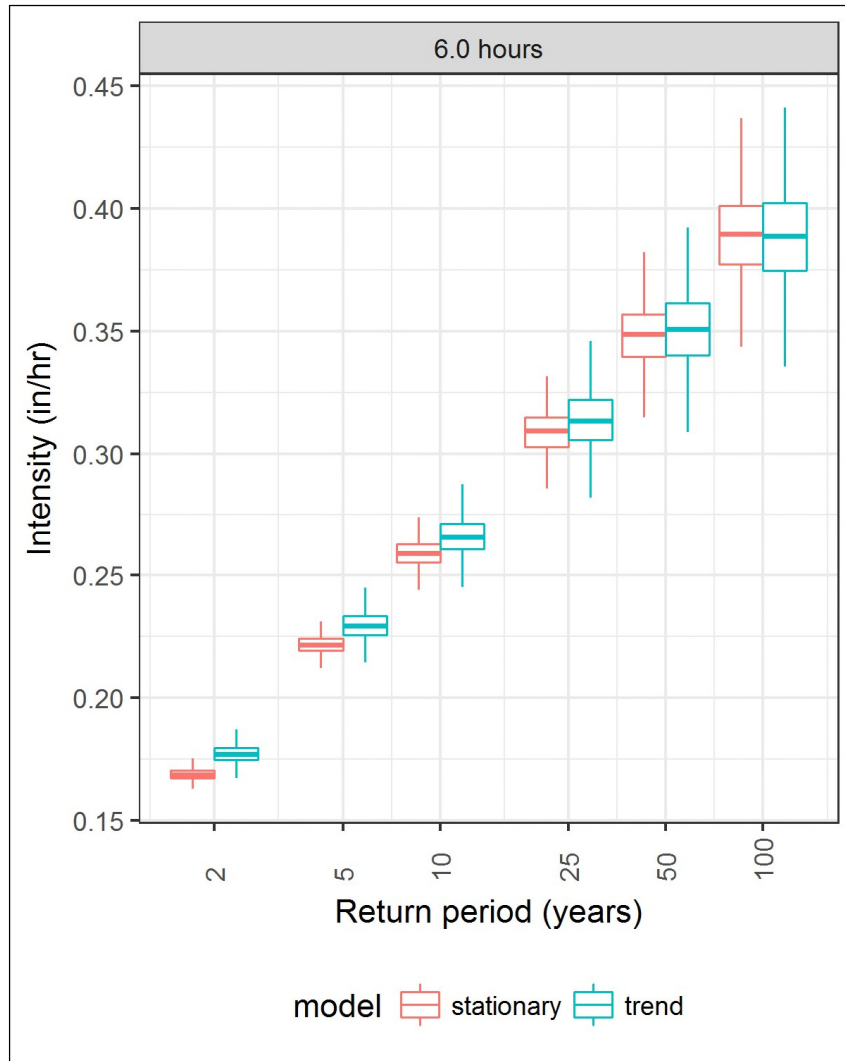
Time and PDO coefficients are fixed to zero.

Figure 63. Comparison of 30-Minute-Duration Intensity Return Levels, Bayesian Time Trend and Stationary



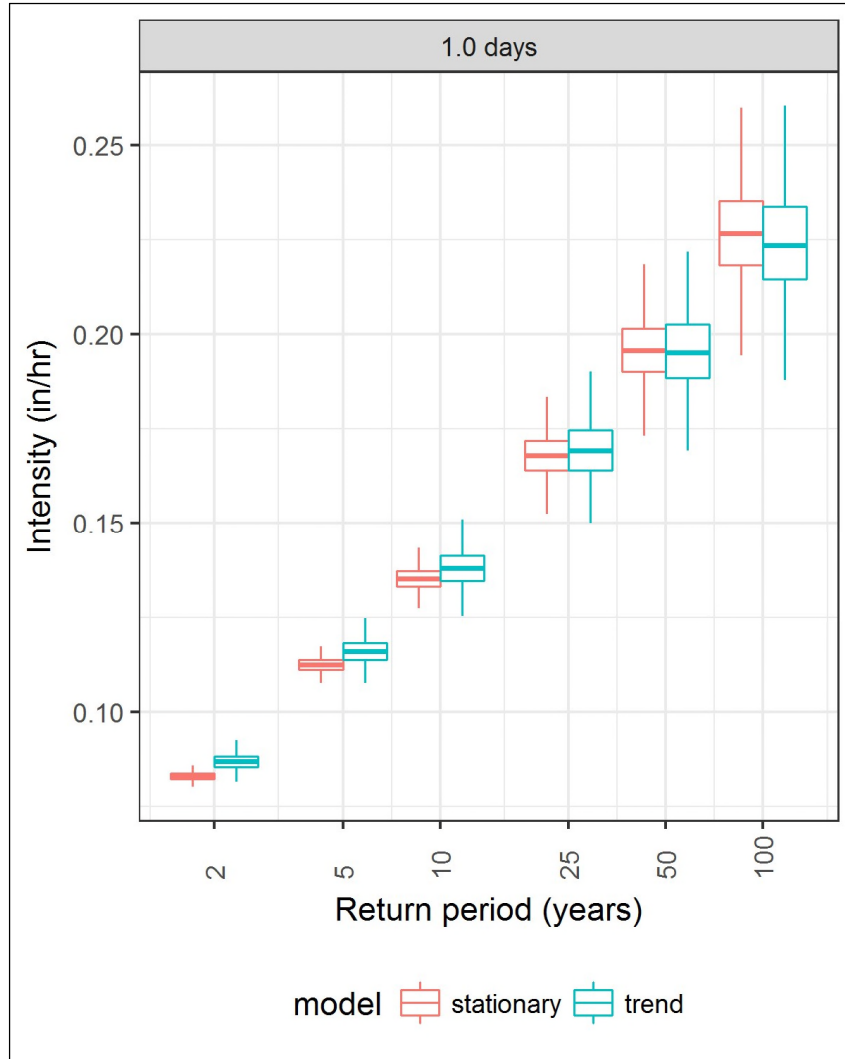
Time and PDO coefficients are fixed to zero.

Figure 64. Comparison of 1-Hour-Duration Intensity Return Levels, Bayesian Time Trend and Stationary



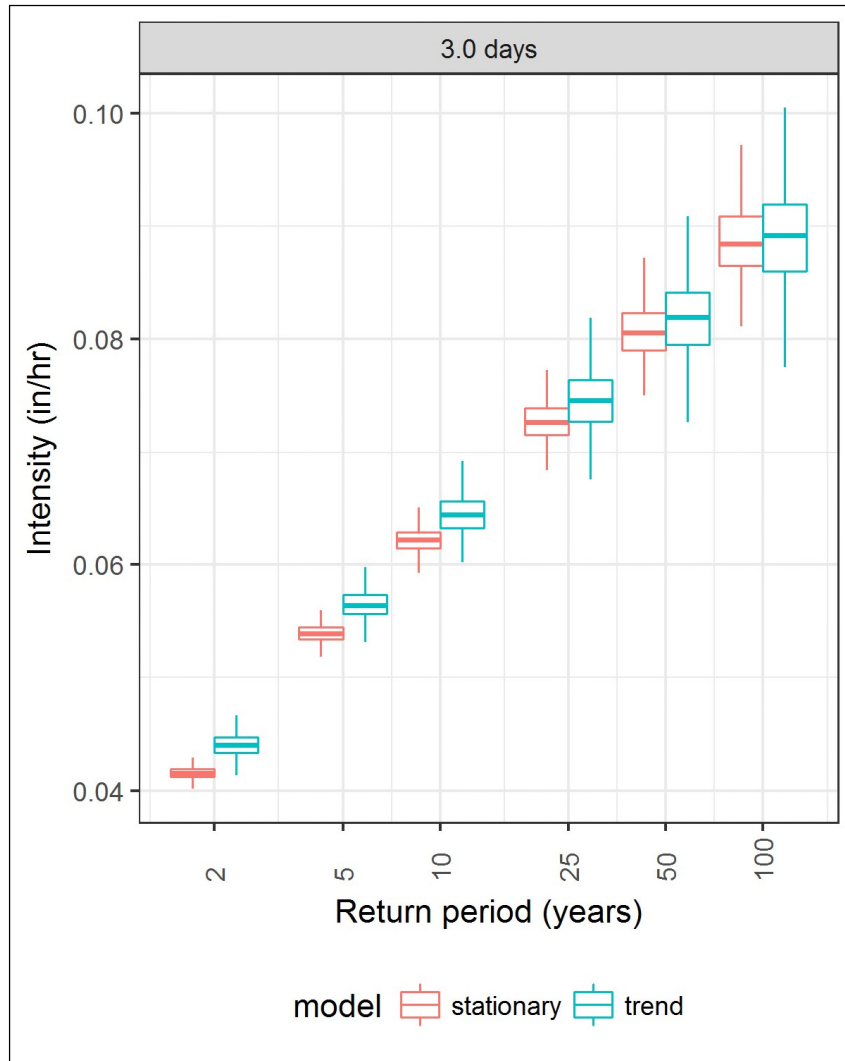
Time and PDO coefficients are fixed to zero.

Figure 65. Comparison of 6-Hour-Duration Intensity Return Levels, Bayesian Time Trend and Stationary



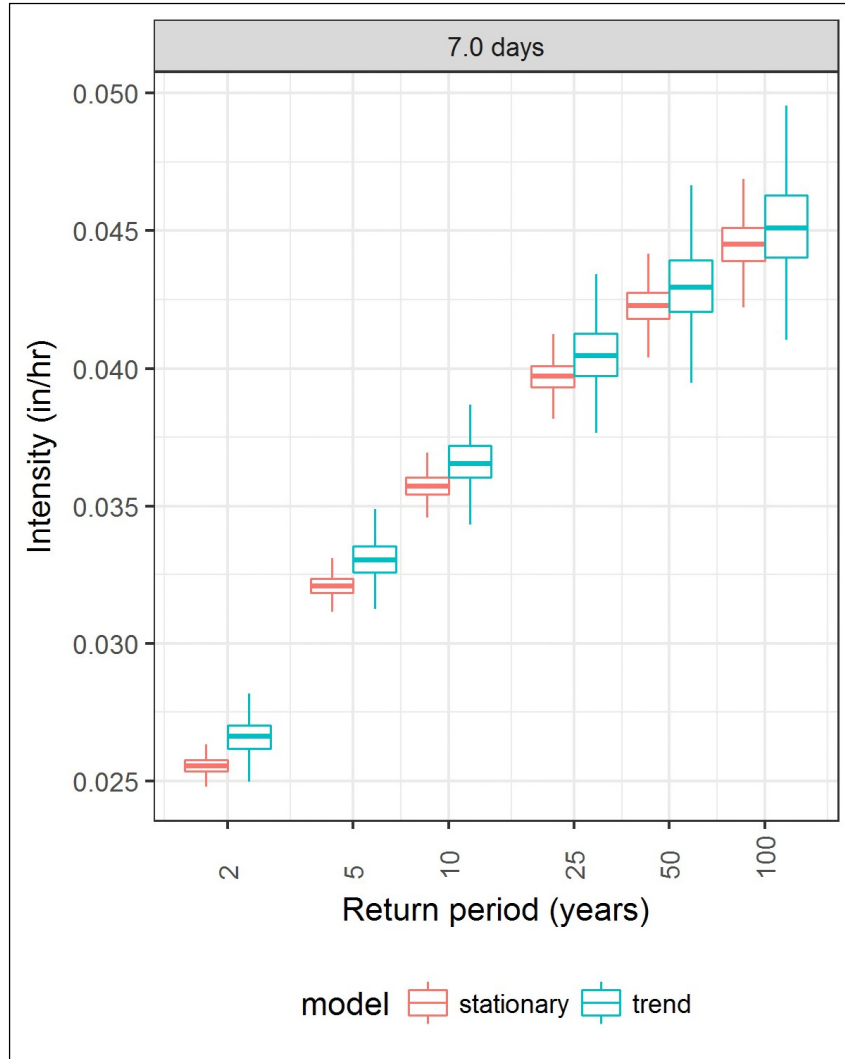
Time and PDO coefficients are fixed to zero.

Figure 66. Comparison of 1-Day-Duration Intensity Return Levels, Bayesian Time Trend and Stationary



Time and PDO coefficients are fixed to zero.

Figure 67. Comparison of 3-Day-Duration Intensity Return Levels, Bayesian Time Trend and Stationary



Time and PDO coefficients are fixed to zero.

Figure 68. Comparison of 7-Day-Duration Intensity Return Levels, Bayesian Time Trend and Stationary

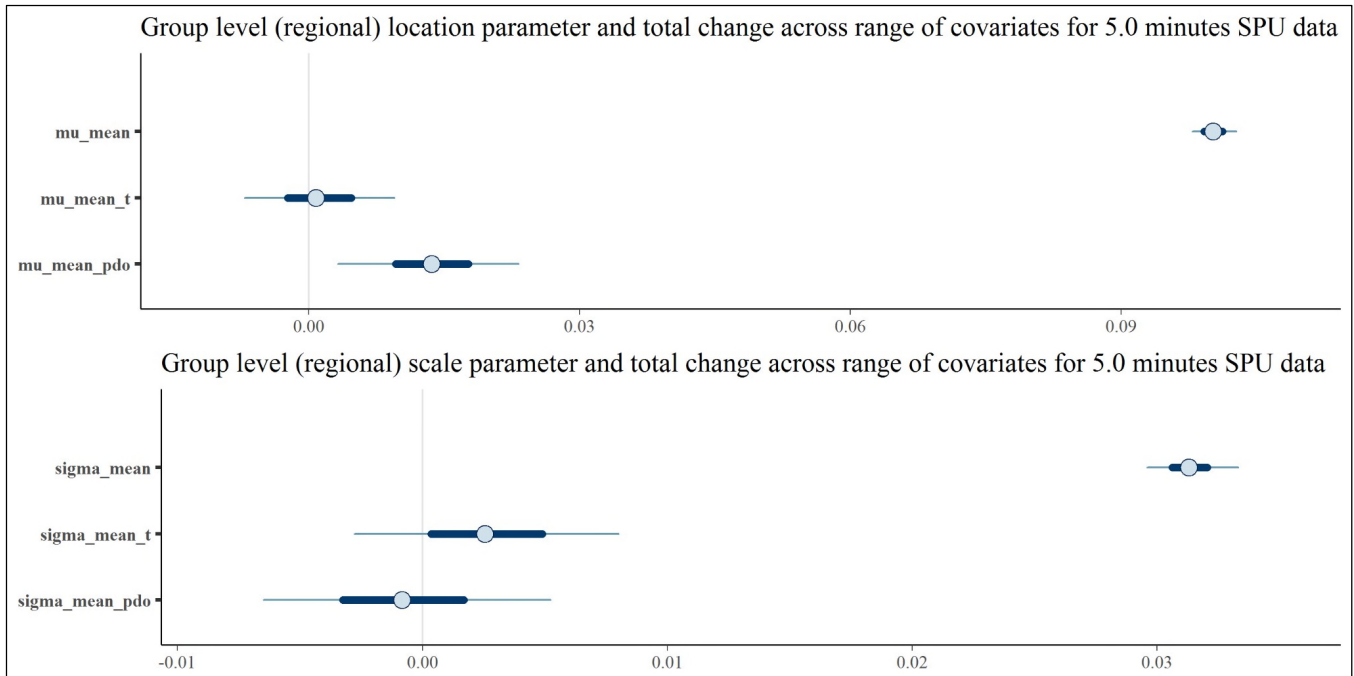


Figure 69. Posterior Medians, 50%, and 90% Intervals for Group-Level GEV Regression Parameters, 5Minute Duration

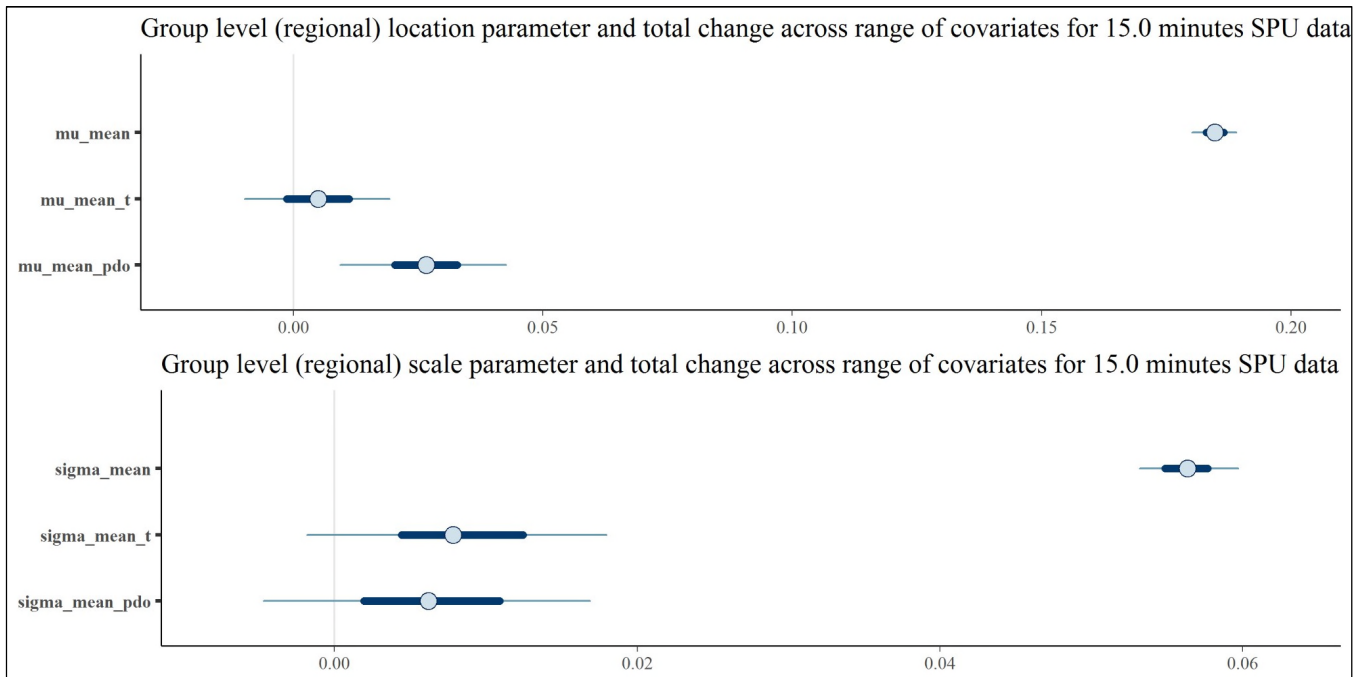


Figure 70. Posterior Medians, 50%, and 90% Intervals for Group-Level GEV Regression Parameters, 15Minute Duration

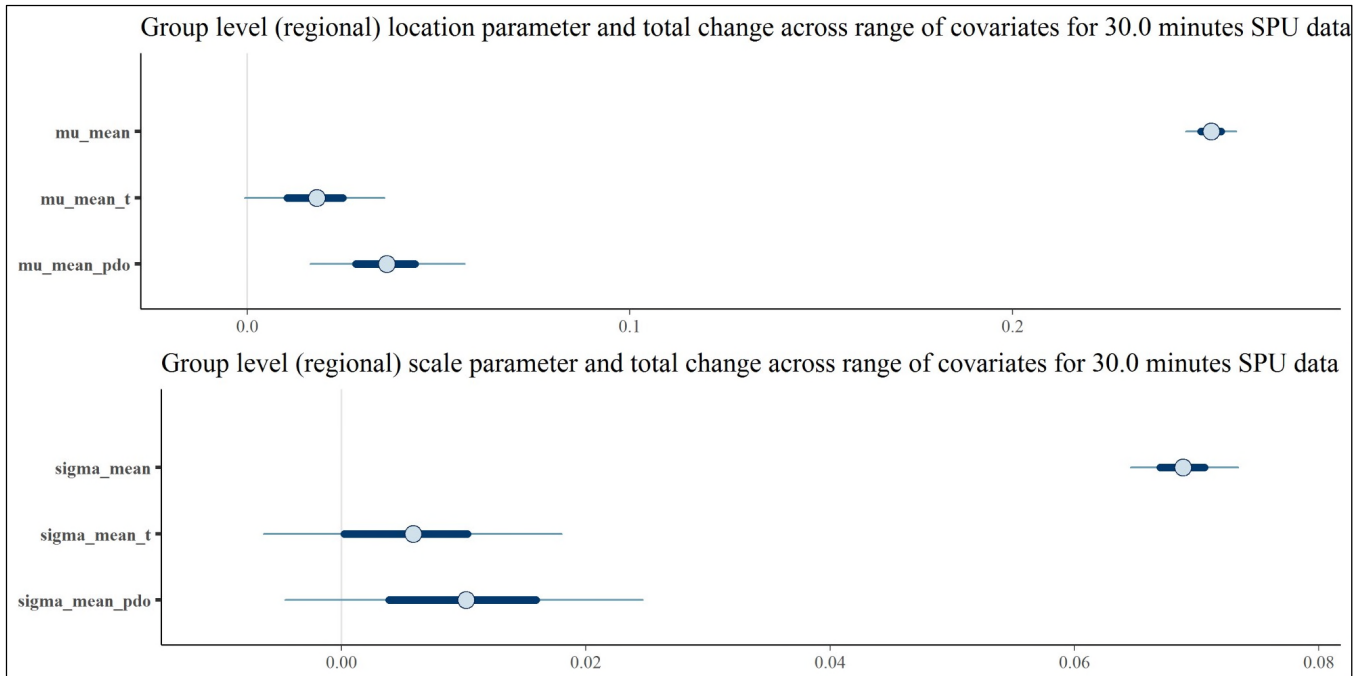


Figure 71. Posterior Medians, 50%, and 90% Intervals for Group-Level GEV Regression Parameters, 30Minute Duration

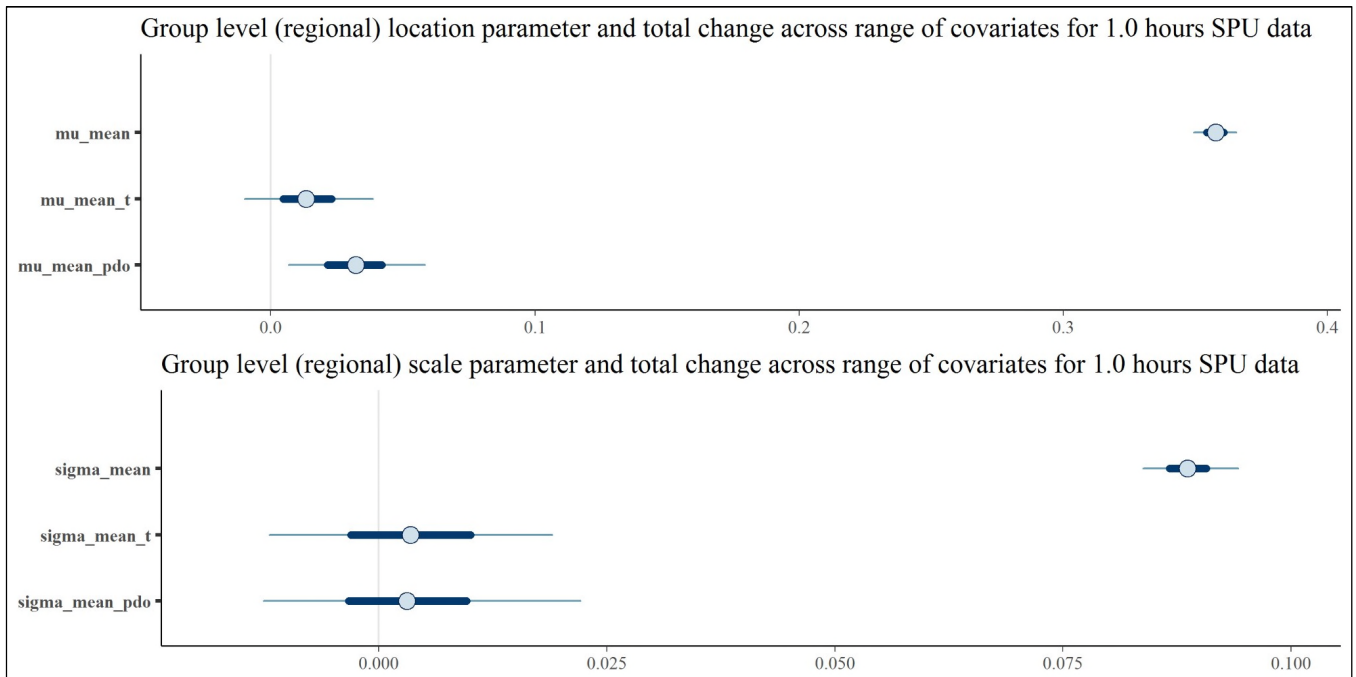


Figure 72. Posterior Medians, 50%, and 90% Intervals for Group-Level GEV Regression Parameters, 1Hour Duration

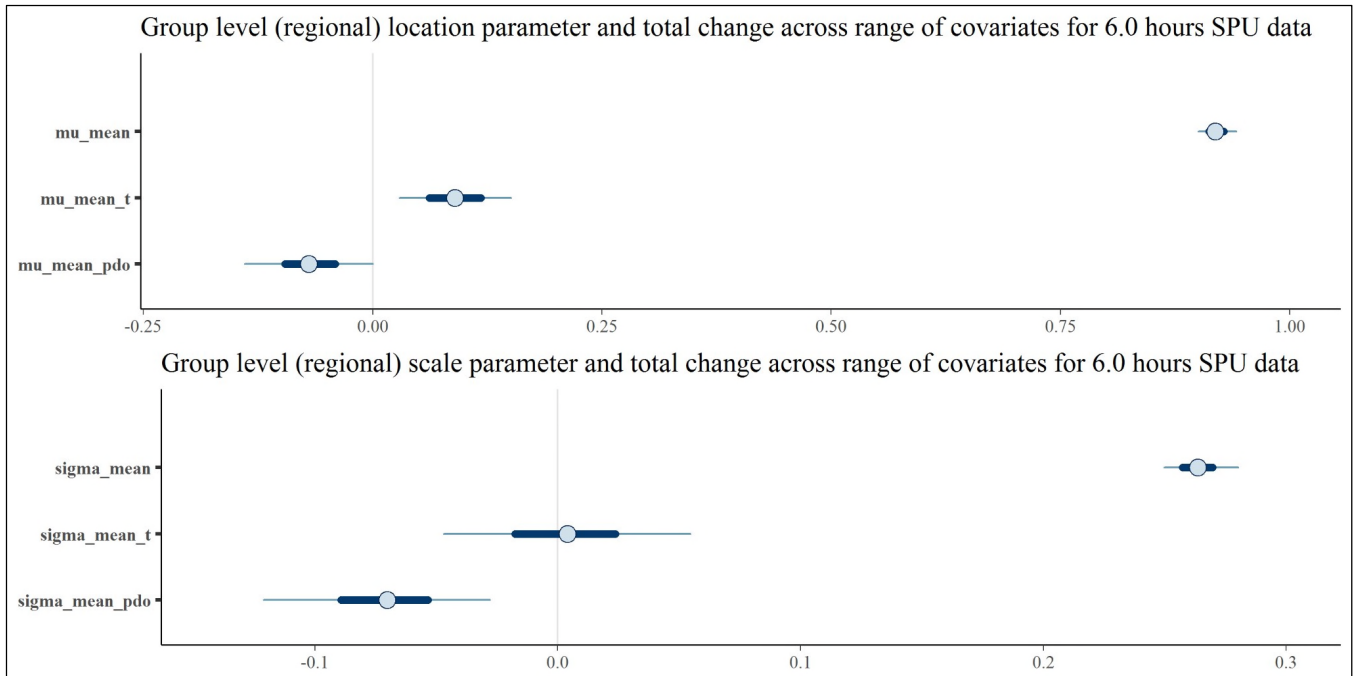


Figure 73. Posterior Medians, 50%, and 90% Intervals for Group-Level GEV Regression Parameters, 6Hour Duration

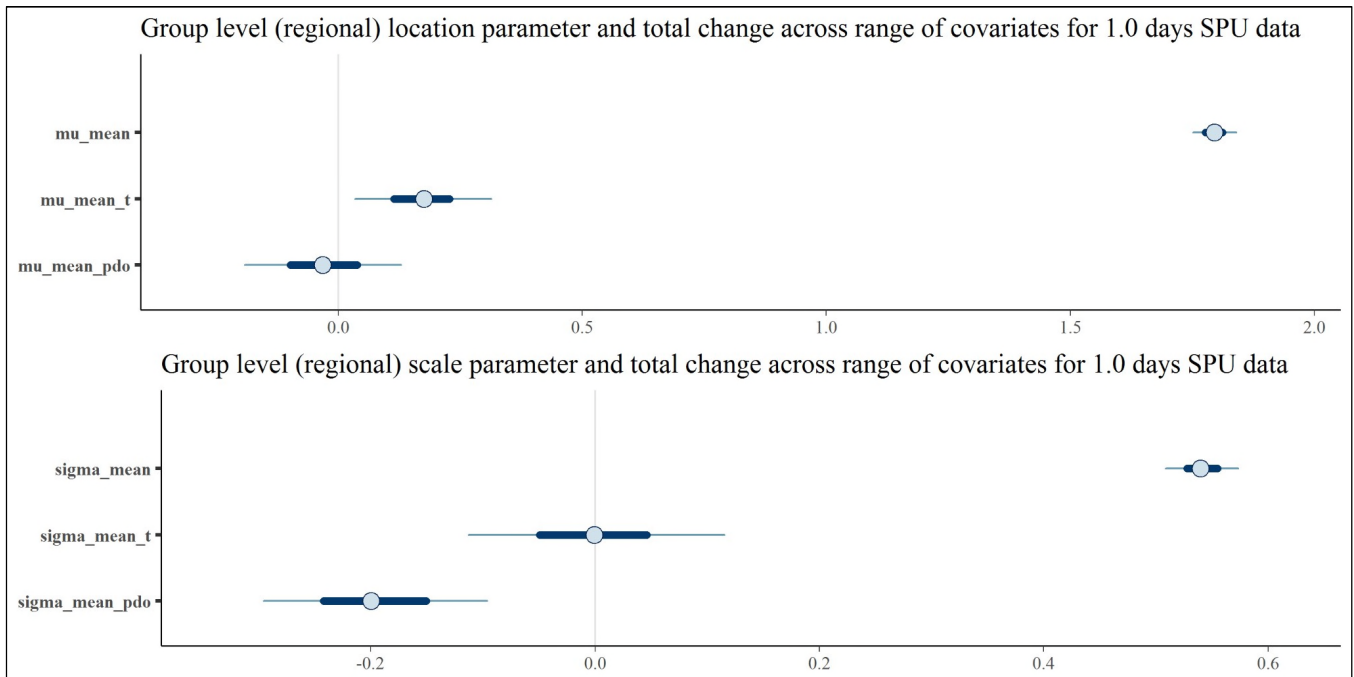


Figure 74. Posterior Medians, 50%, and 90% Intervals for Group-Level GEV Regression Parameters, 1Day Duration

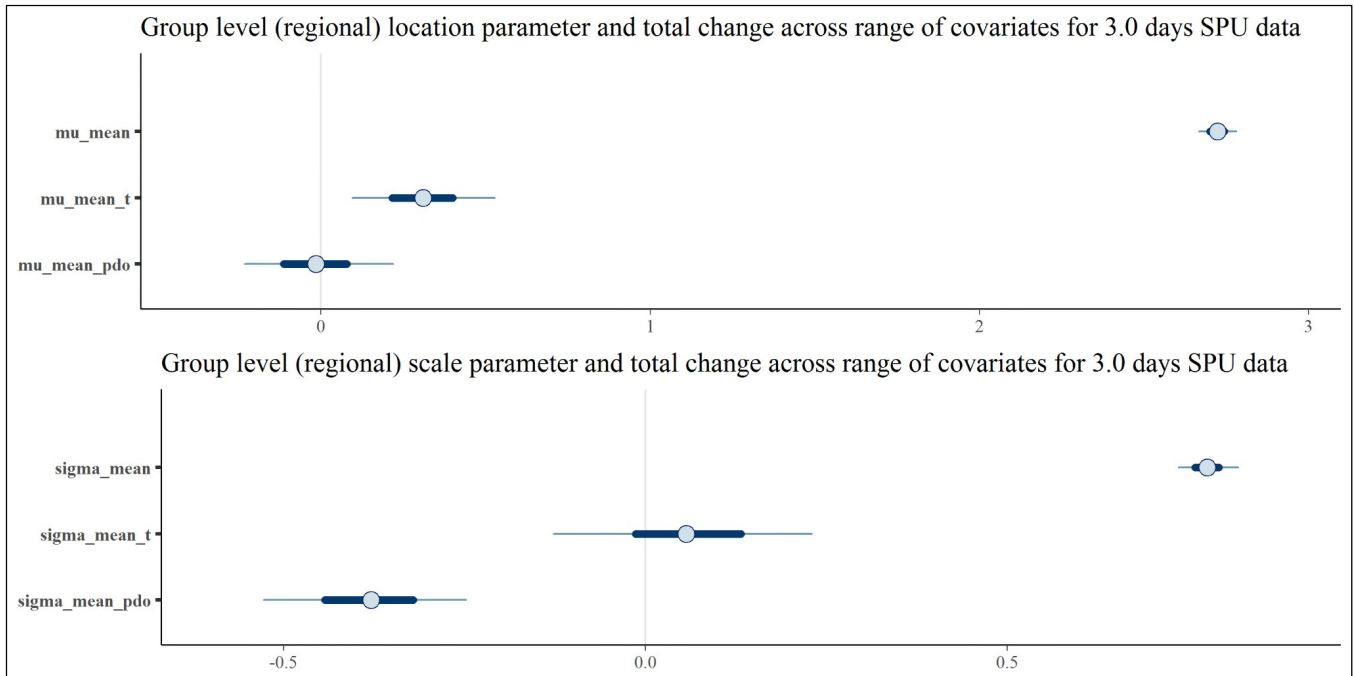


Figure 75. Posterior Medians, 50%, and 90% Intervals for Group-Level GEV Regression Parameters, 3Day Duration

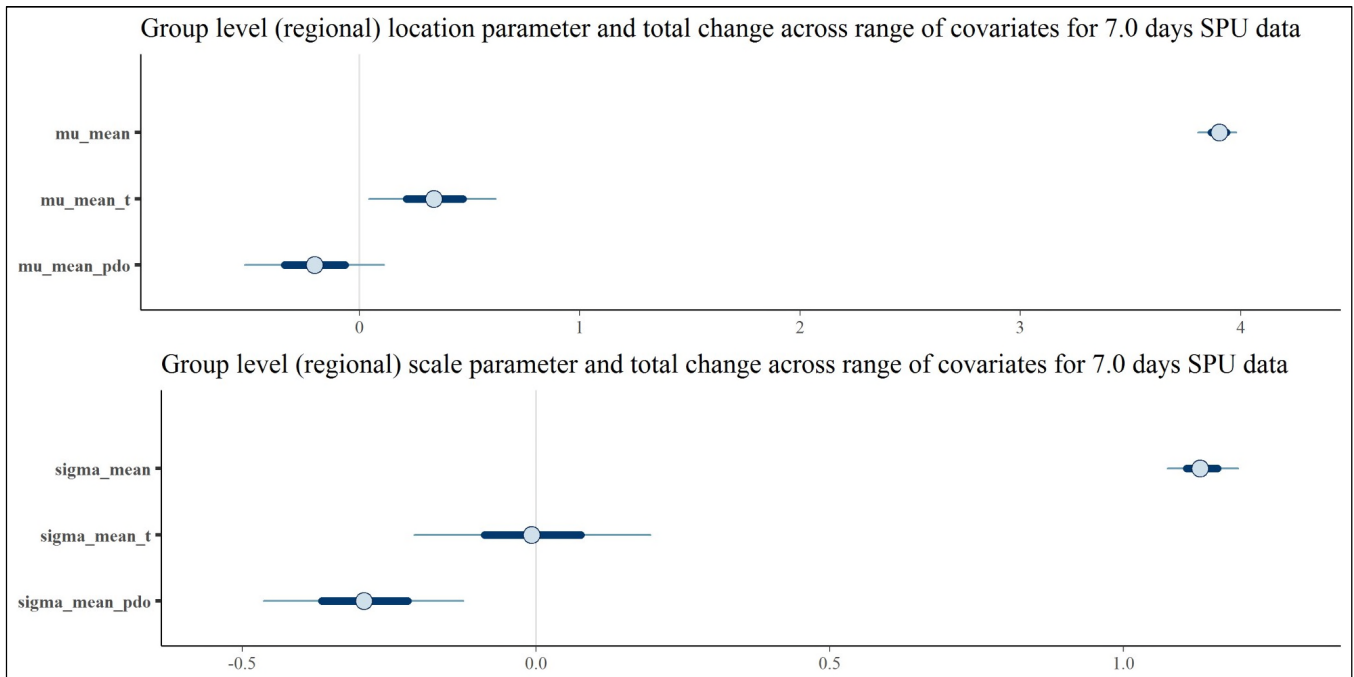
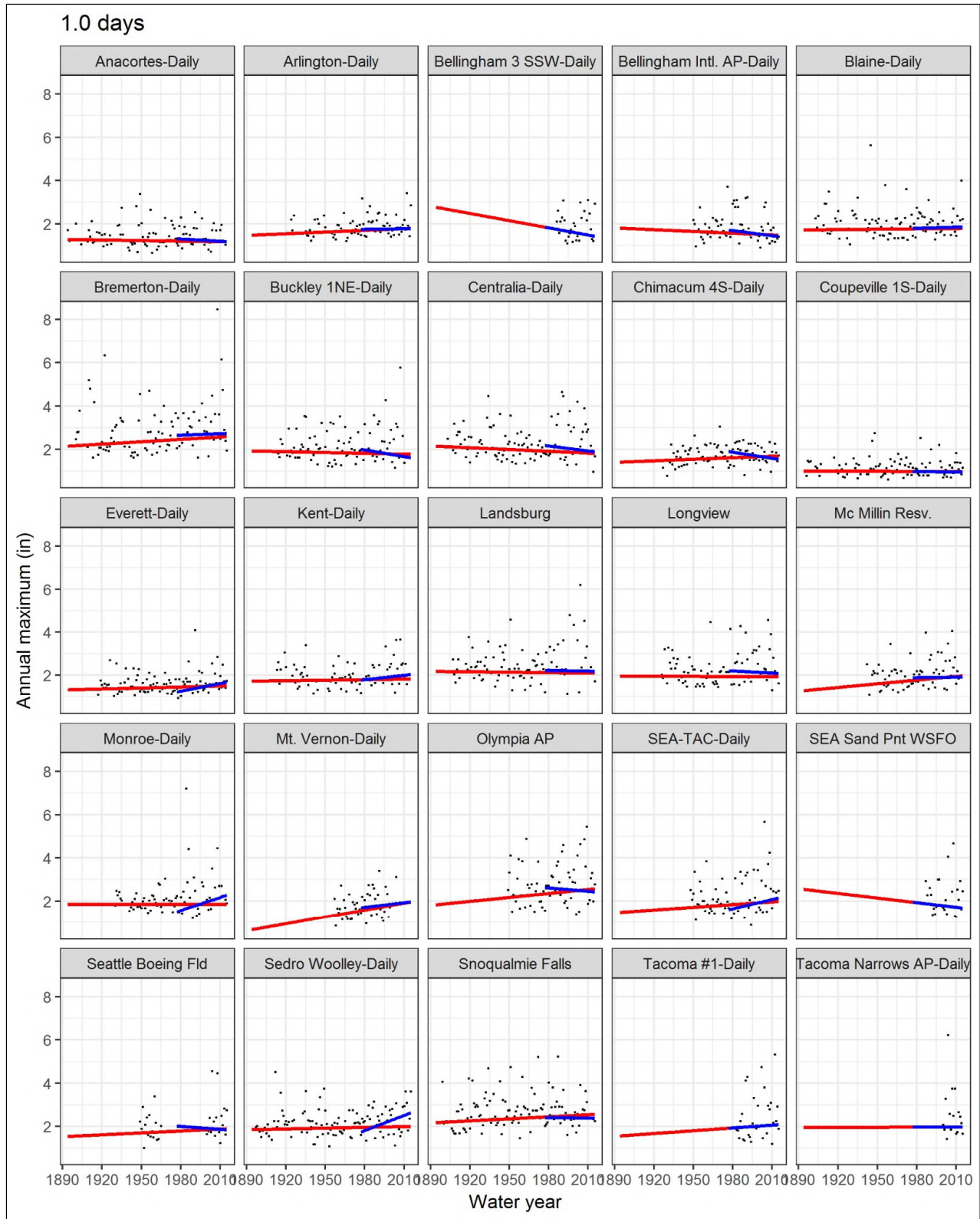
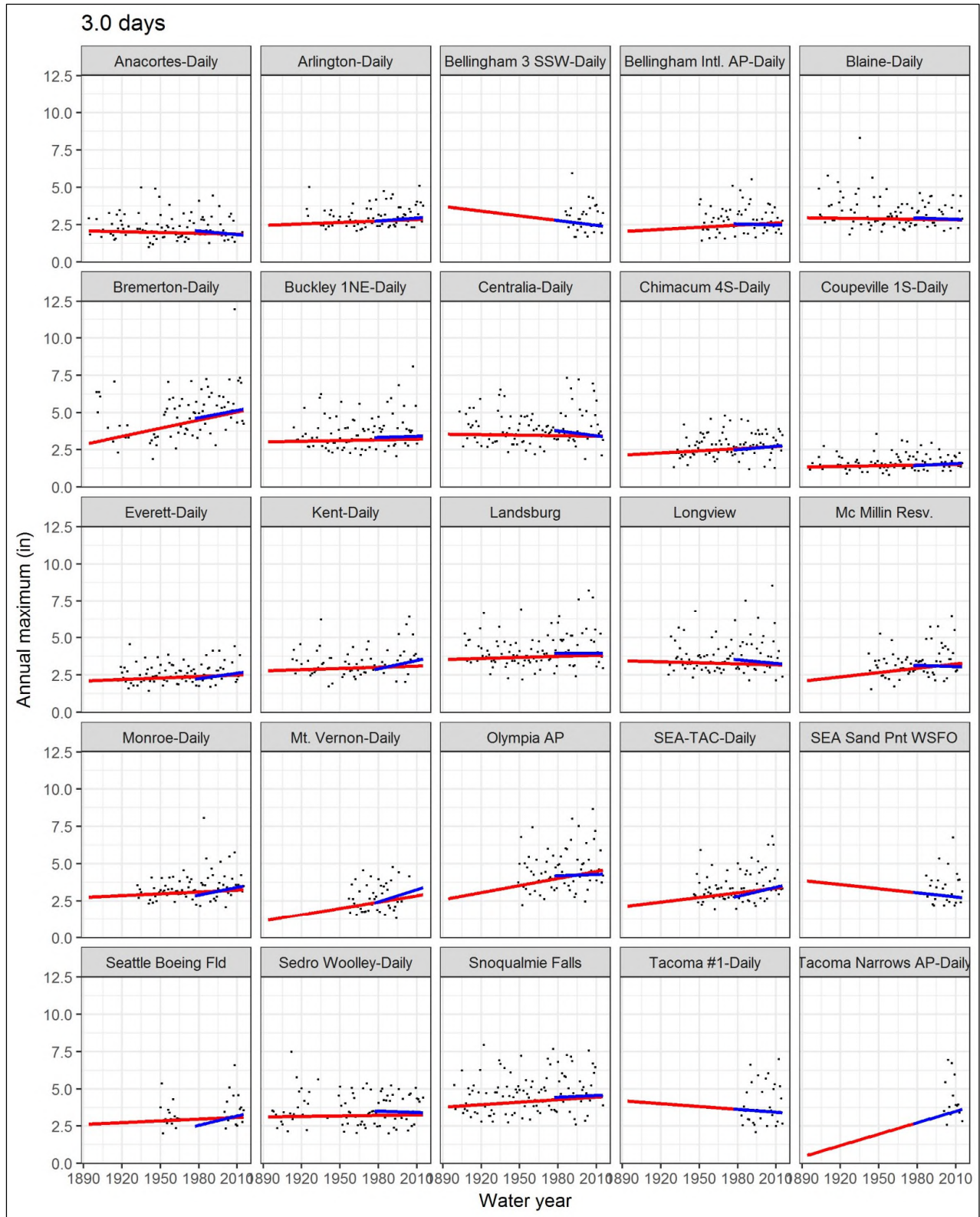


Figure 76. Posterior Medians, 50%, and 90% Intervals for Group-Level GEV Regression Parameters, 7Day Duration



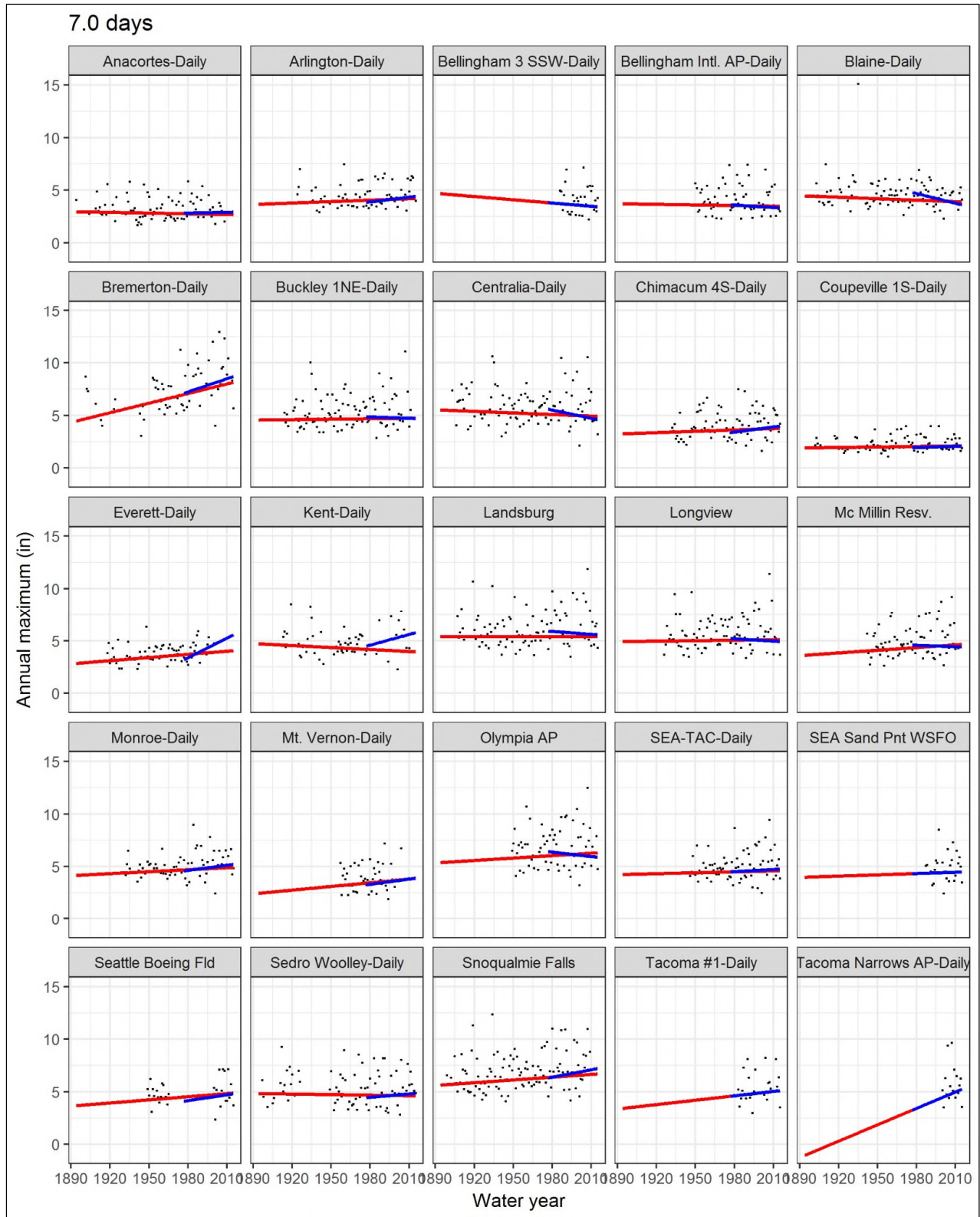
Red indicates all available data, blue indicates starting in 1977, the starting point of provided SPU data.

Figure 77. By-Station Estimates for Trends in Location Parameter of Maximum Likelihood Estimated GEV Regression Model Using NWS Data, 1-Day Duration



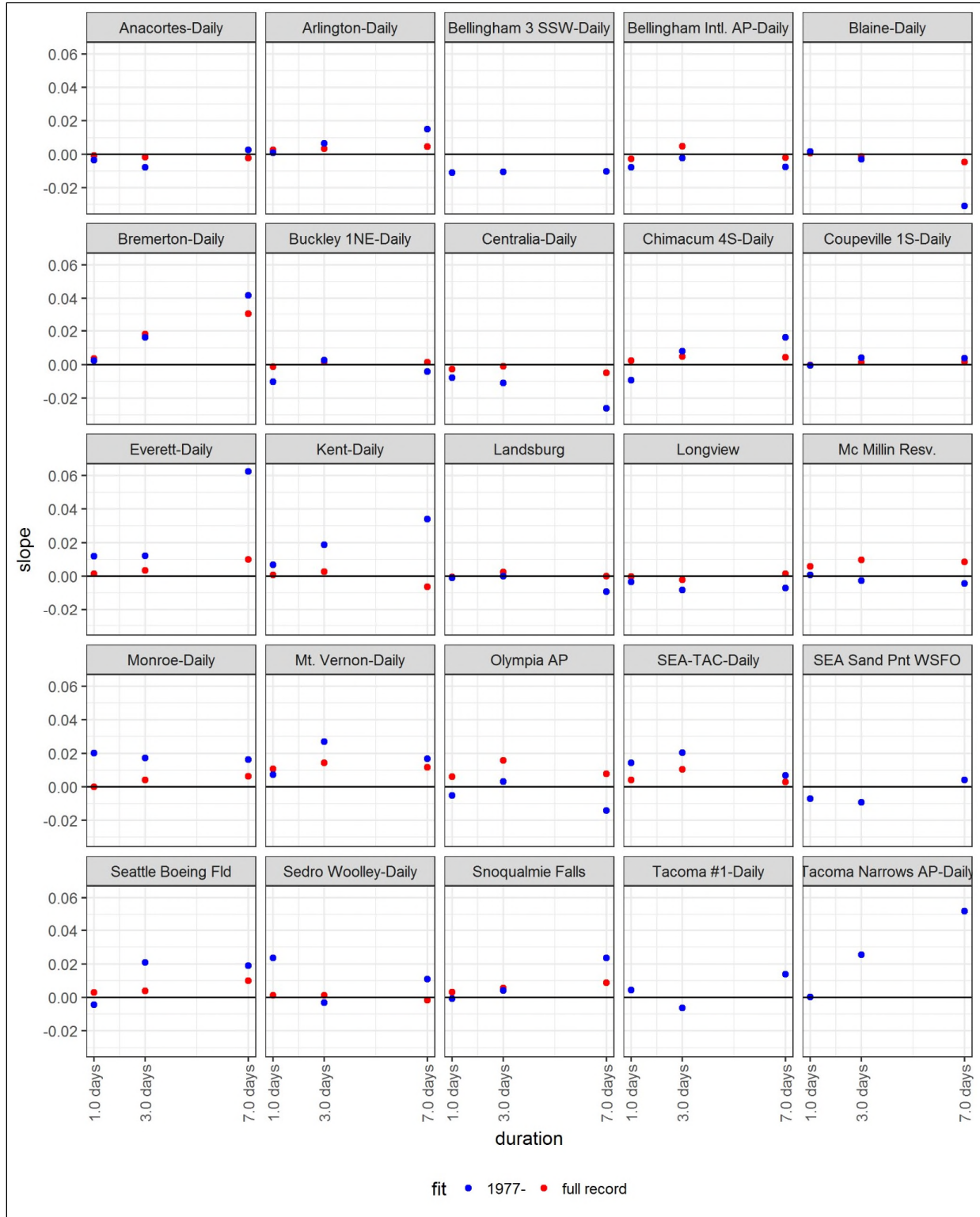
Red indicates all available data, blue indicates starting in 1977, the starting point of provided SPU data.

Figure 78. By-Station Estimates for Trends in Location Parameter of Maximum Likelihood Estimated GEV Regression Model Using NWS Data, 3-Day Duration



Red indicates all available data, blue indicates starting in 1977, the starting point of provided SPU data.

Figure 79. By-Station Estimates for Trends in Location Parameter of Maximum Likelihood Estimated GEV Regression Model Using NWS Data, 7-Day Duration



Red indicates all available data, blue indicates starting in 1977, the starting point of provided SPU data.

Figure 80. By-Station Estimates for Trends in Location Parameter of Maximum Likelihood Estimated GEV Regression Model Using NWS Data. Values greater than zero indicate increasing trend.